6. EXPERIMENTAL RESULTS AND DISCUSSION

6.1 Geochemistry and Mineralogy

6.1.1 XRF Analysis

The XRF analysis was done at Mintek Analytical Services and the results shown in table 20. Kimberlite is a magnesium rich ore as discussed in section 2.1.1. The kimberlites also contain considerable amounts of calcium and iron and minor amounts of potassium. The other elements are not present in significant quantities. What is of particular interest is, firstly, K8, which was identified as a dolomite deposit which is supported by the high calcium content. The composition of K8 does not show the considerable carbonate component and therefore only adds up to ~ 67 %. In addition the high aluminium content of the red kimberlite should also be noted. The sum of elements does not equal 100 due to the loss of ignition not included in the table. The weathering indexes discussed in section 2.3.1.1.3 was fitted to the XRF data but no correlation could be found with weathering results reported later.

Table 20. Results of XRF analysis done at Mintek Analytical Services on the ore samples tested (proportions by mass).

SAMPLE NAME	Na_2O	MgO	Al_2O_3	SiO_2	P_2O_5	K_2O	CaO	TiO_2	Fe_2O_3	MnO	SO_2
	%	%	%	%	%	%	%	%	%	%	ppm
DUTOITSPAN	2.33	25.3	5.94	46.6	0.63	2.03	5.82	0.81	8.45	0.12	< 60
GELUK WES	1.71	25.8	4.44	45.6	0.78	2.86	7.82	1.22	8.89	0.13	233
KOFFIEFONTEIN	1.17	26.3	5.52	49.4	0.33	0.98	5.17	0.75	8.35	0.11	795
CULLINAN	0.80	29.1	4.08	52.6	0.12	1.19	5.15	1.29	9.47	0.15	368
WESSELTON	0.36	32.4	2.07	35.1	1.24	1.86	8.63	1.33	9.83	0.16	244
K1 HYP NE	<300 ppm	32.7	1.6	35.4	0.47	1.57	8.44	0.72	8.25	0.13	346
K1 HYP S	<300 ppm	33.6	0.70	36.6	0.3	0.64	7.18	0.89	8.17	0.12	907
K1 TKB E	0.82	29.0	5.26	47.8	0.15	1.58	3.90	0.50	9.44	0.12	0.1
K2 NE	1.2	25.6	5.93	48.0	0.2	1.18	6.43	0.59	8.7	0.14	96
K2 S	0.6	21.7	5.78	46.5	0.28	1.69	9.88	0.76	8.68	0.19	509
K2 W	0.81	25.7	5.28	47.1	0.28	1.67	7.38	0.75	9.31	0.17	201
K8	<300 ppm	19.1	0.9	14.6	0.28	0.26	27.1	0.67	4.92	0.11	346
Red	1.09	19.6	8.37	51.1	0.18	1.86	4.46	0.72	8.79	0.10	< 60

6.1.2 XRD Analysis

As discussed in the experimental procedure the XRD analysis was done at three different institutions. The results from Mintek are reported in table 21 and 22, although the analysis by the University of Pretoria was used to confirm these results. The original XRD scans from Mintek and the University of Pretoria are shown in Appendix B.

Table 21. XRD Analysis results on Dutoitspan, Geluk Wes, Koffiefontein, Cullinan TKB and Wesselton kimberlites as done by Mintek.

Sample	Mineral group / mineral identified	Probable mineral	Estimated Quantity [Mass %]
Dutoitspan	Smectite	Dioctahedral	30 - 40
	Mica	Biotite / Phlogopite	~ 20
	Calcite		10 – 20
	Pyroxene	Diopside	10 – 20
	Serpentine	Antigorite ?	~ 10
	Magnetite		< 10
	Dolomite		~ 5
	Hematite		< 5
Geluk Wes	Smectite	Dioctahedral	30 - 40
	Calcite		> 20
	Mica	Biotite / Phlogopite	10 - 20
	Serpentine	Lizardite	~ 10
	Pyroxene	Diopside	~ 10
	Feldspar	Albite / Microcline	~ 10
	Magnetite		< 10
	Dolomite		~ 5
	Amphibole	Tremolite	< 5
	Hematite		< 5

Sample	Mineral group / mineral identified	Probable mineral	Estimated Quantity [Mass %]
Koffiefontein	Smectite	Dioctahedral	50 - 60
	Mica	Biotite / Phlogopite	~ 10
	Pyroxene	Augite	< 10
	Serpentine	Antigorite	5 - 10
	Feldspar	Microcline ?	5 - 10
	Dolomite		~ 5
	Calcite		< 5
	Magnetite		< 5
	Quartz		< 5
Cullinan TKB	Mica	Biotite / Hydrobiotite / Phlogopite	~ 25
	Chlorite	Chlinochlore	~ 20
	Magnetite		~ 20
	Talc		~ 15
	Amphibole	Tremolite	10 - 15
	Serpentine	Antigorite	< 10
	Pyroxene	Diopside	< 10
	Smectite	Trioctahedral	~ 5
	Hematite		< 5
	Olivine	Forsterite ?	< 5
	Quartz		< 5
Wesselton	Mica	Biotite	30 - 40
	Calcite		~ 20
	Serpentine	Antigorite ?	~ 20
	Olivine	Forsterite ?	~ 10
	Dolomite		< 10
	Magnetite		< 10
	Goethite		< 5
	Rectorite		~ 5

Table 22. XRD Analysis on Venetia Kimberlites as done by Mintek.

Sample	Mineral group / mineral identified	Probable mineral	Estimated Quantity [Mass %]
K1 HYP NE	Mica	Phlogopite	~ 30
	Calcite		~ 30
	Serpentine	Antigorite	20 - 30
	Magnetite		~ 10
	Chlorite	Chlinochlore	< 5
K1 HYP S	Serpentine	Lizardite	~ 60
	Calcite		20 - 30
	Mica	Biotite	< 10
	Magnetite		< 10
K1 TKB E	Smectite	Dioctahedral	~ 40
	Serpentine	Lizardite / Antigorite	20 - 30
	Mica	Phlogopite	10 - 20
	Amphibole	Tremolite	< 10
	Pyroxene	Diopside ?	< 10
	Dolomite		~ 5
	Magnetite		< 5
	Chlorite	Chlinochlore	< 5
	Calcite		< 5
K2 NE	Smectite	Dioctahedral	~ 45
	Mica	Phlogopite	20 - 30
	Pyroxene	Augite	10 - 20
	Serpentine	Antigorite	~ 10
	Magnetite		< 10
	Amphibole	Tremolite	~ 5
	Calcite		< 5
	Dolomite		< 5

Sample	Mineral group / mineral identified	Probable mineral	Estimated Quantity [Mass %]
K2 S	Smectite	Trioctahedral	~ 40
	Calcite		~ 30
	Mica	Biotite / Phlogopite	~ 20
	Amphibole	Tremolite	10 – 20
	Quartz		~ 10
	Magnetite		Trace
	Serpentine	Lizardite	Trace
K2 W	Smectite	Mixed layer	~ 30
	Pyroxene	Augite	< 30
	Mica	Biotite / Phlogopite	~ 25
	Serpentine	Antigorite	~ 10
	Calcite		~ 10
	Magnetite		< 10
	Dolomite		~ 5
RED KIMB	Smectite	Dioctahedral	~ 40
	Quartz		~ 25
	Calcite		~ 10
	Feldspar	Albite	~ 10
	Serpentine	Lizardite	< 10
	Mica	Phlogopite	~ 5
	Amphibole	Tremolite	< 5
	Magnetite		< 5
K8	Dolomite		> 90
	Calcite		< 10
	Unknown silicate		< 5

Initial test work used Koffiefontein and Wesselton ore. These ores show contrasting weathering behaviour as Koffiefontein weathered in minutes and Wesselton showed very little degradation even after fifteen days of exposure. XRD investigations showed Koffiefontein ore to contain predominantly swelling clays compared to Wesselton containing very little or no swelling clay (see table 21). Based on these preliminary results the hypothesis developed

around swelling clays and was refined through further test work and investigation. Cullinan TKB ore contains very little swelling clay resulting in a very low weathering rate. Geluk Wes contains 30 – 40 % swelling clay and therefore showed a medium to fast weathering behaviour depending on the weathering conditions. Similarly Dutoitspan contains 30 – 40 % swelling clay and shows similar weathering behaviour to Geluk Wes.

The position of the 060 reflection of smectite gives some information whether dioctahedral (montmorillonite, beidellite and nontronite) or trioctahedral (hectorite and saponite) smectites are present (Weaver, 1989). Dioctahedral smectites have reflections at 1.490 – 1.515 Å compared to trioctahedral smectites with reflections at 1.515 – 1.55 Å. This classification was done on the kimberlites used in this study and is given in tables 21 and 22. Note that the smectite was of the dioctahedral type in nearly all cases.

6.1.3 Visual observation of the kimberlite ores

Photographs were taken of all the kimberlites used for test work and these are shown in figure 20. The lumps are ~ 25 mm in size.

Dutoitspan

Geluk Wes

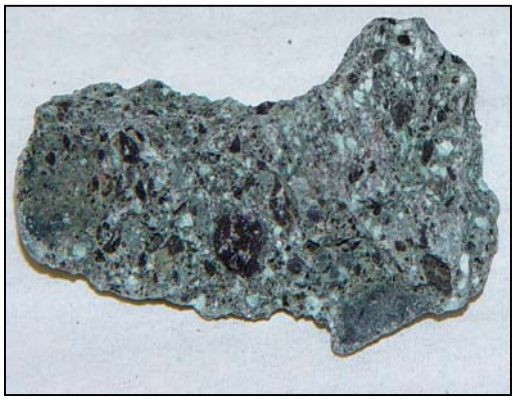

Koffiefontein

Wesselton

Venetia K1 Hypabyssal North East

Venetia K1 Hypabyssal South

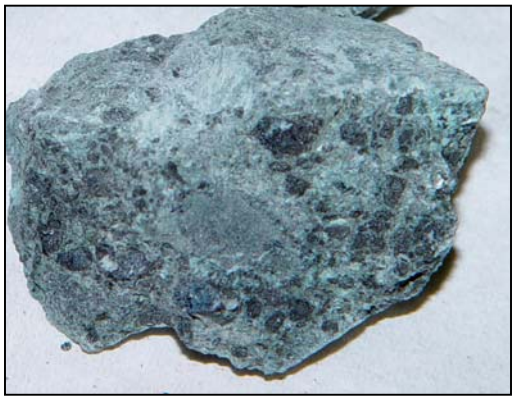

Venetia K1 TKB East

Venetia K2 North East

Venetia K2 South

Venetia K8

Venetia Red

Figure 20. Visual appearance of the untreated kimberlite lumps.

The kimberlite ores exhibit very different physical appearances as shown in figure 20. Colours range from grey, green, yellow, brown to blue and even red. Also the fine-grained matrix and larger xenoliths are easily identified.

6.1.4 Cation Exchange Capacity (CEC)

The cation exchange capacity (CEC) (procedure discussed in section 2.2.2.8) was determined at Agricultural Research Council (ARC) in Pretoria. A pulverised 300 g sample is used for this analysis. The CEC results are given in table 23 below.

Table 23. Cation Exchange Capacities for the kimberlites tested.

Sample Name	CEC
	$cmol_c/kg$
Dutoitspan	41.3
Geluk Wes	33.0
Koffiefontein	44.6
Cullinan TKB	18.7
Wesselton	5.4
V_K1 HYP NE	15.9
V_K1 HYP S	8.3
V_K1 TKB E	45.3
V_K2 NE	41.0
V_K2 S	31.1
V_K2 W	29.2
V_K8	10.4
V_Red	36.5

6.1.5 Conclusion

From the XRF and XRD results it is concluded that the kimberlites obtained for test work, vary extremely in geological and mineralogical properties. All the kimberlites contain considerable amounts of clay material. The predominant mineral species present are: amphibole, calcite, chlorite, feldspar, magnetite, mica, olivine, pyroxene, serpentine, smectite and talc. The smectite content and CEC values of all kimberlites used in this study are compared in figure 21. The cation exchange capacity is strongly influenced by the swelling clay content but also secondarily depends on the amounts of other minerals – for example, chlorite and mica - as they have different capacities to exchange cations. Therefore the ores with no swelling clay do have a non-zero and variable CEC. The cation exchange capacity is a property that can be used to complement the swelling clay content to provide information on the possible

weathering behaviour of a kimberlite. However due to the complexity and cost associated with XRD, CEC is the preferred property.

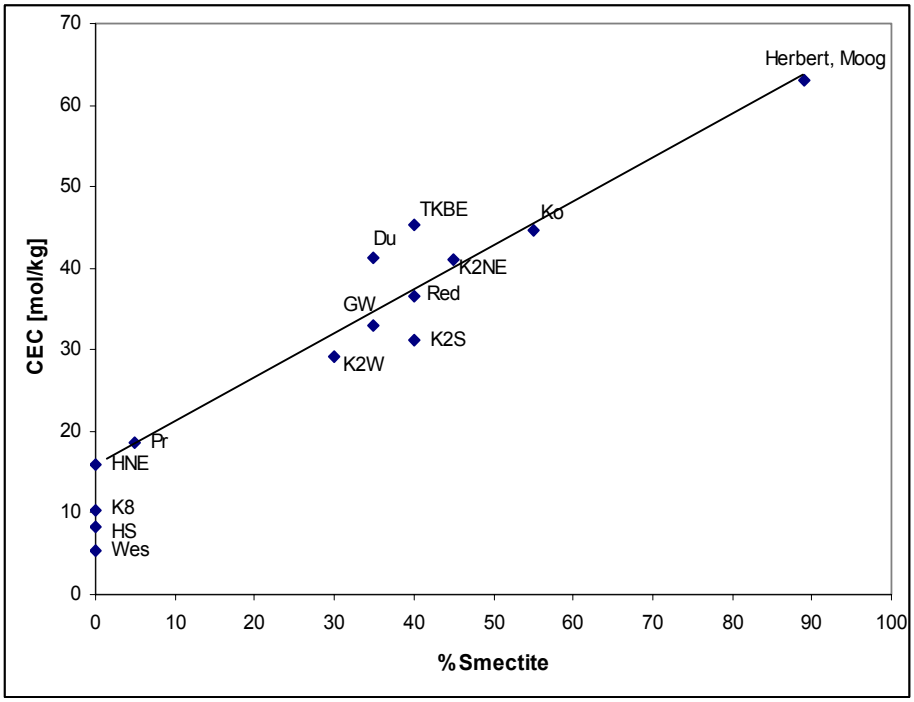

Figure 21. Comparison of the cation exchange capacity (CEC) and % smectite. Additionally a datapoint for a sodium bentonite from Herbert and Moog (1999) are presented.

The smectite - CEC relationship was plotted (figure 21) with the relationship y = 0.57 x + 15.5. A data point from the study of Herbert and Moog (1999) on bentonite clay was added to figure 21.

6.2 Weathering Results

Weathering results are given as the size distribution after milling. The unweathered ore was milled (labelled 0 days) and this size distribution given as the base case for comparison. The size distributions are given on linear scales on both axes as this was found to depict the results optimally. Weathering results at a later time did not utilise milling (as it was not required); the output of these tests is therefore given only as the size distribution after weathering and outdoor drying. The influence of milling on the size distribution is investigated in section 6.2.5.8. The repeatability of results was tested and is discussed in section 6.3.

6.2.1 Koffiefontein

The Koffiefontein sample was found to weather at a very high rate, as it forms fines within hours of contact with distilled water (figure 22). This correlates with the mineralogical investigation reporting this ore to be very rich in swelling clays ~ 50 - 60 %. Figure 22 shows visual breakdown of this ore after 1 and 3 hours of exposure to distilled water.

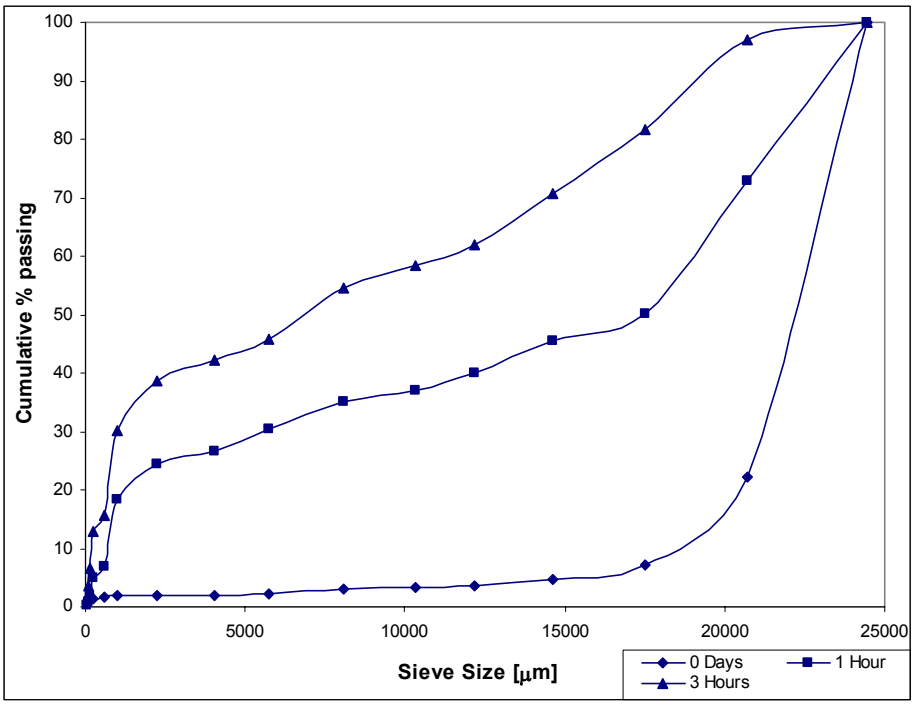

Figure 22. Results of a 1.5 kg (– 26.5 + 22.4 mm) Koffiefontein sample weathered for 1 and 3 hours respectively in distilled water.

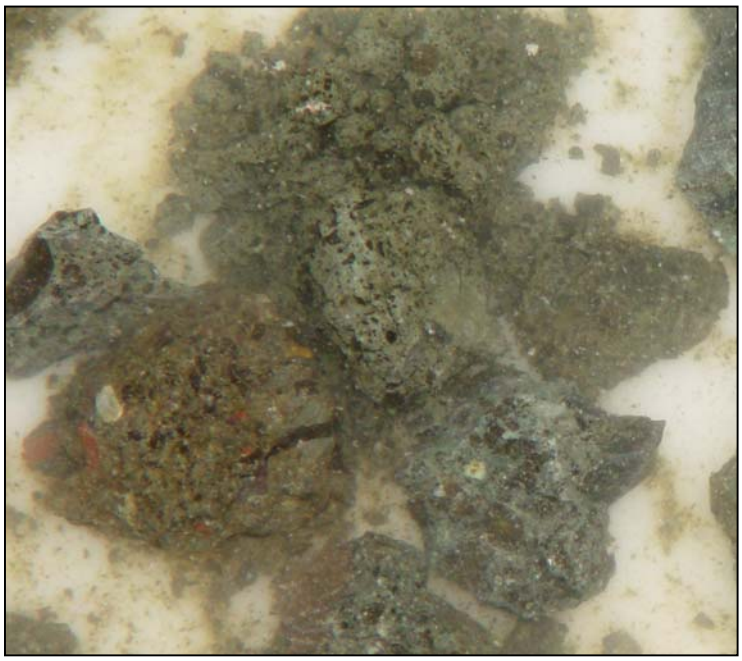

Figure 23. Visual appearance of Koffiefontein ore (- 26.5 + 22.4 mm initial size fraction) weathered for 3 hours in distilled water.

Within 1 hour the cumulative % passing 17.5 mm has increased from 7 to 50 %, which is further increased to 82 % after 3 hours. The particle size distribution shape remains similar but shifts to smaller size fractions. Figure 23 shows that the particles are cracked and some broken into fines already after 3 hours of weathering.

6.2.2 Wesselton

Wesselton ore was tested in different solutions namely water (figure 24), sodium chloride (figure 25), sulphuric acid (figure 26), cyclic wetting with distilled water (figure 27) and copper sulphate (figure 28). The visual appearance of the product of the standard weathering test is shown in figure 29.

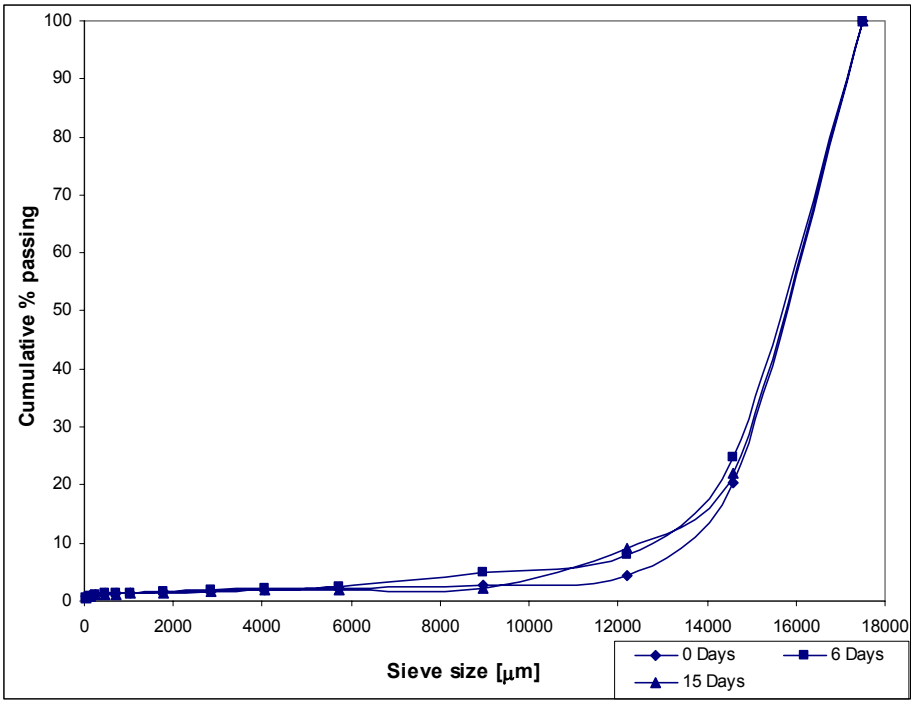

Figure 24. Weathering results from the standard test procedure; 1.5 kg (– 19 + 16 mm) Wesselton ore weathered in distilled water for 0, 6 and 15 days.

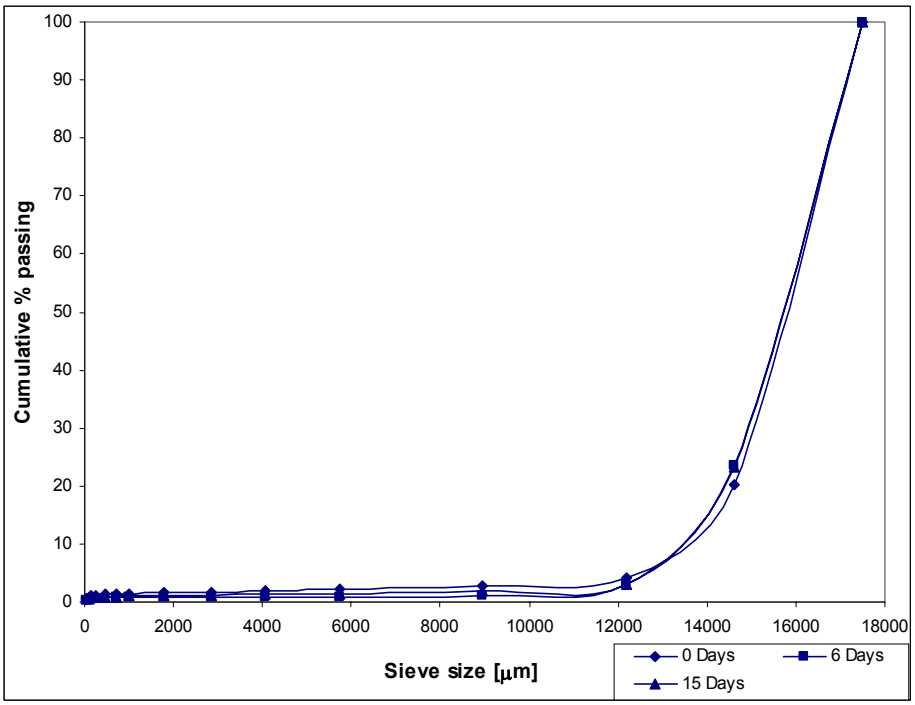

Figure 25. Weathering results from a 1.5 kg (– 19 + 16 mm) Wesselton ore sample weathered in sodium chloride solution (0.2 M) for 0, 6 and 15 days.

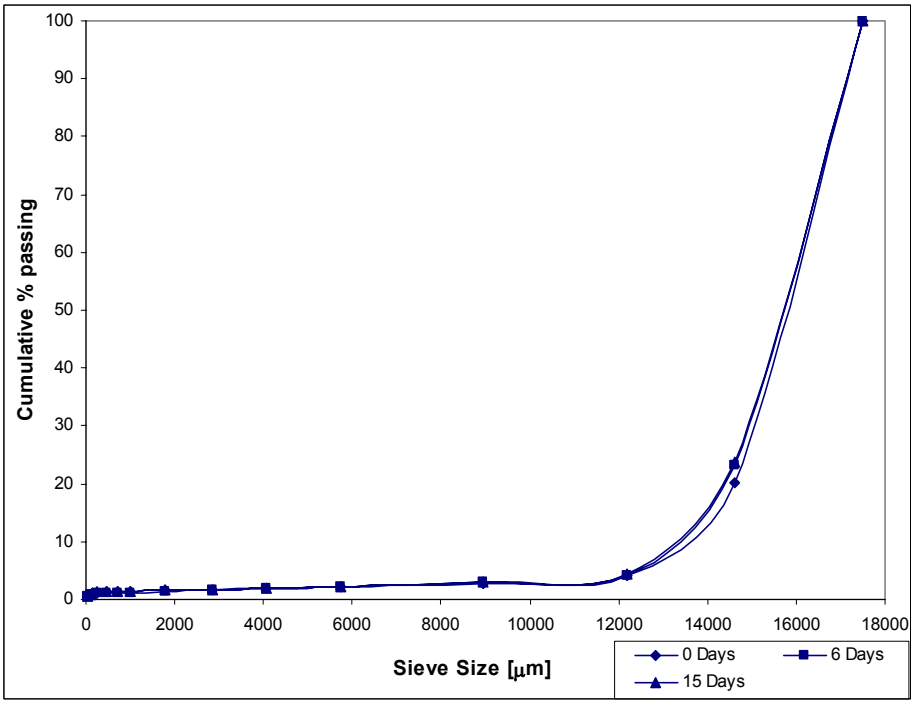

Figure 26. Weathering results from a 1.5 kg (– 19 + 16 mm) Wesselton ore sample weathered in dilute sulphuric acid (pH ~ 3) for 0, 6 and 15 days.

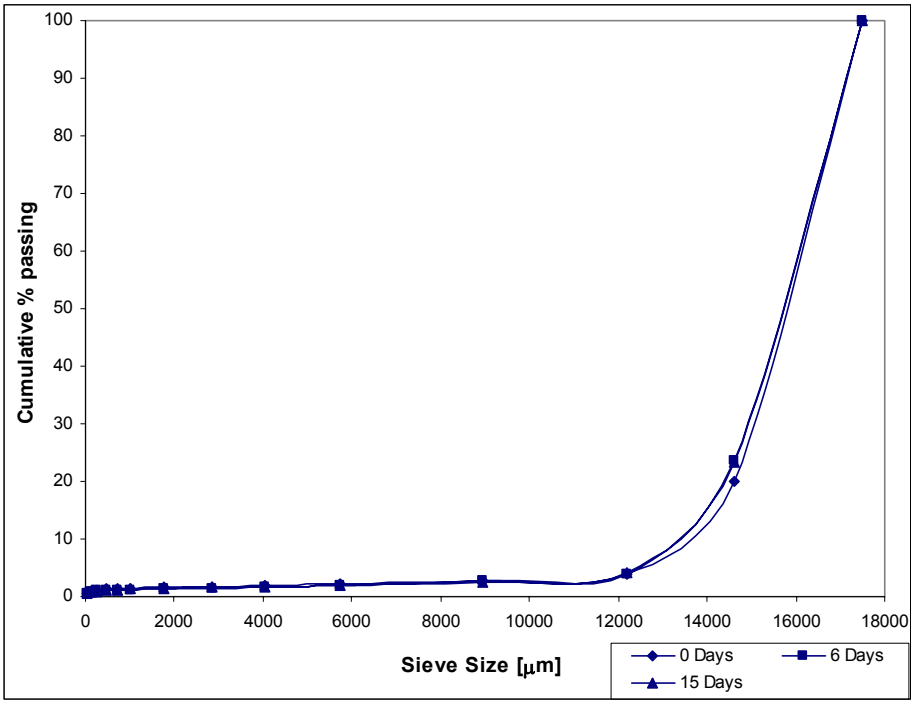

Figure 27. Weathering results from a 1.5 kg (– 19 + 16 mm) Wesselton ore sample weathered by cyclic wetting with 500 ml of distilled water once a day for 0, 6 and 15 days.

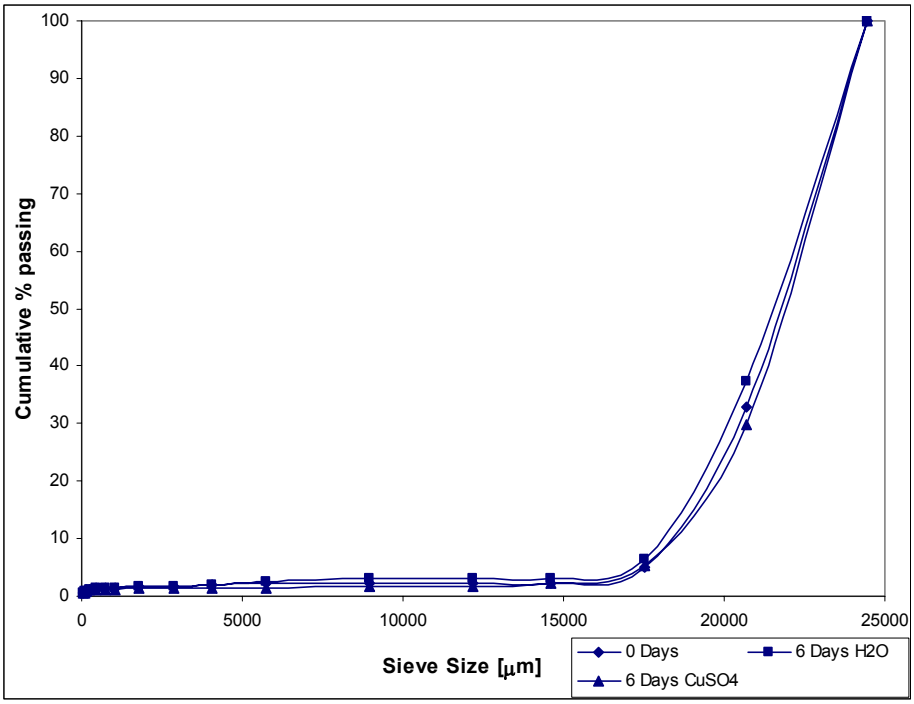

Figure 28. Weathering results from a 1.5 kg (– 26.5 + 22.4 mm) Wesselton ore sample weathered in a 0.2 M copper sulphate solution for 0 and 6 days. The 6 days standard weathering test is shown for comparative purposes.

Figure 29. Visual appearance of Wesselton ore after the standard weathering test (- 19 + 16 mm).

From the results of figures 24 to 27 it is concluded that this type of ore is not weatherable even under severely aggressive conditions. The absence of weathering is attributed to the fact that the ore does not contain any swelling clays (see section 6.1.2). Even the copper solution (figure 28), which showed severe attack on other ores made no significant impact on this ore.

6.2.3 Cullinan

Cullinan ore (- 19 + 16 mm) was weathered according to the standard weathering test (figure 30) and also in a 0.2 M sodium chloride solution (figure 31).

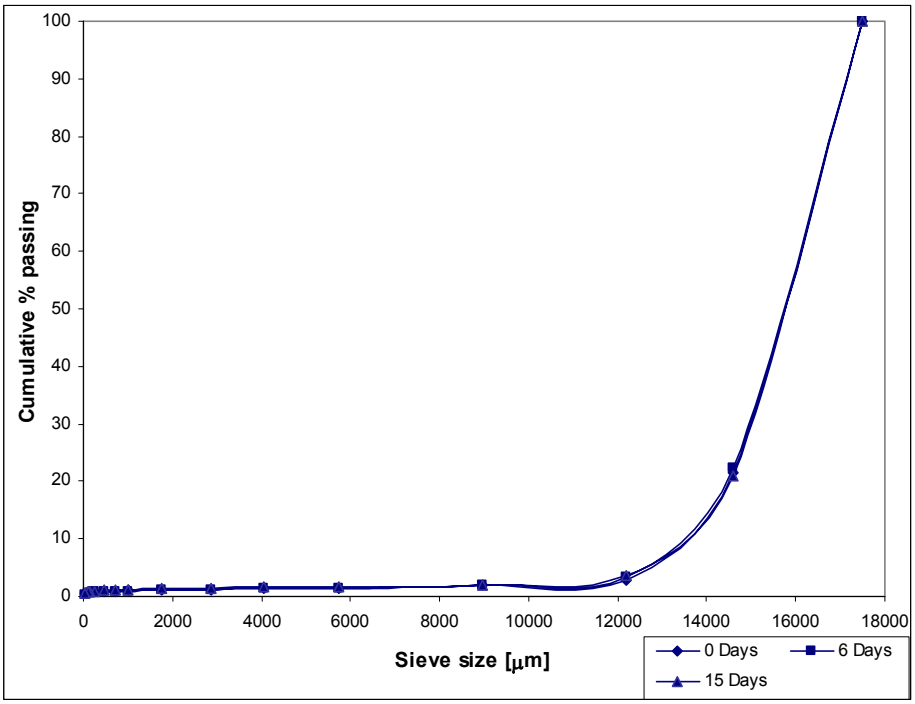

Figure 30. Weathering results from a 1.5 kg (– 19 + 16 mm) Cullinan TKB ore sample weathered by the standard test method for 0, 6 and 15 days.

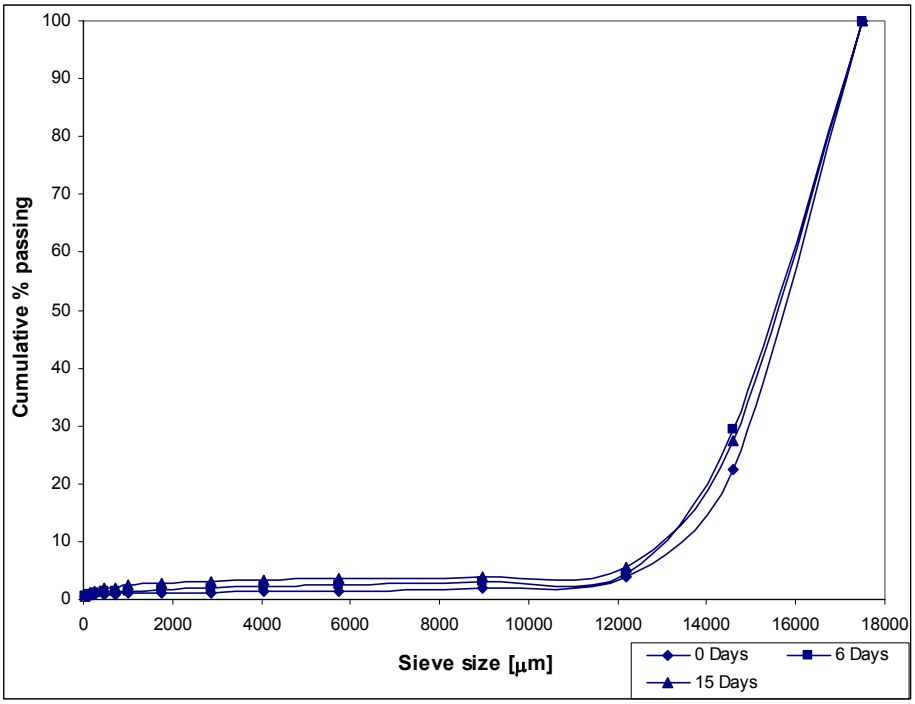

Figure 31. Weathering results from a 1.5 kg (– 19 + 16 mm) Cullinan TKB ore sample weathered in a 0.2 M sodium chloride solution for 0, 6 and 15 days.

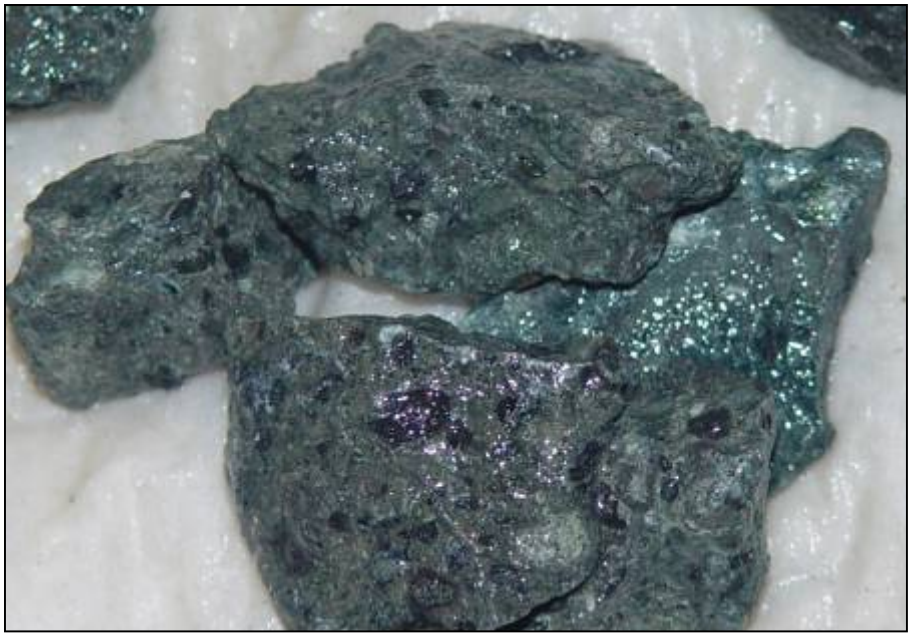

Figure 32. Visual appearance of Cullinan TKB ore after the standard weathering test (-19 + 16 mm).

This ore also shows very little change when weathered (no change in particle size distribution). There is slightly enhanced weathering (~ 5 % increase in cumulative % passing 12.2 mm) in sodium chloride. This is however not a large enough increase to be considered a

significant influence. This ore contains less than five percent swelling clays, which is the presumed reason why weathering is very slow. The product of the standard weathering test is shown in figure 32.

6.2.4 Geluk Wes

This ore was weathered according to the standard conditions and then the effect of some cations (sodium, aluminium and lithium) was tested. The sodium chloride solution test was repeated with the addition of sulphuric acid to investigate the influence of pH.

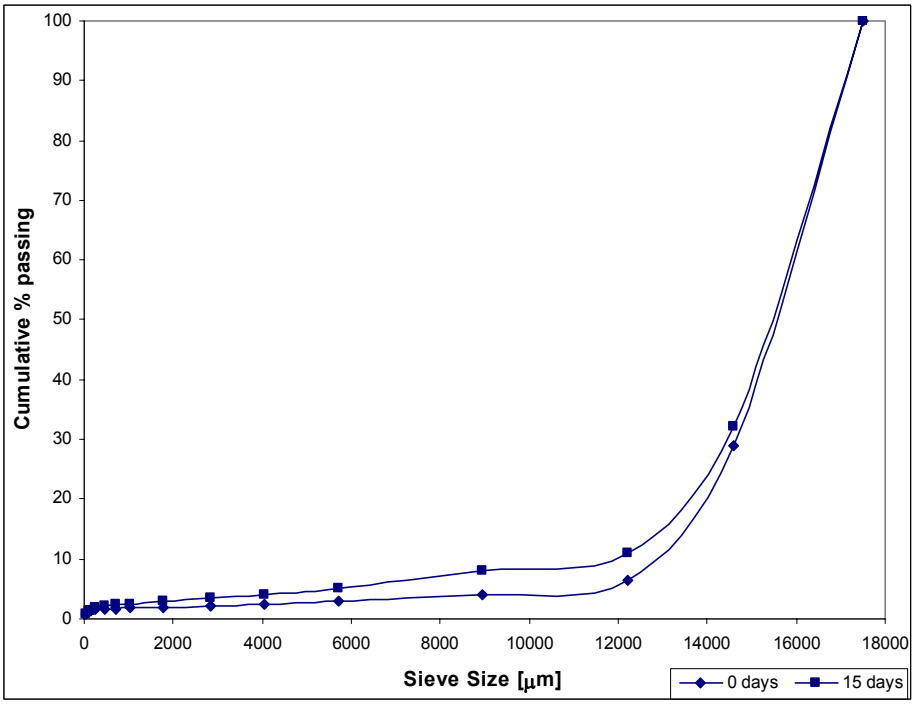

Figure 33. Weathering results from a 1.5 kg (– 19 + 16 mm) Geluk Wes ore sample weathered by the standard test method for 0 and 15 days.

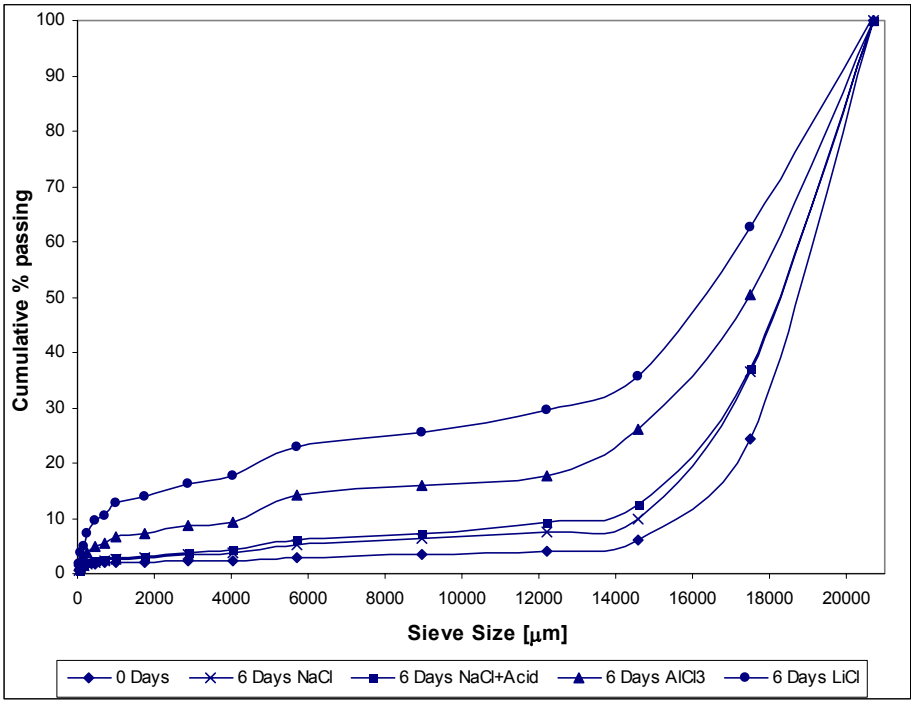

Figure 34. Weathering results from a 1.5 kg (– 22.4 + 19 mm) Geluk Wes ore sample weathered in 0.2 M sodium chloride, acidified sodium chloride at low pH (~ 2.5), aluminium chloride and lithium chloride solutions, all for 6 days.

Weathering of Geluk Wes ore in water shows a maximum of 5 % increase in cumulative % passing over the whole size range, after 15 days. Therefore under normal plant conditions this ore will show degradation to a limited extent.

Figure 34 shows the influence of cations on the weathering process. The results show a nominal increase (compared to water weathering) of 10 % in cumulative % passing 17.5 mm with the addition of sodium chloride, 25 % with aluminium chloride and 35 % with lithium chloride. It also shows that the addition of acid to the sodium medium did not enhance weathering and therefore acidification has no significant influence on weathering in this case. However the pH will influence the complex formation and precipitation reactions of cations. Figures 35, 36 and 37 show photographs of the weathered products using sodium chloride, aluminium chloride and lithium chloride solutions, respectively. Note the increase in broken material and fines from the sodium medium to the aluminium medium and then the lithium medium. These results led to further test work on the effect of cations using the Dutoitspan ore.

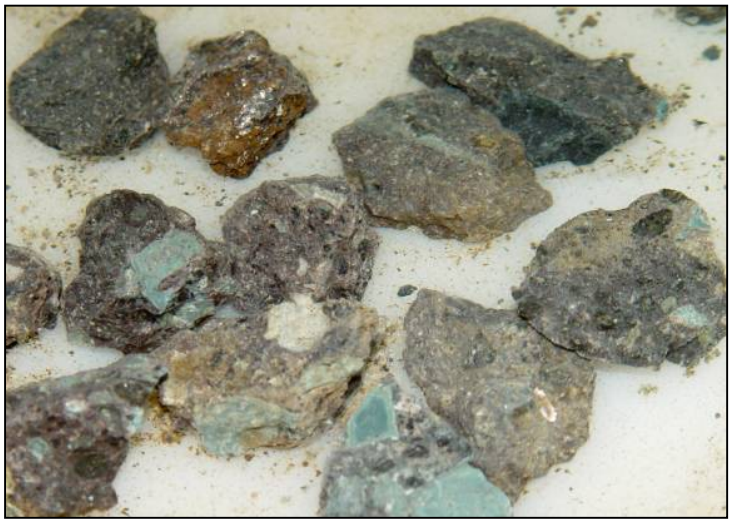

Figure 35. Visual appearance of Geluk Wes ore (initial size -22.4 + 19 mm) weathered in sodium chloride solution (0.2 M) for 6 days.

Figure 36. Visual appearance of Geluk Wes ore (initial size - 22.4 + 19 mm) weathered in aluminium chloride solution (0.2 M) for 6 days.

Figure 37. Visual appearance of Geluk Wes ore (initial size -22.4 + 19 mm) weathered in lithium chloride solution (0.2 M) for 6 days.

6.2.5 Dutoitspan

6.2.5.1 Standard weathering test

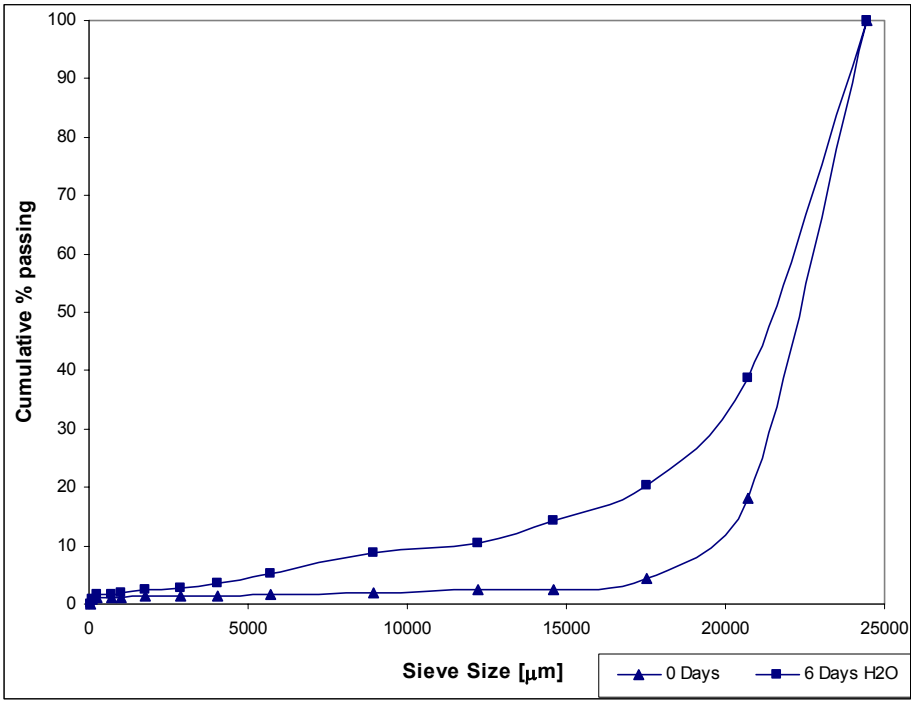

Figure 38. Weathering results from a 1.5 kg (– 26.5 + 22.4 mm) Dutoitspan ore sample weathered for 6 days in a distilled water medium.

Figure 38 shows the results of the standard weathering test on the Dutoitspan kimberlite. The unweathered sample, milled, gave 3.7 % passing 12.2 mm. The 6 days distilled water weathered sample resulted in 13 % passing 12.2 mm. The standard weathering test therefore gave a ~ 9 – 10 % change in the product size distribution. This test gives an indication of what might be expected under plant conditions from this ore, which again shows some degradation but not full disintegration.

6.2.5.2 Influence of cation species on weathering

Monovalent Cations

The results for weathering in a potassium-, sodium-, ammonium- and lithium chloride solution are shown in figure 43. Photos of the products are shown in figures 39-42.

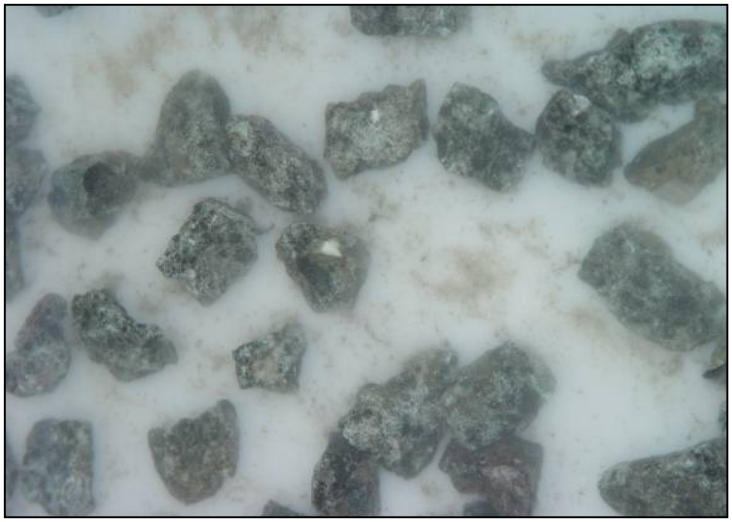

Figure 39. Visual appearance of Dutoitspan ore (initial size - 26.5 + 22.4 mm) weathered in potassium chloride solution (0.4 M) for 6 days.

Figure 40. Visual appearance of Dutoitspan ore (initial size - 26.5 + 22.4 mm) weathered in lithium chloride solution (0.4 M) for 6 days.

Figure 41. Visual appearance of Dutoitspan ore (initial size - 26.5 + 22.4 mm) weathered in ammonia chloride solution (0.4 M) for 6 days.

Figure 42. Visual appearance of Dutoitspan ore (initial size - 26.5 + 22.4 mm) weathered in sodium chloride solution (0.4 M) for 6 days.

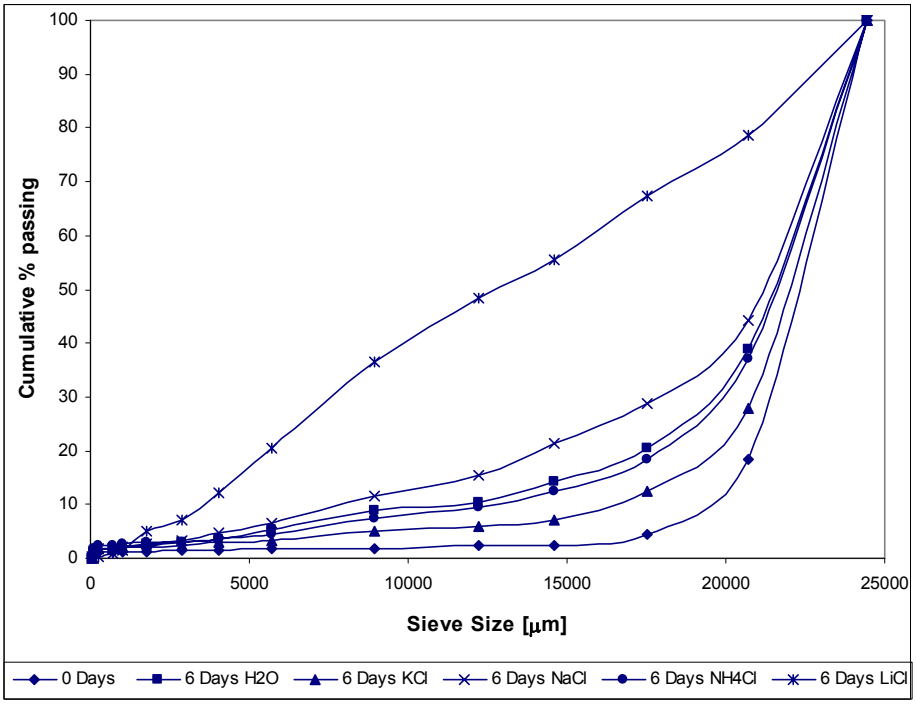

Figure 43. Results of the investigation on the influence of monovalent cations on the weathering behaviour of Dutoitspan ore. Tests were done utilising 1.5 kg (initial size – 26.5 + 22.4 mm) ore weathered in a 0.4 M cation solution for 6 days.

Visual appearances of the weathering tests are shown in figures 39 – 42 for the monovalent cations. The results of figure 43 show that, as suggested in literature (Vietti, 1994) the weathering behaviour can be decelerated by potassium, which in this case decreased the ore passing 17.5 mm by 6 %. Water and ammonium chloride showed similar weathering

behaviour, with sodium showing increased weathering of ~ 9 % compared to distilled water. Lithium showed the maximal weathering behaviour with 67 % ore passing 17.5 mm which is a substantial increase of ~ 50 %.

Divalent Cations

The results for weathering in a calcium-, cupric-, ferrous- and magnesium chloride solution are shown in figure 48. Photos of the products are shown in figures 44-47.

Figure 44. Visual appearance of Dutoitspan ore (initial size - 26.5 + 22.4 mm) weathered in calcium chloride solution (0.4 M) for 6 days.

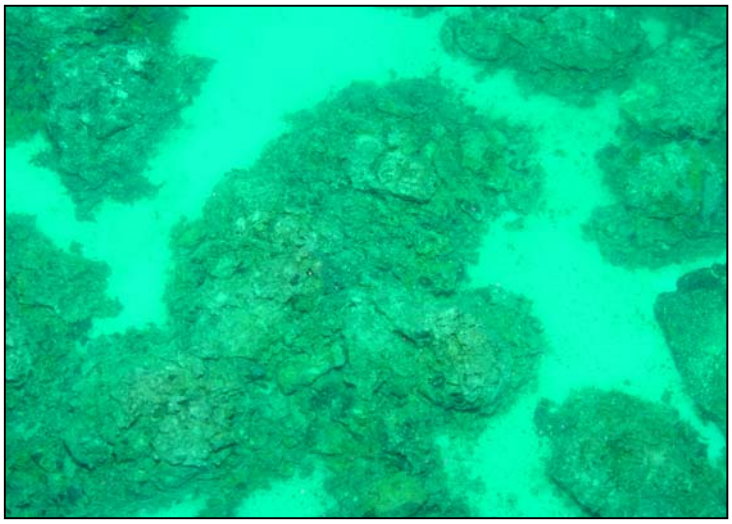

Figure 45. Visual appearance of Dutoitspan ore (initial size - 26.5 + 22.4 mm) weathered in cupric chloride solution (0.4 M) for 6 days.

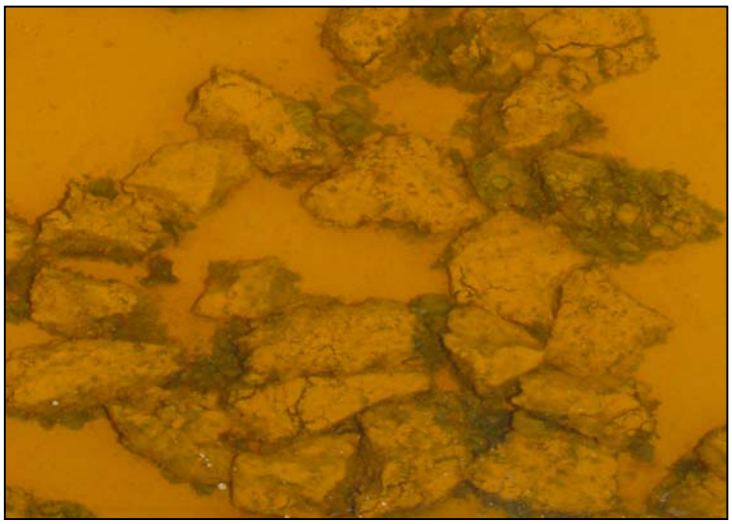

Figure 46. Visual appearance of Dutoitspan ore (initial size - 26.5 + 22.4 mm) weathered in ferrous chloride solution (0.4 M) for 6 days.

Figure 47. Visual appearance of Dutoitspan ore (initial size - 26.5 + 22.4 mm) weathered in magnesium chloride solution (0.4 M) for 6 days.

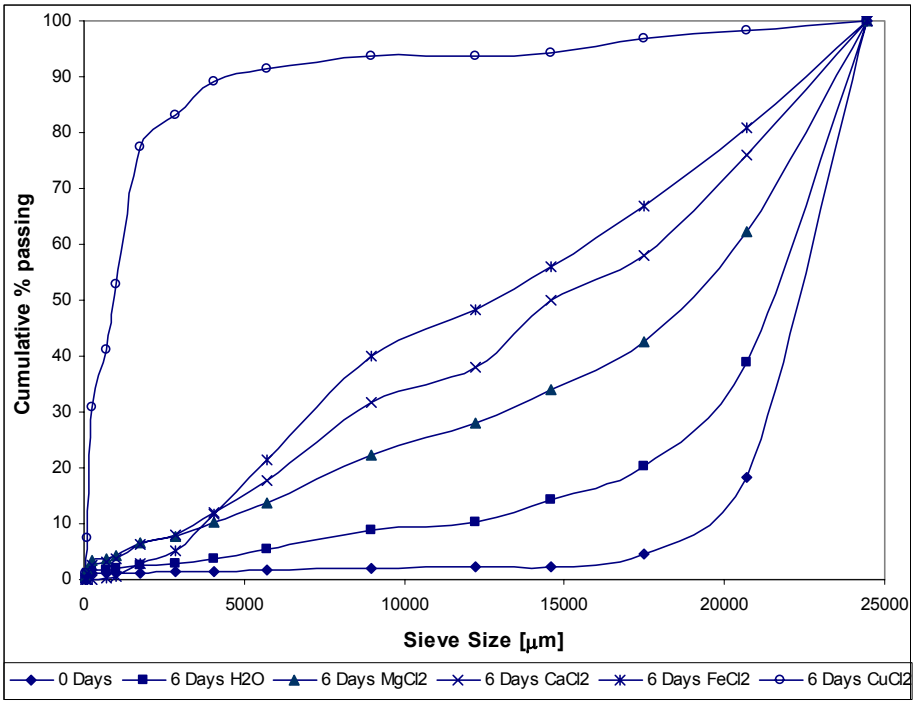

Figure 48. Results of the investigation on the influence of divalent cations on the weathering behaviour. Tests were done utilising 1.5 kg (initial size – 26.5 + 22.4 mm) Dutoitspan ore weathered in 0.4 M cation solution for 6 days.

Of the divalent cations copper was the most efficient cation, followed by iron, then calcium and lastly magnesium. Magnesium produced 42 % passing 17.5 mm, an increase of some 22 % relative to water weathering. Calcium results in 58 % passing 17.5 mm with ferrous iron giving 67 %. Copper showed unique weathering behaviour, moving the whole size distribution to the left to 90 % passing 4 mm. The shapes of the size distribution curves remain similar for unweathered, water, magnesium, calcium and ferrous iron, but copper produces a totally different form of size distribution.

Trivalent Cations

Tests on the influence of trivalent cations used aluminium and ferric ions at a 0.4 M concentration (with chloride as the anion).

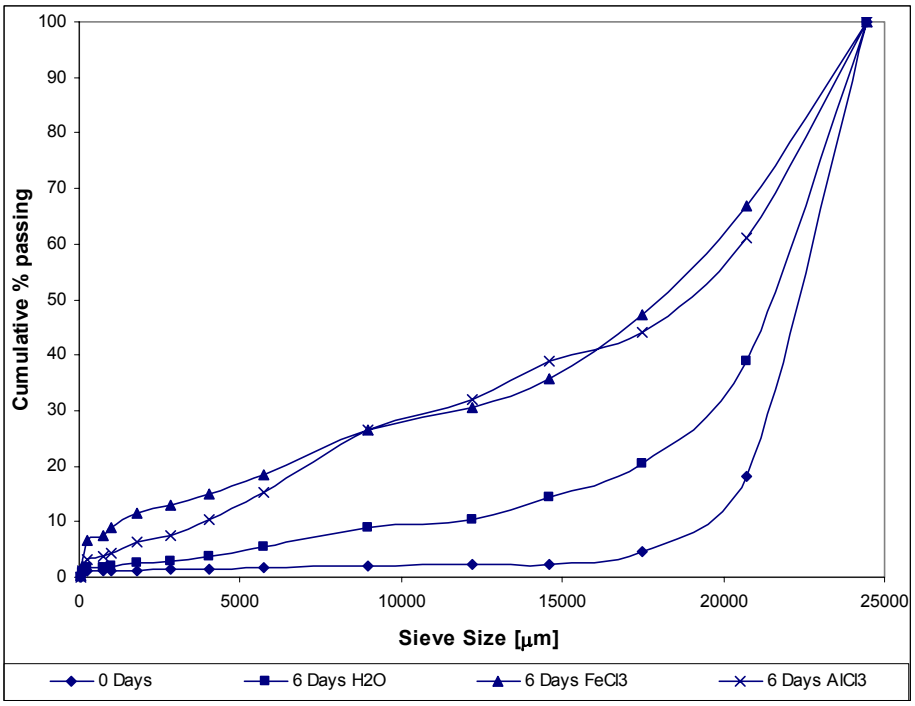

Figure 49. Results of the investigation on the influence of trivalent cations on the weathering behaviour. Tests were done utilising 1.5 kg (initial size – 26.5 + 22.4 mm) Dutoitspan ore weathered in a 0.4 M cation solution for 6 days.

Aluminium and ferric cation solutions showed similar weathering behaviour with ~ 45 % passing 17.5 mm.

Comparison of the weathering effect for differently charged cations is shown in figure 50.

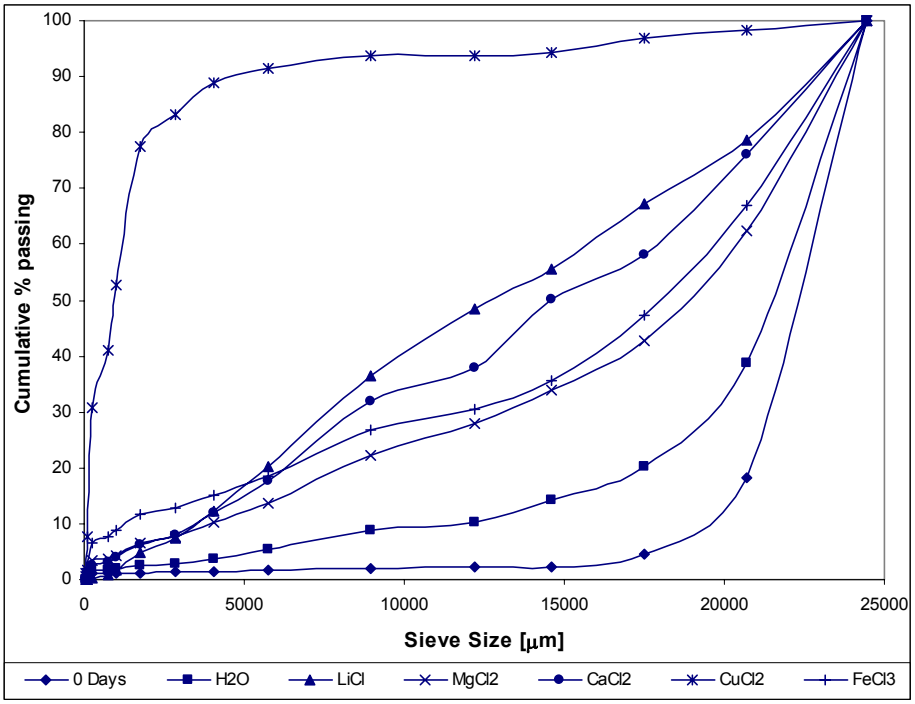

Figure 50. Comparing the influence of different charged cations on weathering behaviour. The tests were done on a 1.5 kg (- 26.5 + 22.4 mm) sample weathered for 6 days in a 0.4 M solution.

Comparison of differently charged cations yields the weathering series from most effective to least effective, as $Cu^{2+} > Li^{+} > Ca^{2} > Fe^{3+} > Mg^{2+}$. Newman (1987) showed that Mg^{2+} and Ca^{2+} hydrate to two sheet complexes under controlled humidity whereas Sr and Ba tend to form single layer complexes. All the cations Mg^{2+}, Ca^{2+}, Sr^{2+} and Ba^{2+} cause the clay to swell to 19 Å in water, but never swell macroscopically. Newman (1987) showed that K^{+} easily dehydrates in the interlayer spacing, tending towards spacings of 12 – 13 Å in water. NH_4^{+} behaves similar to K^{+} with the exception that it can dissociate into H^{+} and NH_3. Cs^{+} and Rb^{+} are large enough to prevent swelling and both form ~ 12 Å interlayer spacings independent of water content. Al^{3+} is shown by Newman (1987) to wet up to 19 Å but can increase to ~ 22 Å at high pH values due to the formation of Al-OH polymers.

The ionic potential (Z/r_{eff}) is an indication of the strength of hydration of cations of valency Z and effective ionic radius r_{eff}. Ferrage *et al* (2005) showed a correlation between the ionic potential and interlayer spacing (as measured by XRD). The ionic potential was therefore investigated for possible correlation with weathering results as shown in figure 51. The r_{eff} values were obtained from Shannon (1976), using the values for 6-fold coordination. Disregarding trivalent cations (which tend to form hydroxy interlayers, rather than simply exchanging into the interlayer), the relationship between observed weathering behaviour and ionic potential is strong. The weathering effects of Cu^{2+}, Fe^{2+} and Li^{+} clearly lie above the trend formed by the other monovalent and divalent cations. It has been reported that all three

of these ions adsorb at other positions (such as crystal edges) in addition to exchanging into the interlayer (Strawn *et al*, 2004, Hofstetter *et al*, 2003, Anderson *et al*., 1989). This might explain the strong weathering effects of these three cations; it is argued later in this thesis that their strong weathering effect is probably related to a reduction in surface energy, so reducing the work required to generate fresh crack surfaces. The ionic potential correlation studied by Ferrage *et al* (2005) was not validated for trivalent cations as the clay structure was found to be very heterogeneous and assessment of the degree of saturation was difficult. Trivalent cations especially Al^{3+} and Fe^{3+} tend to form hydroxy species in the clay interlayer as utilised in pillared clay formation (Belver *et al*, 2004; Newman, 1987). Polycation pillaring of smectites has also been investigated. This suggests that the mechanism of adsorption for trivalent cations are very different than mono- and divalent cation adsorption and could possible explain the poor correlation in figure 51.

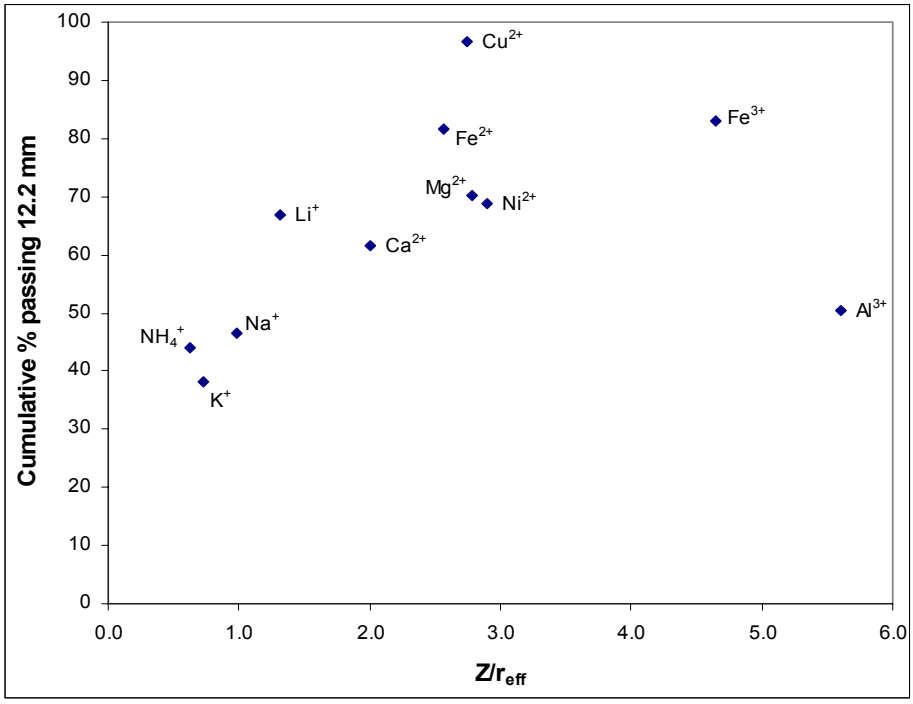

Figure 51. Weathering results of differently charged cations as a function of ionic potential. Weathering tests were performed with 300 g of – 16 + 13.2 mm Dutoitspan kimberlite, weathered in a 0.5 M cation solution for 6 days.

Based on the observed weathering acceleration, further tests were done on the concentration and time dependence when using cations in the weathering solution.

6.2.5.3 Time dependence of weathering

The time dependence of weathering was tested in magnesium and copper containing media.

Magnesium Chloride Medium

The time dependence of weathering was tested in a magnesium chloride solution (0.2 M) for 2, 6 and 15 days. Results are shown in figures 52 and 53.

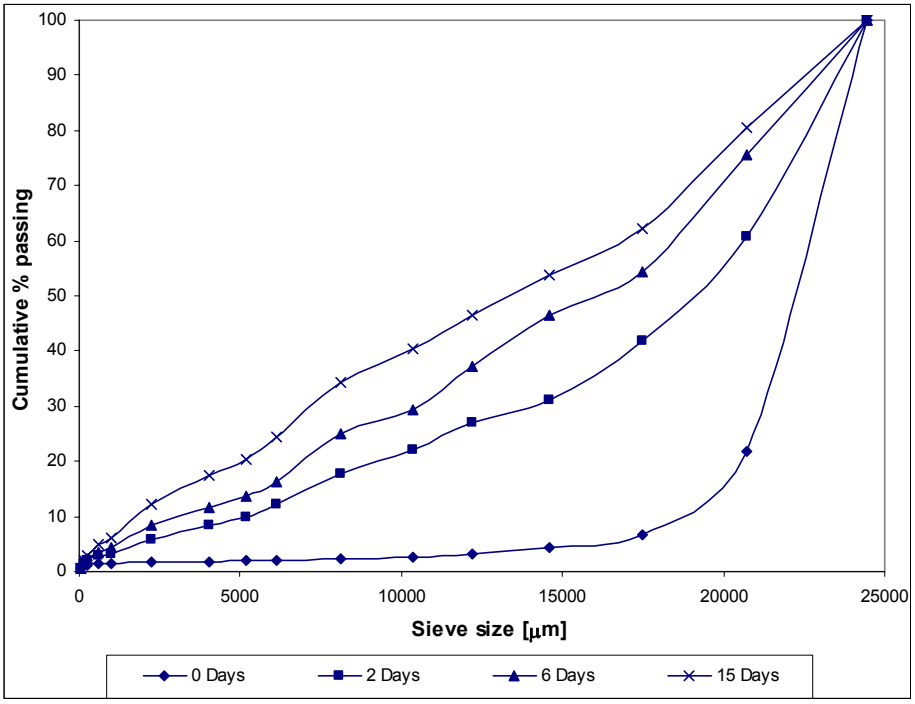

Figure 52. Weathering results from a 1.5 kg (initial size – 26.5 + 22.4 mm) Dutoitspan ore sample weathered in a 0.2 M magnesium chloride solution for 0, 2, 6 and 15 days.

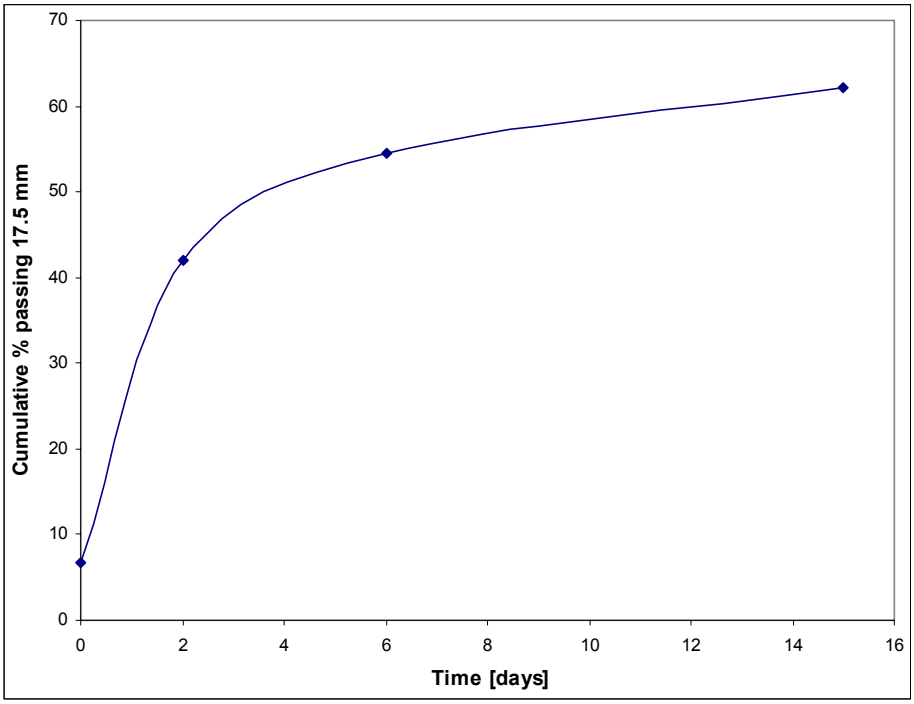

Figure 53. Summarised weathering results from a 1.5 kg (initial size – 26.5 + 22.4 mm) Dutoitspan ore sample weathered in a 0.2 M magnesium chloride solution for 0, 2, 6 and 15 days (from figure 52).

Figure 52 shows the results of time dependence tests done on Dutoitspan ore. Figure 53 was produced from figure 52 by plotting the cumulative % passing 17.5 mm vs. time. This graph shows a very high weathering rate for the first two days which subsequently decreases in rate. After 6 days the rate is considerably lower but not zero. Around 66 % of the total weathering for 15 days took place in the first two days and 88 % in the first six days.

Cupric Sulphate Medium

The time dependence of weathering was also tested in a cupric medium (0.2 M). Photos at 12, 24 and 144 hours clearly display the disintegration as time passes (figures 54 – 56).

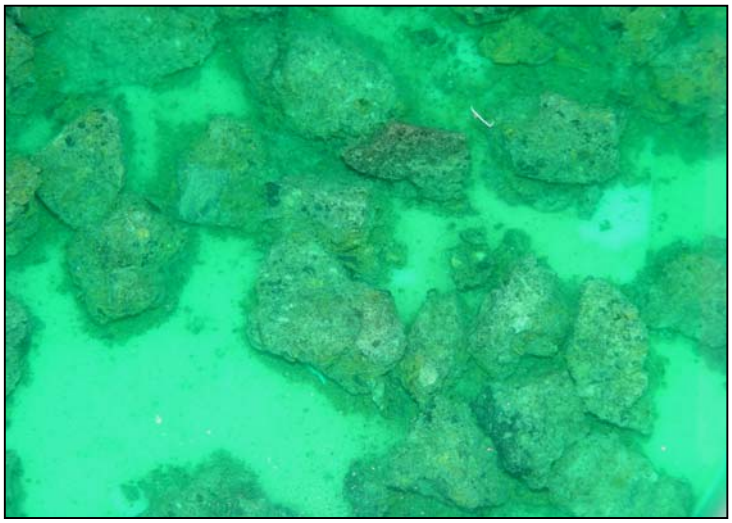

Figure 54. Visual appearance of Dutoitspan ore (initial size - 26.5 + 22.4 mm) weathered in cupric sulphate solution (0.2 M) for 12 hours.

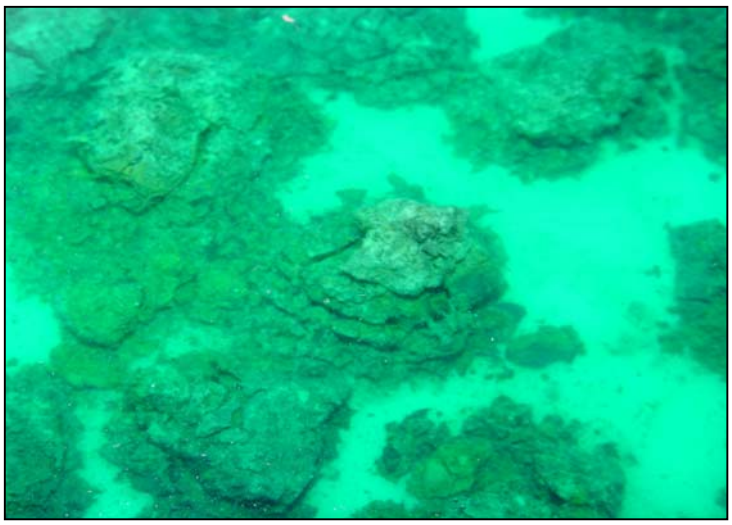

Figure 55. Visual appearance of Dutoitspan ore (initial size - 26.5 + 22.4 mm) weathered in cupric sulphate solution (0.2 M) for 24 hours.

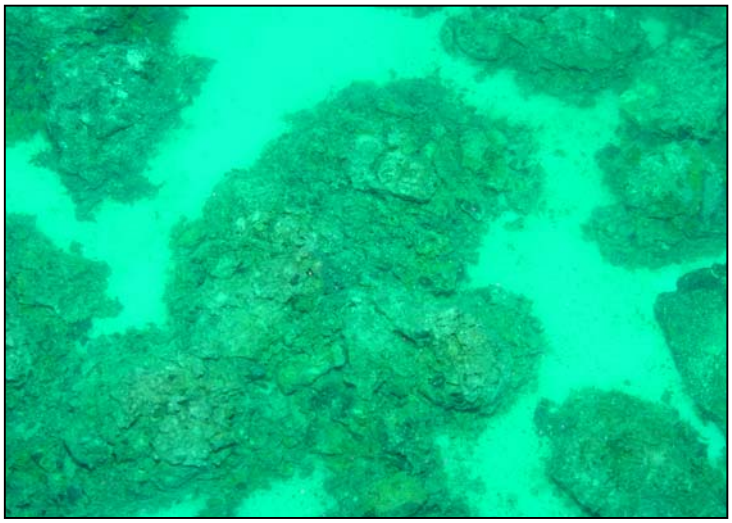

Figure 56. Visual appearance of Dutoitspan ore (initial size - 26.5 + 22.4 mm) weathered in cupric sulphate solution (0.2 M) for 6 days (144 hours).

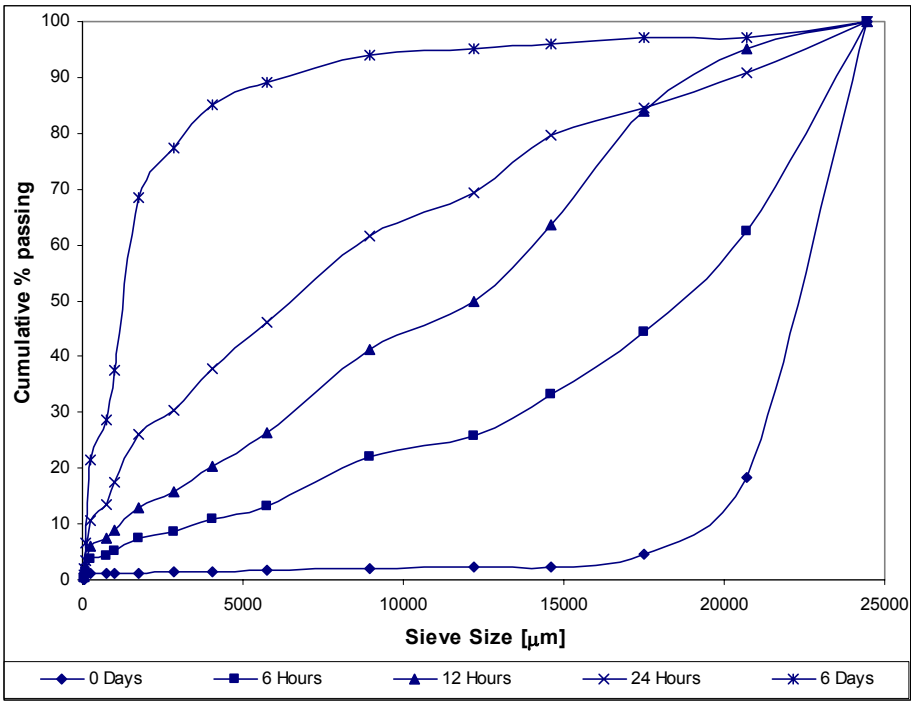

Figure 57. Weathering results from a 1.5 kg (initial size – 26.5 + 22.4 mm) Dutoitspan ore sample weathered in a 0.2 M cupric sulphate solution for 6, 12, 24 and 144 hours (6 days).

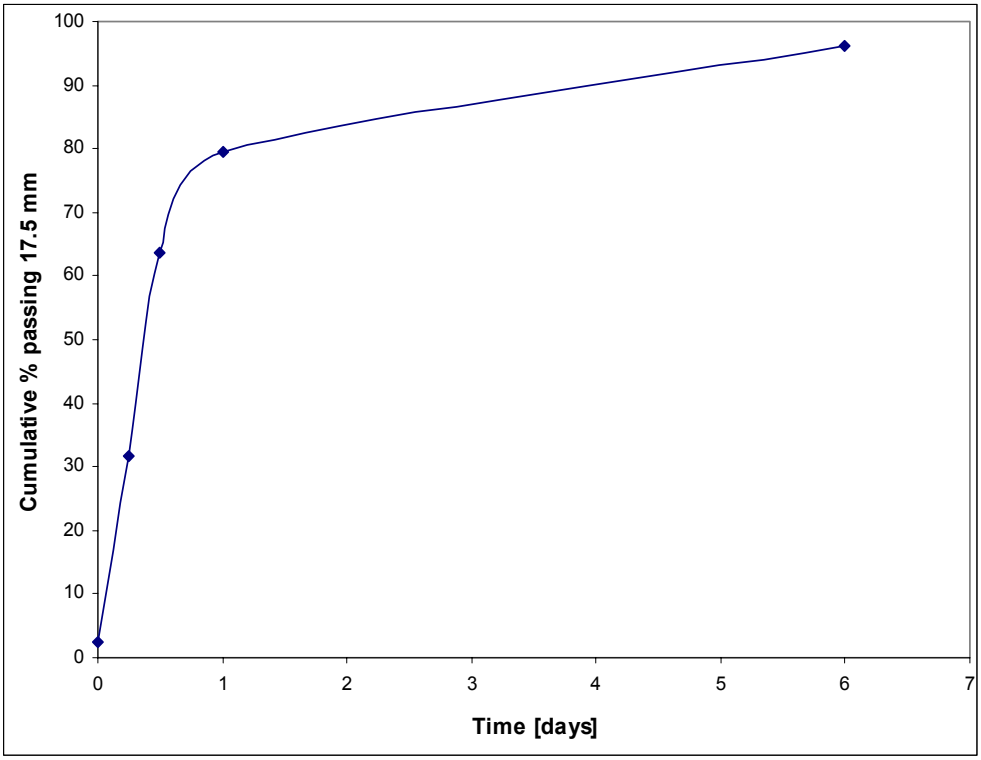

Figure 58. Results from the investigation of the time dependence of kimberlite weathering. Drawn from figure 57 as cumulative % passing 17.5 mm.

Results of time dependence tests using cupric suphate as weathering medium are shown in figures 57 and 58. Weathering is fast for the first 24 hours whereafter the rate decreases but does not seem to reach zero even in 6 days; this corresponds to the magnesium solution results. The results show that at this concentration of 0.2 M copper sulphate, 83 % of the weathering that took place over six days occurred within the first 24 hours.

Another test was done to investigate the effect of time, but the test was run for up to 30 days. The work was done with 250 – 300 g Dutoitspan kimberlite at 0.5 M copper concentration for 4 hours, 8 hours , 24 hours, 48 hours, 168 hours (7 days), 360 (15 days) and 720 hours (30 days). In this case a sample of – 16 + 13 mm kimberlite was used, as the -26 + 22.4 kimberlite fraction has all been utilised. The results are shown in figures 59 and 60. At a concentration of 0.5 M the weathering reached steady conditions after ~ 7 days. Again 80 % of the weathering took place in the first 24 hours. Comparison of figures 58 and 60 shows that concentration plays a role, which is discussed in the next section.

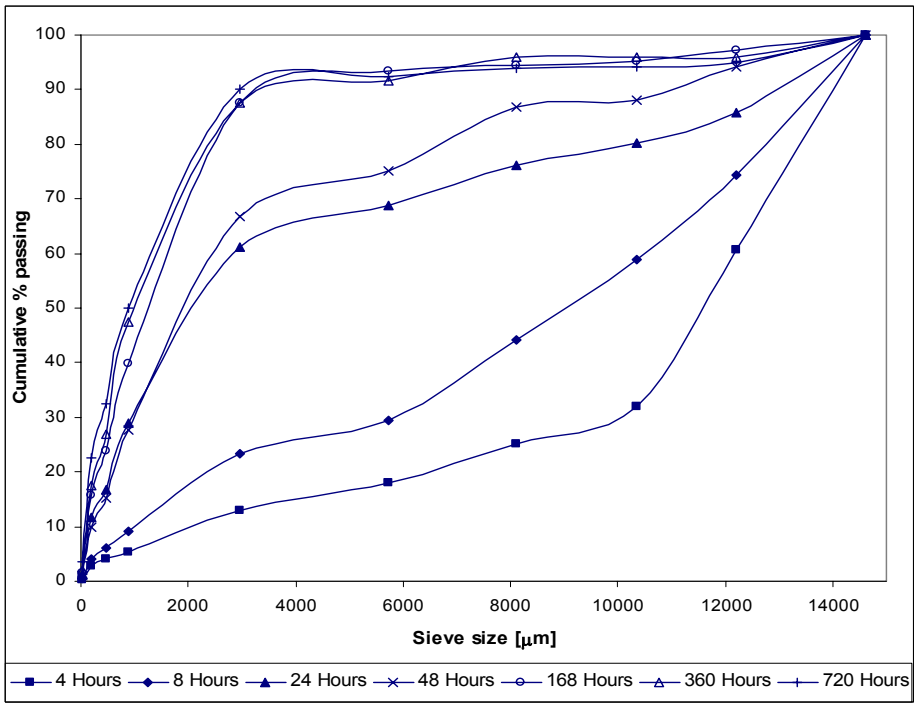

Figure 59. Weathering results from a 300 g (initial size – 16 + 13.2 mm) Dutoitspan ore sample weathered in a 0.5 M cupric sulphate solution for up to 30 days.

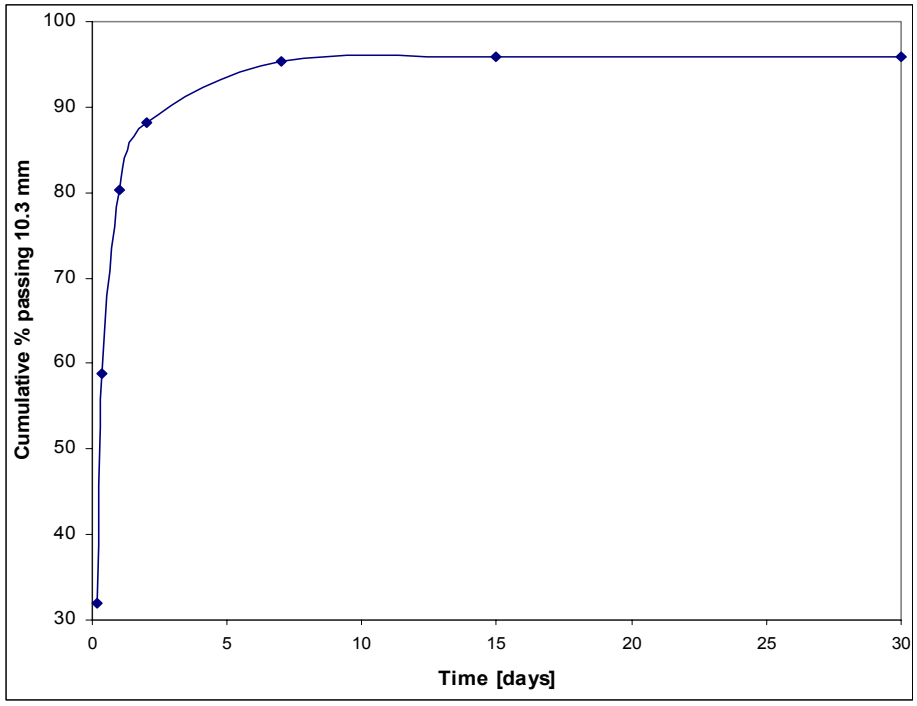

Figure 60. Results from the investigation of the time dependence of kimberlite weathering. Drawn from figure 59 as cumulative % passing 10.3 mm.

6.2.5.4 Influence of cation concentration on weathering

The influence of the cation concentration on accelerated weathering was tested in a cupric medium between 0.005 and 0.4 M concentration.

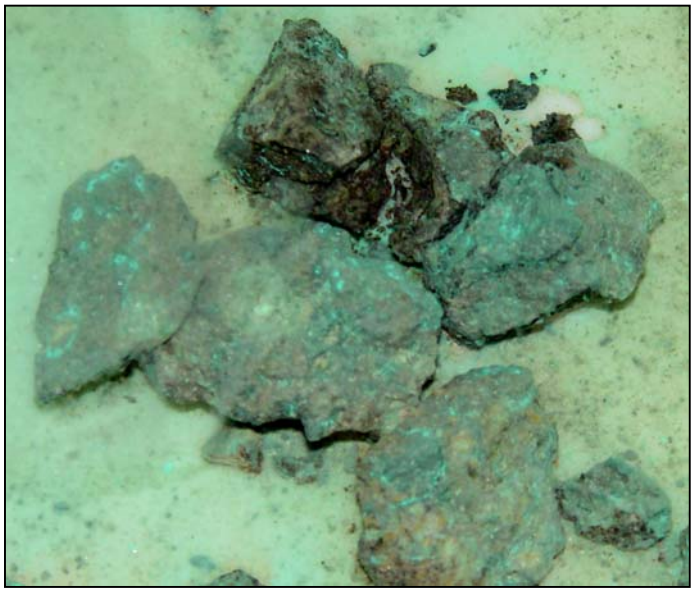

Figure 61. Visual appearance of Dutoitspan ore (initial size -26.5 + 22.4 mm) weathered in a 0.005 M cupric sulphate medium for 6 days.

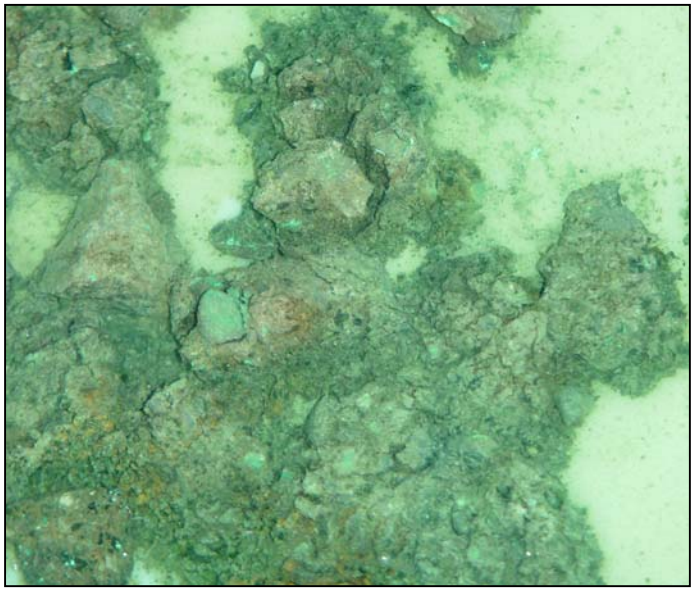

Figure 62. Visual appearance of Dutoitspan ore (initial size -26.5 + 22.4 mm) weathered in a 0.1 M cupric sulphate medium for 6 days.

Figure 63. Visual appearance of Dutoitspan ore (initial size -26.5 + 22.4 mm) weathered in a 0.4 M cupric sulphate media for 6 days.

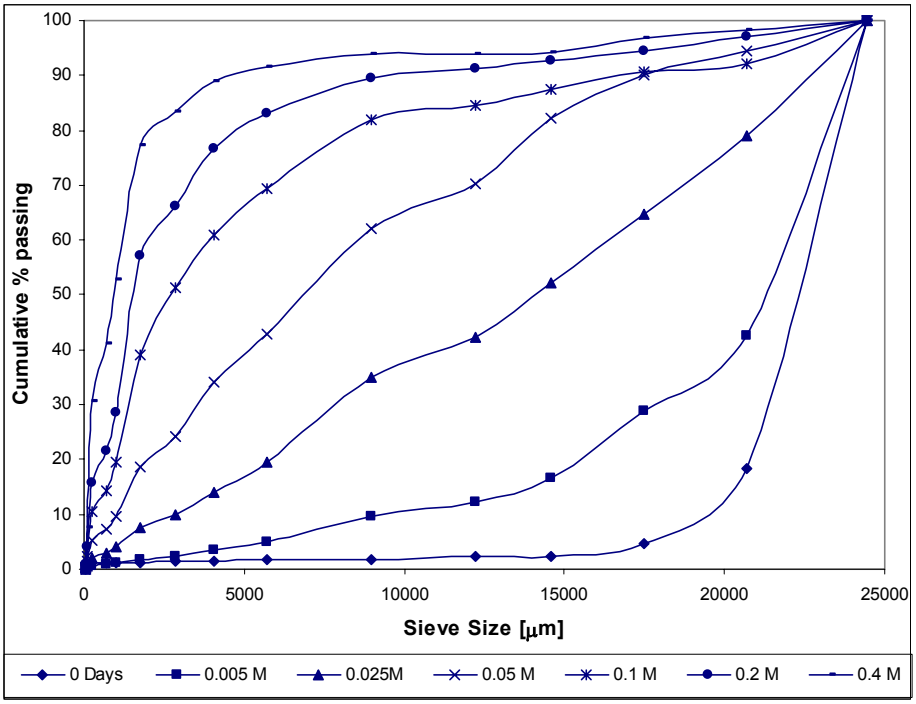

Figure 64. Results of the investigation to determine the influence of cation concentration. The tests were conducted on 1.5 kg of –26.5 +22.4 mm Dutoitspan ore. Copper sulphate concentrations were 0.005, 0.025, 0.05, 0.1, 0.2 and 0.4 M. The weathering time was constant at 6 days.

The influence of copper concentration on the efficiency of accelerated weathering was tested and results reported in figure 64 and 65. It is concluded from the tests that the concentration of cations is critical to the weathering of kimberlite. A very strong dependence is displayed up to 0.05 M whereafter the effect of concentration is less strong but still not negligible.

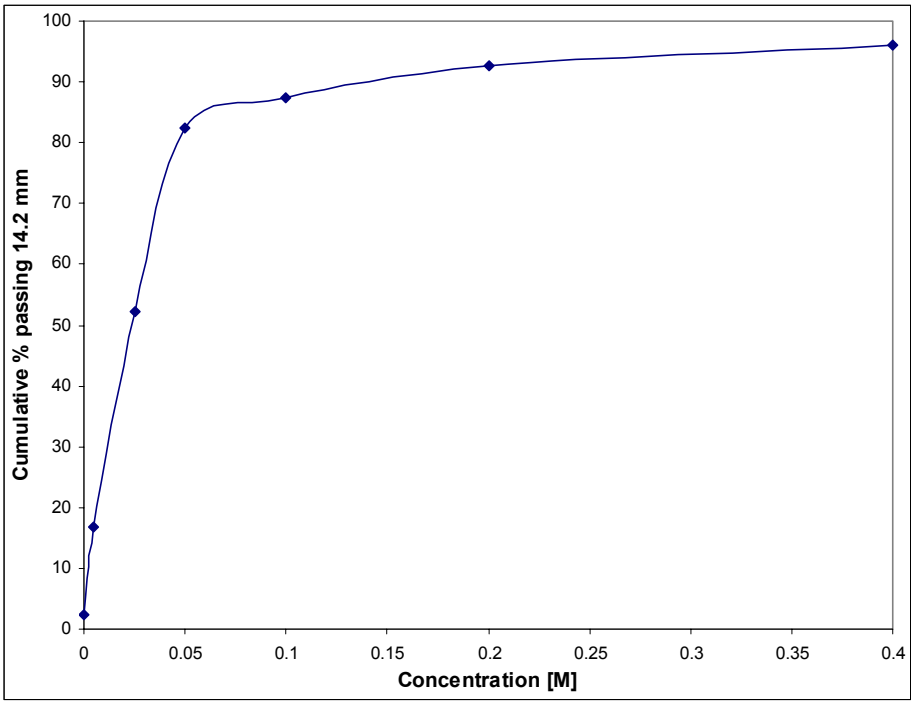

Figure 65. Weathering as a function of cation (cupric) concentration. The weathering is reported as the cumulative percent passing 14.2 mm from figure 64.

6.2.5.5 Influence of temperature on weathering

The influence of temperature was tested in a distilled water and magnesium chloride solution (0.2 M concentration) at 40 °C compared to room temperature (~ 20 °C). Results are shown in figure 66.

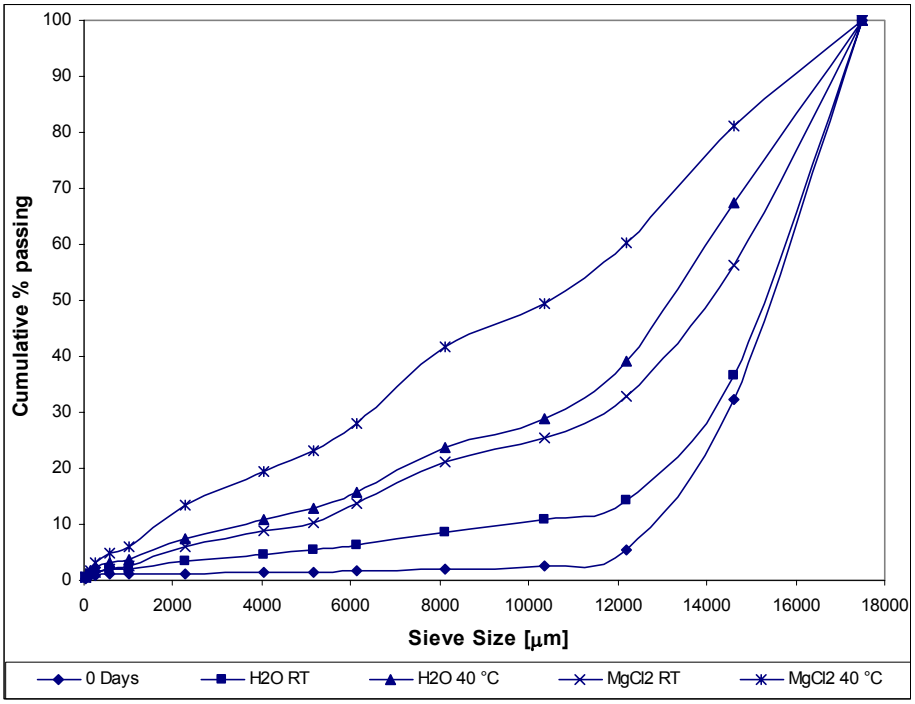

Figure 66. Results of the investigation of the influence of temperature on the weathering behaviour. The results include the standard test at room temperature and the standard test at 40 °C. The weathering tests in a 0.2 M $MgCl_2$ solution for 6 days at room temperature and 40 °C are also shown. All the tests were done on a 1.5 kg (initial size – 19 + 16 mm) Dutoitspan kimberlite sample.

Figure 66 shows the influence of higher temperature on the weathering process. The magnesium chloride solution was used as it shows limited accelerated weathering and therefore will allow for sensitive investigation of the effect of temperature. For the standard weathering test the higher temperature caused a 25 % increase in the cumulative mass % passing 12.2 mm. The influence of temperature is strong and comparable with that of cations in the weathering medium. The higher temperature combined with the magnesium chloride resulted in a further ~ 20 % increase in weathering over the room temperature magnesium chloride solution. The combination of 0.2 M $MgCl_2$ solution and 40 °C cause an increase of 55 % in the cumulative mass % passing at 12.2 mm compared to the unweathered material.

6.2.5.6 Influence of anions

The influence of anions was tested by comparing weathering results in a cupric chloride and cupric sulphate solution at 0.3 M for 6 days. From results shown in figure 67 it is concluded that the anion species does not influence the weathering process (an effect might be expected if the anion influences the solubility of the cation).

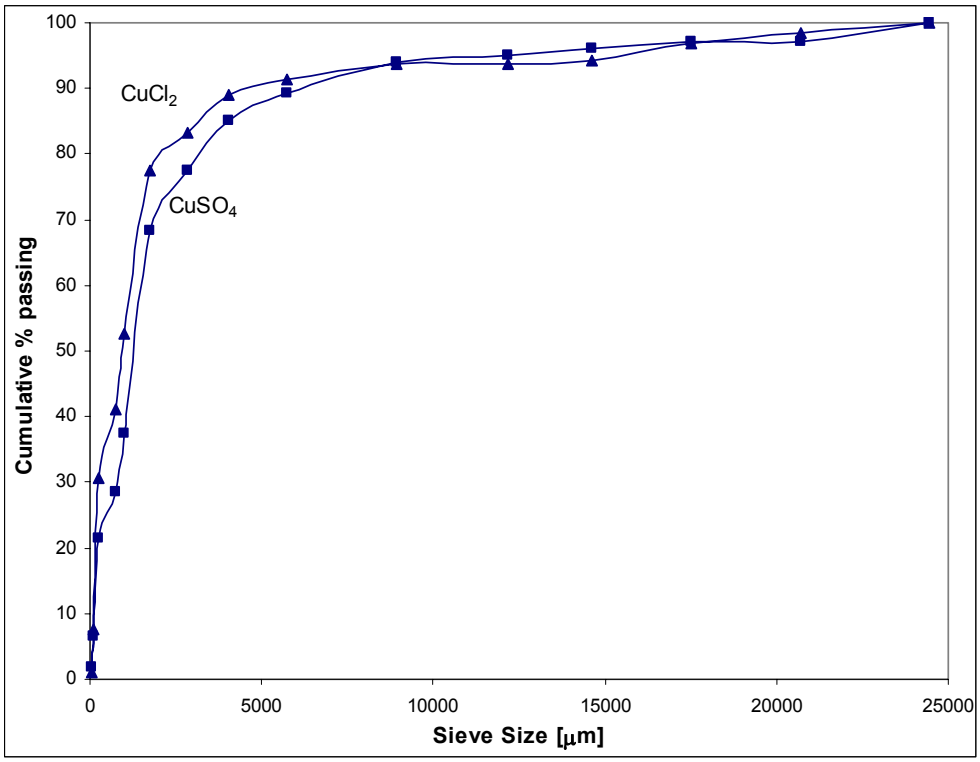

Figure 67. Results of tests to determine the influence of the type of anion on weathering. Tests conducted on a 1.5 kg -26.5 + 22.4 mm Dutoitspan ore sample at 0.3 M cupric chloride and cupric sulphate solution for 6 days.

6.2.5.7 Influence of particle size

The influence of particle size was determined using 4 size intervals weathered for 6 days in a 0.2 M $MgCl_2$ solution.

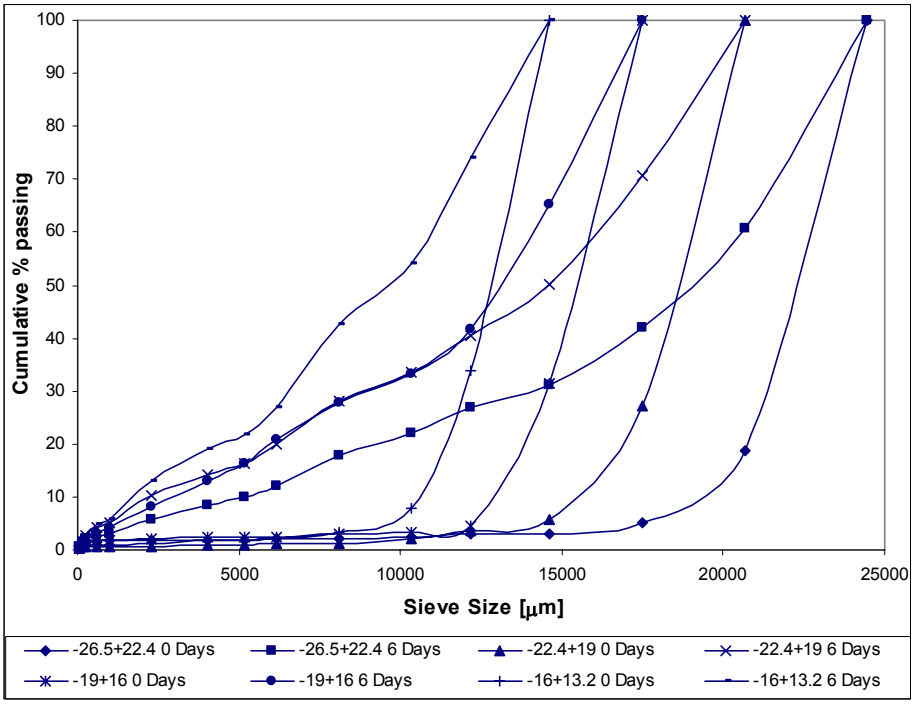

Figure 68. Results of the investigation to determine the influence of particle size. The tests were conducted in 0.2 M magnesium chloride solution for 6 days. The particle sizes used were –26.5 + 22.4, -22.4 + 19, -19 + 16 and -16 + 13.2 mm, using Dutoitspan ore.

The results are shown in figure 68 and comparative results in figure 69. The comparative results are shown at 70 % of the starting material size as this is the position in the size distribution curve where weathering is shown best. The conclusion from these results is that the starting size of the particles does not play a significant role in the efficiency of weathering. The starting particle sizes used in this test work are however similar in exposed surface area and work on finer size fractions (higher surface area) should be done for accurate conclusions.

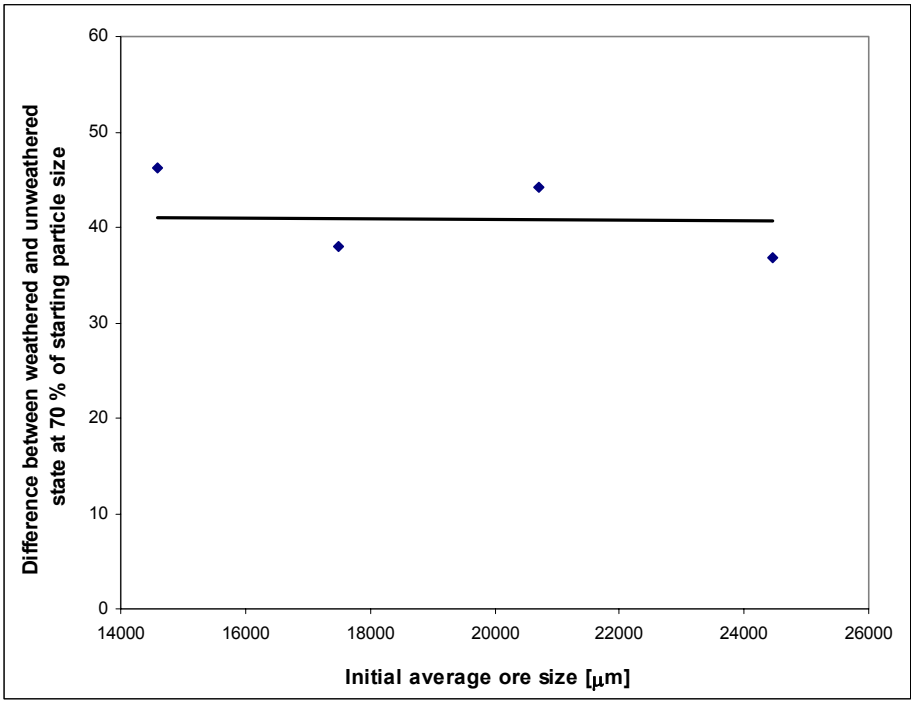

Figure 69. Results from the investigation of particle size. Comparison of the size distribution curves for the unweathered and weathered states at 70 % of the starting material size.

6.2.5.8 Influence of milling on weathering results

The usefulness of the autogeneous batch mill test was investigated and results are given in figure 70. The results show that the milling test does increase the size reduction after weathering. The milled sample seems to have less larger sized particles (> 15 mm) compared to the unmilled sample, which might be due to abrasion. Milling can increase the sensitivity of weathering tests especially in cases where small differences in weathering are investigated. With the copper medium the influence of weathering is so strong that the size degradation is large and no milling is required.

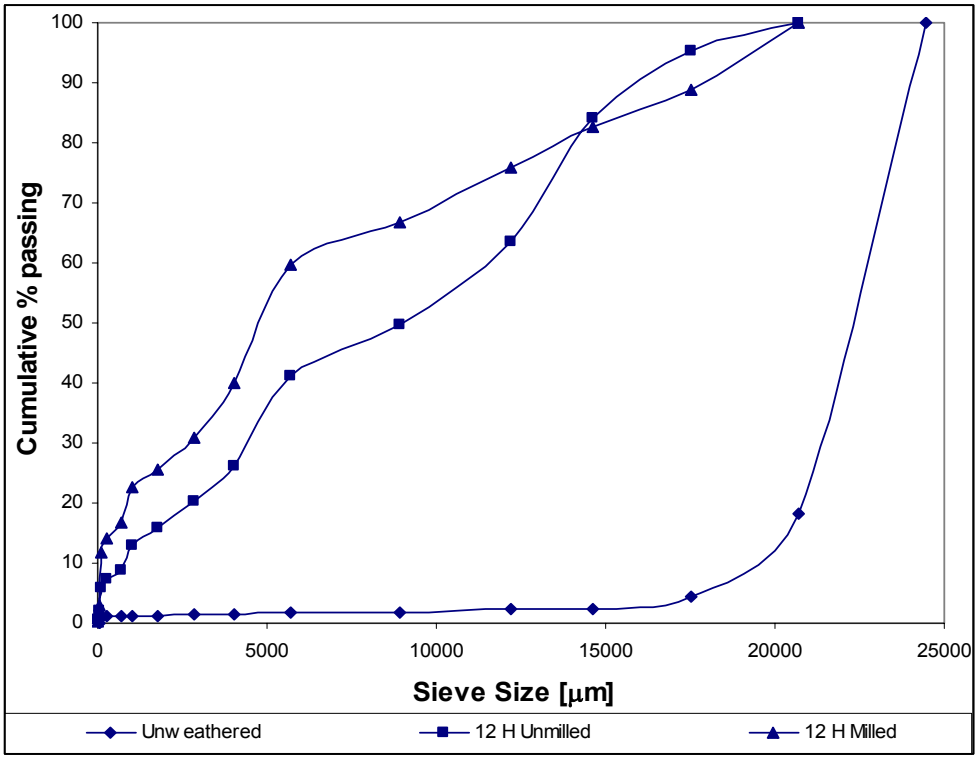

Figure 70. Investigation of the influence of milling on weathering tests. Weathering tests were performed in a 0.2 M cupric sulphate solution (initial size - 26.5 + 22.4 mm) Dutoitspan ore for 12 hours and the unmilled and milled sample product size distributions compared.

6.2.5.9 The effect of a stabilising cation vs. swelling cation

The effects of a potassium (stabilising cation) and copper (a swelling cation) on weathering were investigated. The test utilised 200 - 250 g of Dutoitspan kimberlite (initial size - 16 + 13.2 mm) weathered in a 0.5 M potassium solution for 4, 8 and 144 hours. The tests were repeated in a 0.5 M copper solution at 4, 8, 24, 48, 168 (7 days) and 360 hours (15 days). The weathering results in the potassium medium are shown in figure 71. The results for copper are shown in figure 70. Photos of both products are shown in figure 73.

These results show that cations can be utilised to influence the weathering behaviour of kimberlite by either increasing the extent of weathering as with copper cations or alternatively decreasing the extent of weathering as is the case with potassium cations. It is compared in this section to show the extremes of the influence of cations on weathering behaviour.

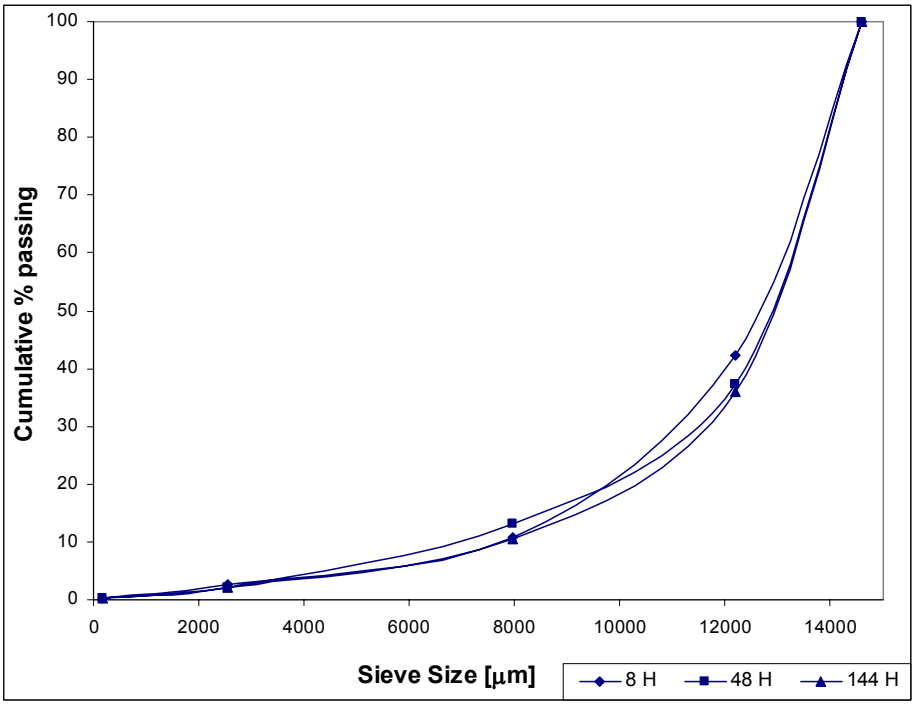

Figure 71. Investigation of the influence of potassium on weathering tests. Weathering tests were performed on a 250 - 300 g -16 + 13.2 mm Dutoitspan kimberlite in a 0.5 M potassium solution for 8, 48 and 144 hours.

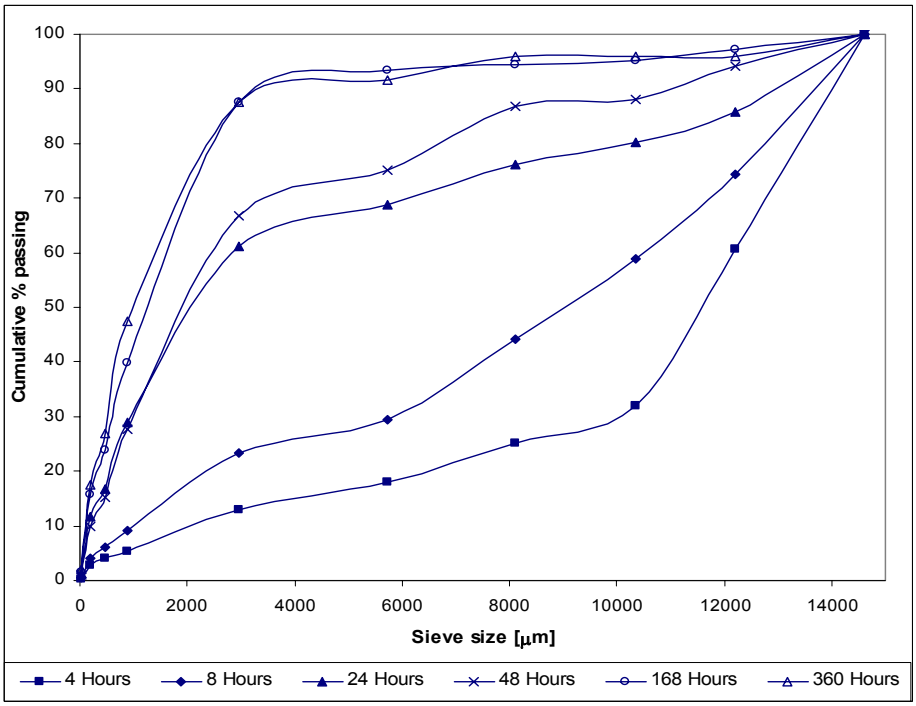

Figure 72. Investigation of the influence of copper on weathering tests. Weathering tests were performed on a 250 - 300 g -16 + 13.2 mm Dutoitspan kimberlite in a 0.5 M copper solution for up to 15 days.

Figure 73. Comparison of the effect of copper (swelling cation) on the left and potassium (stabilising cation) on the right and their effect on the weathering of kimberlite (photos taken after 6 days for potassium and 15 days for copper medium).

6.2.6 Venetia

The samples received from Venetia (- 26.5 + 22.4 mm) were weathered in a 0.05 M cupric sulphate solution for 6 days. The unweathered and weathered samples are shown for comparative purposes (figures 74 – 81).

K1 Hypabyssal North East

Figure 74. Venetia K1 Hypabyssal North East kimberlite unweathered (left) compared to the weathered product (right). Weathering was done in a 0.05 M cupric sulphate solution for 6 days.

K1 Hypabyssal South

Figure 75. Venetia K1 Hypabyssal South kimberlite unweathered (left) compared to the weathered product (right). Weathering was done in a 0.05 M cupric sulphate solution for 6 days.

K1 TKB East

Figure 76. Venetia K1 TKB East kimberlite unweathered (left) compared to the weathered product (right). Weathering was done in a 0.05 M cupric sulphate solution for 6 days.

K2 South

Figure 77. Venetia K2 South kimberlite unweathered (left) compared to the weathered product (right). Weathering was done in a 0.05 M cupric sulphate solution for 6 days.

K2 North East

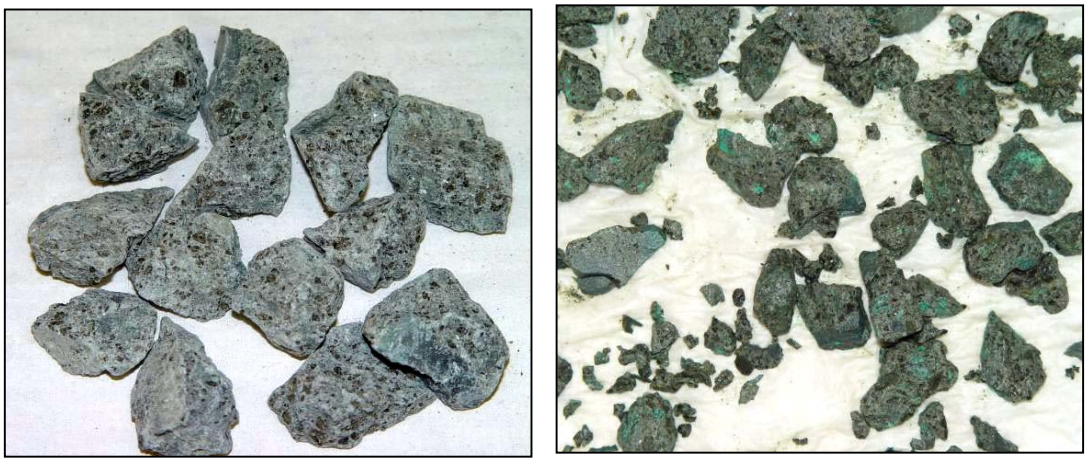

Figure 78. Venetia K2 North East kimberlite unweathered (left) compared to the weathered product (right). Weathering was done in a 0.05 M cupric sulphate solution for 6 days.

K2 West

Figure 79. Venetia K2 West kimberlite unweathered (left) compared to the weathered product (right). Weathering was done in a 0.05 M cupric sulphate solution for 6 days.

K8

Figure 80. Venetia K8 unweathered (left) compared to the weathered product (right). Weathering was done in a 0.05 M cupric sulphate solution for 6 days.

Red Kimberlite

Figure 81. Venetia Red kimberlite unweathered (left) compared to the weathered product (right). Weathering was done in a 0.05 M cupric sulphate solution for 6 days.

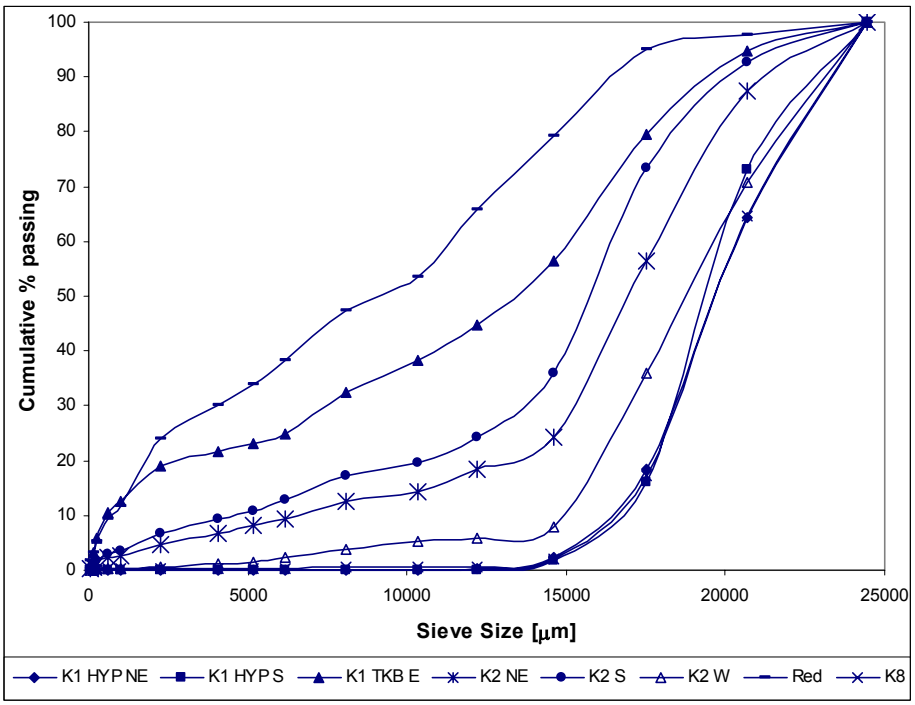

Figure 82. Results of weathering tests performed on Venetia kimberlites (- 26.5 + 22.4 mm) in a 0.05 M cupric sulphate solution for 6 days.

Both hypabyssal ores showed no weathering at all (figure 82), and both contained no swelling clay and had low CEC values, in line with the suggestion that the presence of swelling clay is the parameter that renders a kimberlite amenable to weathering. K8, although not classified as a kimberlite, also contains no swelling clay and has a correspondingly low CEC value, with

no weathering observed. Kimberlites with no swelling clay are concluded to be resistant to weathering even under aggressive conditions.

The K2W kimberlite displayed some signs of weathering with 8 % passing 14.6 mm after weathering. The K2NE kimberlite ranked next with 25 % passing 14.6 mm after weathering, followed by K2S with 36 %, K1 TKB E with 56 % and Red kimberlite with 80 %. The swelling clay content was the same (at 40 %) for the K1 TKB E, K2S and Red kimberlites even though these kimberlites behaved differently during weathering. Therefore, while the swelling clay content does give an indication of the expected weathering behaviour, it cannot give a fully quantitative prediction of weathering. This might be related to the inherent inaccuracy of the semi-quantitative phase determination by XRD analysis. In addition, when a kimberlite is rendered weatherable by the presence of swelling clay, other factors, such as the cations in the ore and weathering solution (and the associated hydration and complexation properties of the cations) play a role, as these will determine the amount of swelling.

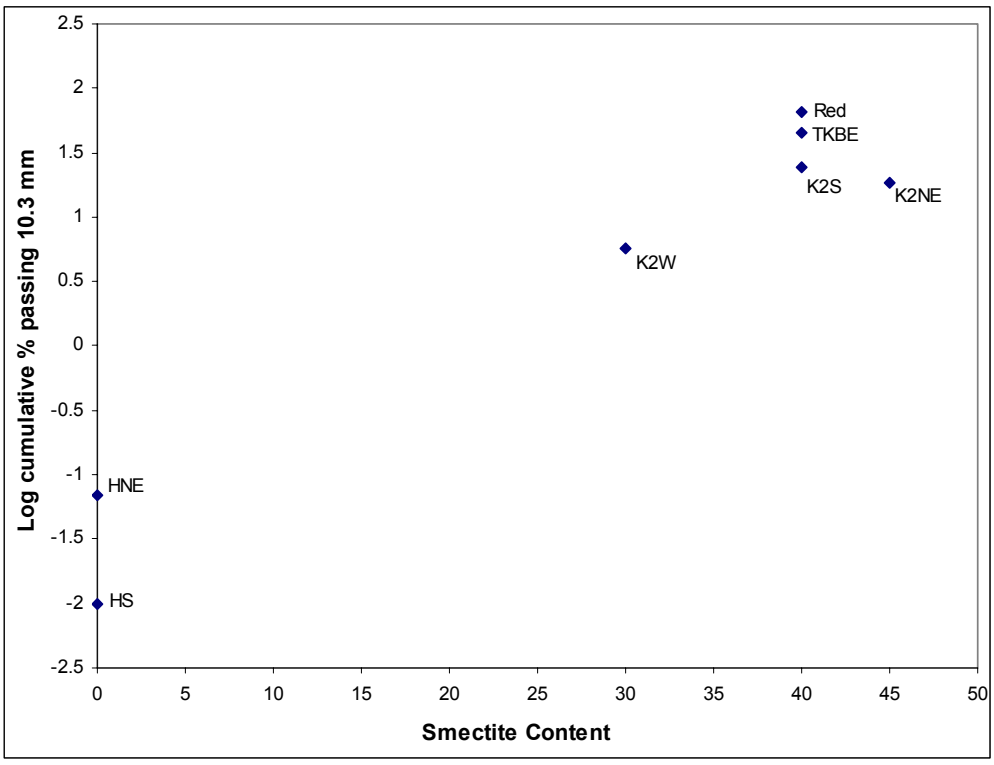

Figure 83a. Comparing weathering results with the smectite content of Venetia ores. Weathering is shown as log cumulative % passing at 10.3 mm from figure 82 (6 days' weathering in 0.05 M copper sulphate).

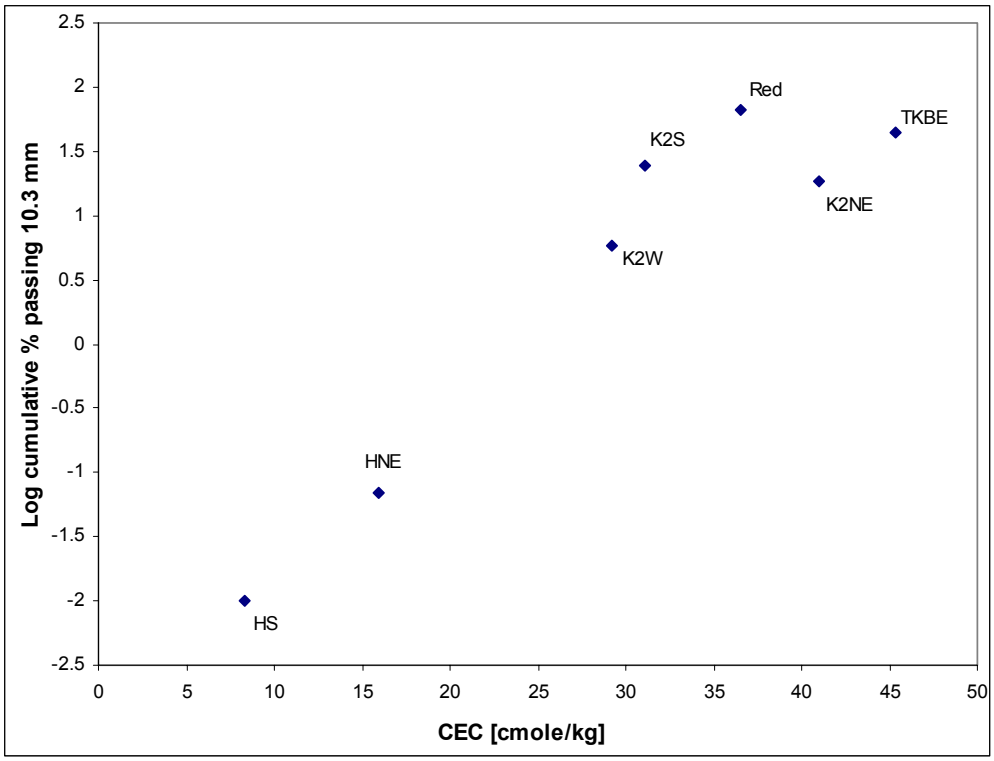

Figure 83b. Comparing weathering results with cation exchange capacity of Venetia ores. Weathering is shown as log cumulative % passing at 10.3 mm from figure 82 (6 days' weathering in 0.05 M copper sulphate).

The weathering behaviour correlates well with both the cation exchange capacity and the swelling clay content (figure 83 a and b). However, determination of the swelling clay content is tedious and expensive. CEC is therefore the preferred parameter to characterise kimberlitic ores and their weathering behaviour.

6.3 Repeatability of results

The repeatability of the experimental results was tested by repeating test work in triplicate at 0.025, 0.1 and 0.5 M copper concentration. The tests were done on 300 g -16 +13.2 Dutoitspan kimberlite for 2 days. The results (figure 84) show that all results consistently fall in a 7 % interval. Statistical analysis of the results is shown in table 24, which includes the standard deviation and the 95 % confidence limits. The largest standard deviation value is 3.8 %. The largest difference between the 95 % confidence lower and upper limit is 19 %. This could be improved by increasing the number of tests.

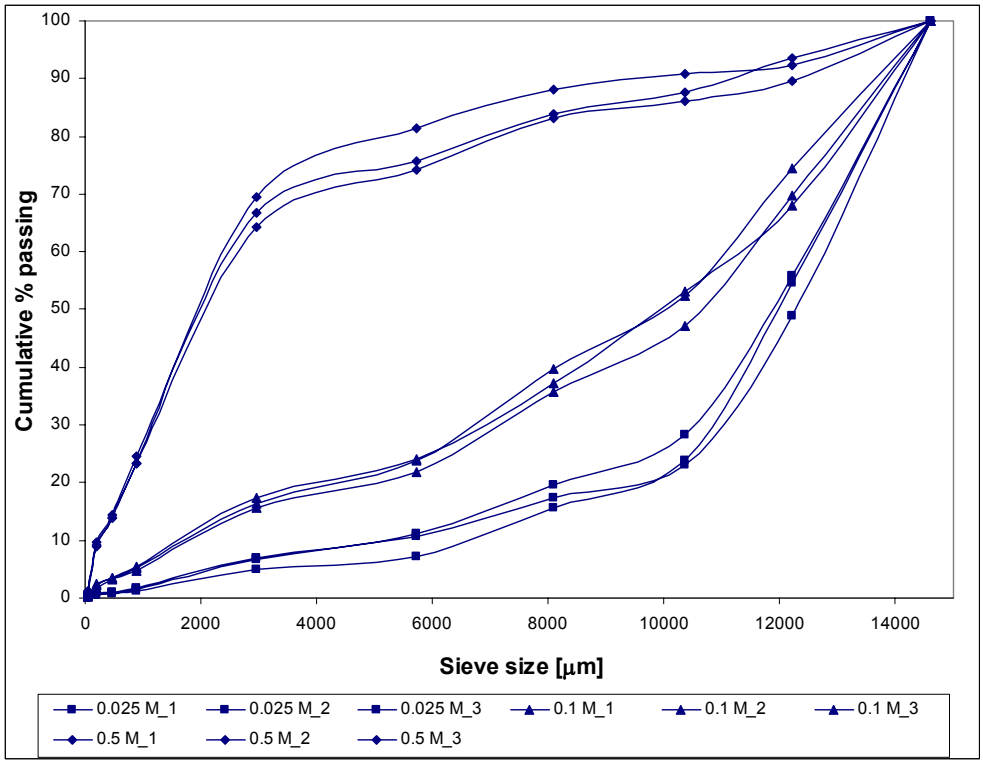

Figure 84. Repeatability of the weathering tests were evaluated by triplicate tests at 0.025, 0.1 and 0.5 M copper concentration. Tests were done on 300 g, -16 + 13.2 mm Dutoitspan kimberlite.

Table 24. Statistical evaluation of repeatability results.

2 Days 0.025 M Cu				
Ave particle size (μm)	Mean cum % passing	Standard deviation	95 % confidence lower limit	95 % Confidence higher limit
14600	100.00	0.00	100.00	100.00
12200	53.12	3.73	43.85	62.39
10350	25.12	2.82	18.11	32.14
8100	17.51	2.00	12.55	22.47
5725	9.59	2.16	4.22	14.96
2965	6.26	1.08	3.57	8.95
890	1.48	0.28	0.79	2.18
467.5	0.90	0.17	0.48	1.33
205	0.58	0.11	0.31	0.85
37.5	0.05	0.00	0.05	0.05
2 Days 0.1 M Cu				
Ave particle size (μm)	Mean cum % passing	Standard deviation	95 % confidence lower limit	95 % Confidence higher limit
14600	100.00	0.00	100.00	100.00
12200	70.73	3.38	62.34	79.11
10350	50.79	3.25	42.71	58.87
8100	37.53	1.94	32.72	42.34
5725	23.18	1.17	20.28	26.08
2965	16.45	0.82	14.42	18.49
890	5.11	0.28	4.41	5.81
467.5	3.38	0.09	3.15	3.61
205	2.21	0.31	1.44	2.97
37.5	0.39	0.03	0.32	0.45
2 Days 0.5 M Cu				
Ave particle size (μm)	Mean cum % passing	Standard deviation	95 % confidence lower limit	95 % Confidence higher limit
14600	100.00	0.00	100.00	100.00
12200	91.80	2.08	86.64	96.97
10350	88.17	2.48	82.01	94.32
8100	85.03	2.68	78.36	91.69
5725	77.09	3.80	67.65	86.53
2965	66.79	2.69	60.11	73.46
890	23.70	0.80	21.71	25.68
467.5	14.07	0.28	13.36	14.77
205	9.28	0.43	8.23	10.34
37.5	1.05	0.09	0.84	1.27

Table 25. ICP analysis results of copper weathering solution as a function of time.

0.025 M Copper						
Time	Cu	Na	K	Mg	Ca	Al
[hours]	mmol/l	mmol/l	mmol/l	mmol/l	mmol/l	mmol/l
0	23.60	0.57	0.069	0.014	0.052	0.000
3	15.11	15.66	0.921	0.041	0.127	0.000
24	3.93	38.28	1.662	0.086	0.187	0.000
48	1.57	41.76	1.816	0.103	0.195	0.000
72	0.77	42.19	1.842	0.111	0.195	0.000
168	0.41	43.50	1.944	0.132	0.187	0.000
360	0.007	43.50	2.072	0.156	0.217	0.000
720	0.004	47.85	2.200	0.202	0.185	0.000
0.1 M Copper						
Time	Cu	Na	K	Mg	Ca	Al
[hours]	mmol/l	mmol/l	mmol/l	mmol/l	mmol/l	mmol/l
0	95.99	0.48	0.02	0.02	0.13	0.005
3	83.40	24.79	1.56	0.13	0.47	0.009
24	51.93	69.60	3.84	0.45	1.37	0.089
48	39.34	82.65	4.35	1.03	1.90	0.010
72	34.62	87.00	5.63	0.86	2.30	0.025
168	25.18	100.04	5.63	1.73	2.74	0.141
360	18.88	104.39	6.14	2.43	4.24	0.289
720	14.48	104.39	6.65	3.17	6.24	0.070
0.5 M Copper						
Time	Cu	Na	K	Mg	Ca	Al
[hours]	mmol/l	mmol/l	mmol/l	mmol/l	mmol/l	mmol/l
0	448.49	0.43	0.00	0.02	0.09	0.01
3	432.76	28.71	2.10	0.31	1.02	0.05
24	393.42	95.69	7.16	2.39	5.49	0.27
48	379.25	108.74	8.44	3.13	8.73	0.48
72	372.96	108.74	8.18	3.54	10.48	0.52
168	346.21	113.09	9.72	6.58	16.72	2.85
360	336.76	113.09	9.21	9.87	21.21	1.07
720	330.47	121.79	10.49	14.81	27.45	2.82

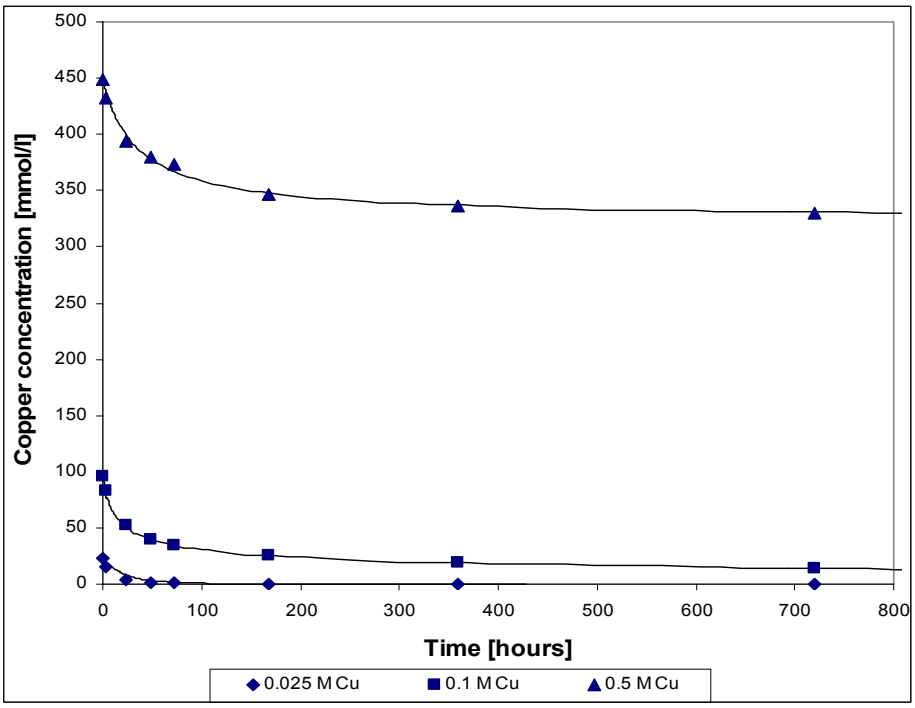

Figure 85. ICP analysis results displaying the steady decrease of the concentration of copper in the weathering solution as a function of time. The lines are fitted curves for simple n^{th} - order kinetics (parameters of curve fits in table 25).

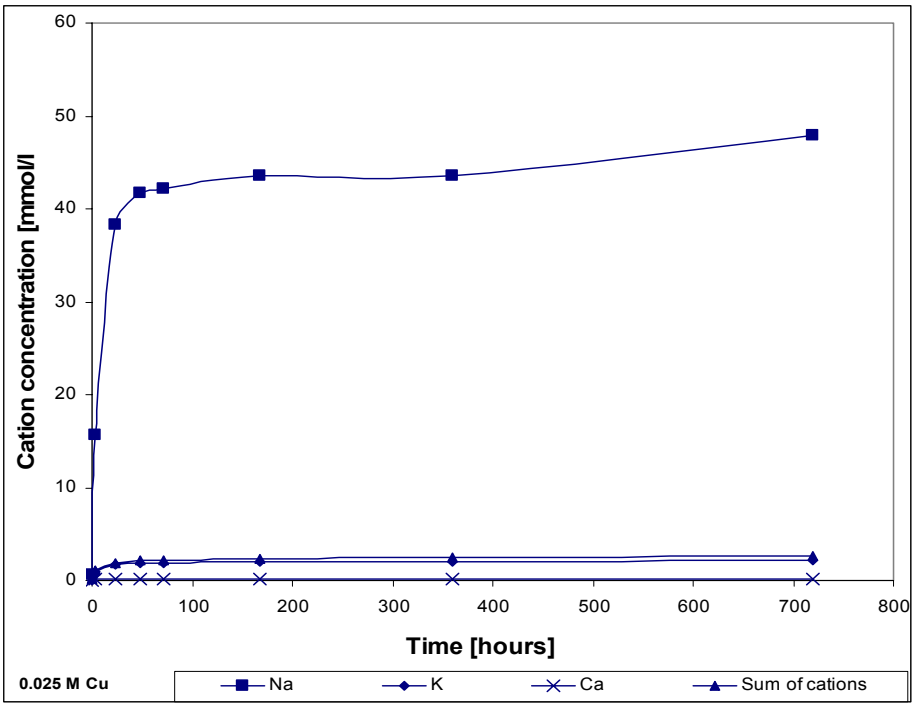

Figure 86. ICP analysis results displaying the release of sodium, potassium, calcium and the sum of minor cations (K^+, Ca^{2+}, Mg^{2+} and Al^{3+}) from the kimberlite into the 0.025 M copper solution.

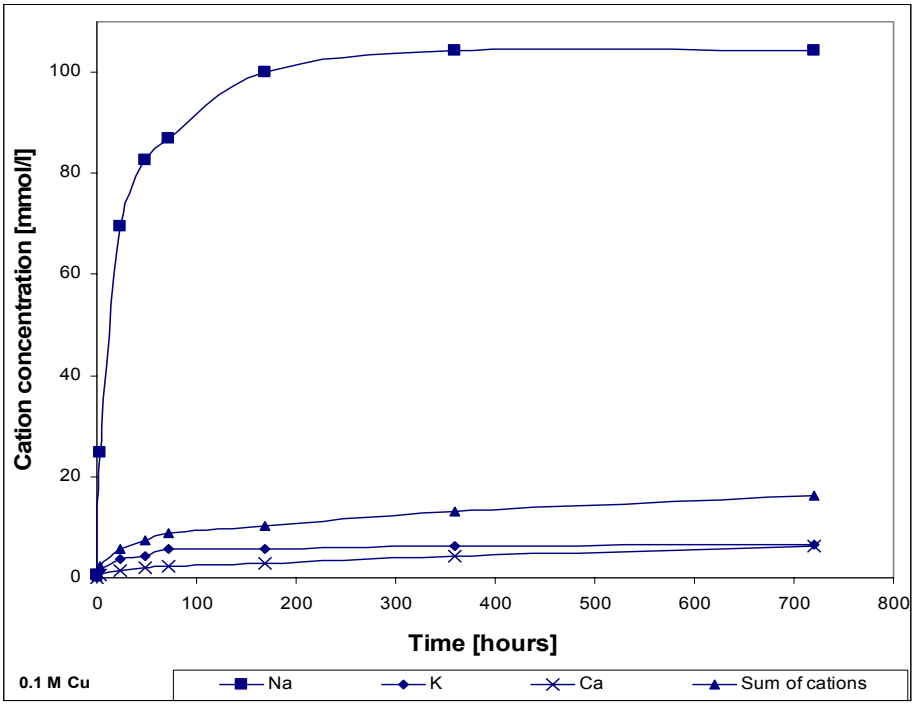

Figure 87. ICP analysis results displaying the release of sodium, potassium, calcium and the sum of minor cations (K^+, Ca^{2+}, Mg^{2+} and Al^{3+}) from the kimberlite into the 0.1 M copper solution.

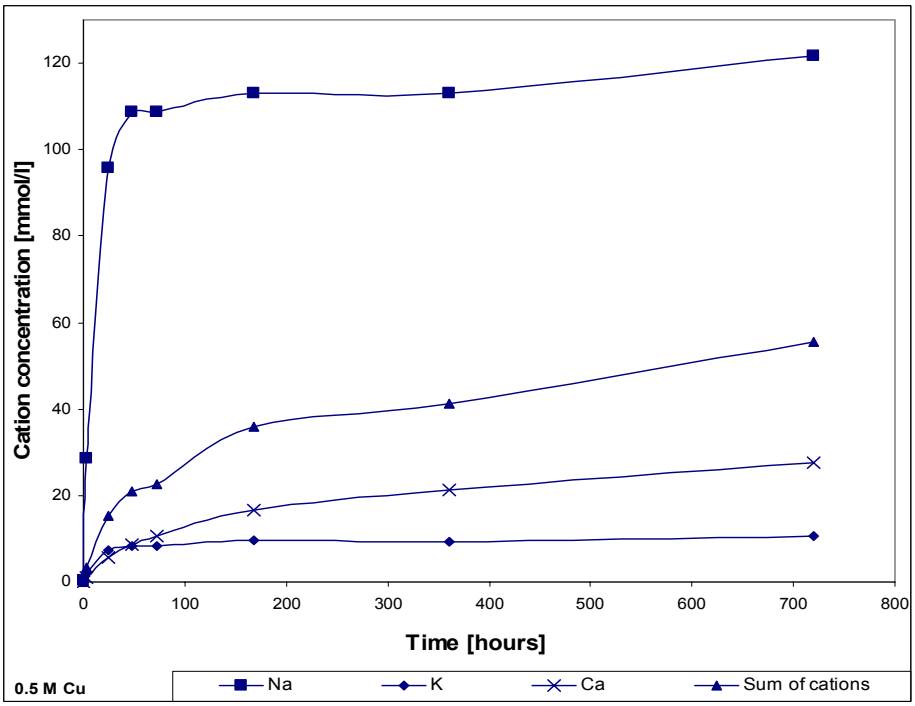

Figure 88. ICP analysis results displaying the release of sodium, potassium, calcium and the sum of minor cations (K^+, Ca^{2+}, Mg^{2+} and Al^{3+}) from the kimberlite into the 0.5 M copper solution.

6.4 Kinetic evaluation of cation exchange

Cupric Medium

The kinetics of the cation exchange reaction was investigated by utilising 300 g of Dutoitspan kimberlite (-16 + 13 mm) weathered in 0.025, 0.1 and 0.5 M cupric chloride solutions at room temperature (20 °C) with 1 L weathering solution. The Dutoitspan kimberlite showed medium weatherability compared to the other kimberlites (see section 6.2.5). Samples of the solution were removed (~ 50 ml) at 0, 4 hours, 24 hours, 48 hours, 72 hours, 168 hours (7 days), 360 hours (15 days) and 720 hours (30 days) for ICP analysis to follow the uptake of copper by the kimberlite. The release of other cations from the kimberlite into the solution was monitored simultaneously. The ICP results are given in table 25 and include the concentration of copper, sodium, calcium, potassium, magnesium and aluminium. The decrease in the concentration of copper in the three solutions is shown in figure 85. The decrease in copper concentration is rapid initially and then the reaction becomes slower at around 7 days; thereafter the concentration changes very little. The expected initial concentrations compared well with the analyses for the 0.025 and 0.1 M concentrations but not for the 0.5 M concentration. The reason for the difference in initial concentration could be the fact that the samples removed initially were kept in storage and sent for analysis with the other samples taken up to 30 days later. This could results in minor precipitation of copper sulphate, especially for the high concentrations. In some cases small flakes could be observed at the bottom of the sample holder.

The increase in sodium, potassium, calcium and sum of minor cations (the total of potassium, calcium, magnesium and aluminium) are shown in figure 86 for the 0.025 M copper solution, figure 87 for the 0.1 M copper solution and figure 88 for the 0.5 M copper solution. In the 0.025 M solution it is essentially only sodium that is replaced from the kimberlite (up to ~ 48 mmol/l) and the sum of minor cations remains lower at ~ 2.6 mmol/l. In the 0.1 M copper solution the amount of sodium replaced from the kimberlite is considerably higher (~ 104 mmol/l) but the concentration of other cations that are replaced is also significant (sum of minor cations ~ 16 mol/l). The sodium concentration for the 0.5 M copper solution only increases up to ~ 122 mmol/l, but the concentration of the other cations increases significantly to ~ 56 mmol/l. This increase in concentration of other cations was primarily due to calcium and potassium that were being replaced from the kimberlite.

The release of sodium from the kimberlite into the three copper solutions is compared in figure 89, and also the sum of other cations in figure 90. It is concluded that sodium is the cation most easily replaced from the kimberlite. Initially with the increase in copper concentration from 0.025 to 0.1 M, the release of sodium into the solution is increased from 48 to 104 mmol/l at long times. The further increase in copper concentration does not increase the sodium concentration in solution drastically. The sum of minor cations (shown in figure 90) for the different copper solutions, show that the sum of minor cations for the 0.025 M solution is relatively low (2.6 mmol/l) which is increased to around 16 mmol/l for the 0.1 M copper solution and drastically increased to 56 mmol/l for the 0.5 M copper solution. Therefore at low weathering cation concentration it is primarily sodium that is replaced from the kimberlite, but as the concentration of cations in the weathering solution increases, so does the driving force for replacing other cations as well. Sodium is the smallest hydrated cation present in the kimberlite and the hydration energy is not as large as for di- or trivalent cations. Sodium is therefore assumed to be the most easily replaced although the quantities of different cations present in the kimberlite should also influence the observed cation exchange process. Equilibrium exchange behaviour from literature is usually done on a single cation saturated clay and usually do not contain different cations as in this present case. Grim (1968) showed the selectivity order on Ba saturated clay as $Na^{+} < K^{+} < Mg^{2+} < Ca^{2+}$. This agrees with the observed behaviour that sodium is the most easily replaced cation.

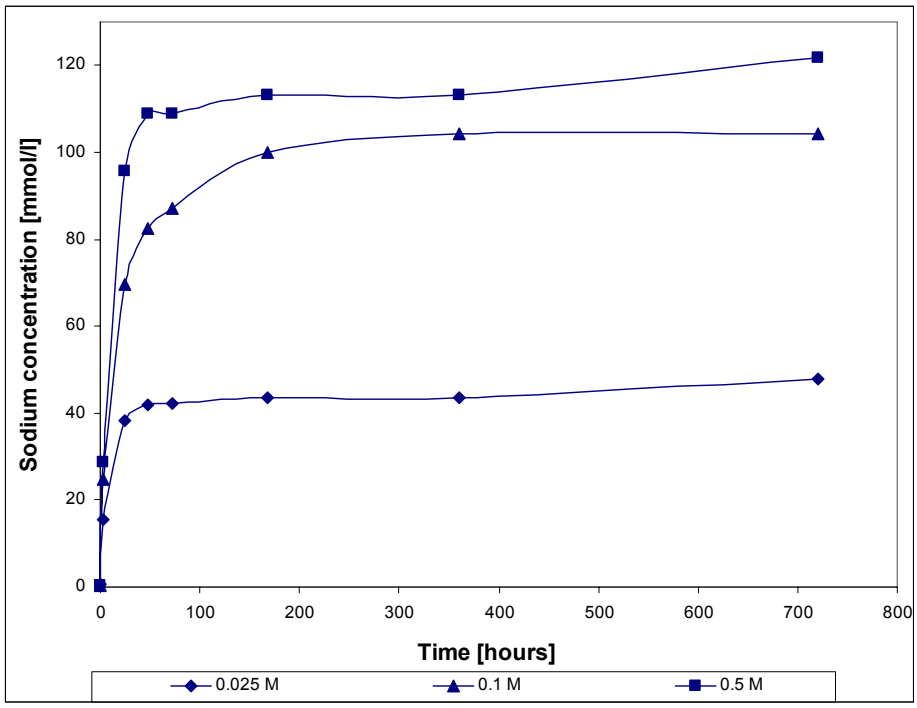

Figure 89. ICP analysis results displaying the release of sodium from the kimberlite into the solution at 0.025, 0.1 and 0.5 M copper concentration.

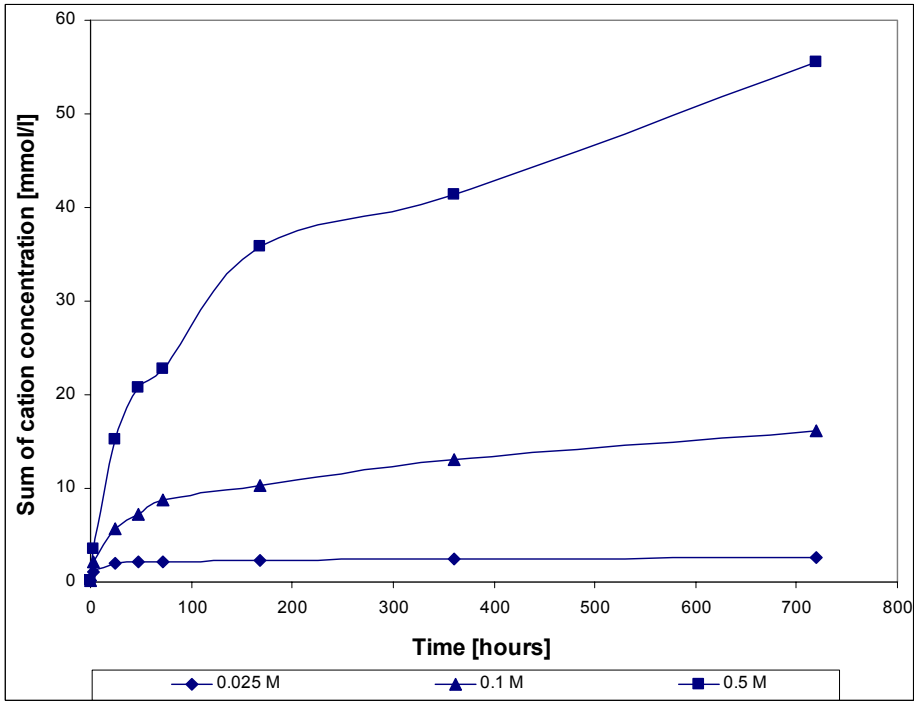

Figure 90. ICP analysis results displaying the release of the sum of other cations (K^+, Ca^{2+}, Mg^{2+} and Al^{3+}) from the kimberlite into the solution at 0.025, 0.1 and 0.5 M copper concentration.

The following simple n^{th}-order kinetic equation was used to fit the data for the change of copper concentration with time:

$$dC/dt = -k(C-C_\infty)^n \quad (32)$$

where C is the concentration in solution, k the rate constant, n the apparent reaction order, and C_∞ the equilibrium concentration. The integrated form of this equation, assuming C_∞, k and n to be constant with time, is as follows:

$$(C- C_\infty)^{(1-n)} – (C_0-C_\infty)^{(1-n)} = kt(n-1) \quad (33)$$

This equation was written with time as the subject, and fitted to the experimental data (measured concentrations at different times) by using the curve-fitting facility of the package SigmaPlot. The values of k, n, R^2 and the standard error for the three cases are given in table 26. The fitted curves are shown in figure 85.

Table 26. Results of fitting kinetic equation 33 to weathering data.

Variable	Coefficient	Std. Error
0.025 M		
C_o (mmol/l)	23.6	-
C_∞(mmol/l)	0.0042	1.57E-06
k	0.0316	0.0002
n	1.1342	0.0014
R^2	0.9806	-
0.1 M		
C_o (mmol/l)	96.0	-
C_∞(mmol/l)	0.3382	0.6785
10^7k	6.6642	5.5389
n	3.5313	0.0975
R^2	1.0000	
0.5 M		
C_o (mmol/l)	448.5	
C_∞(mmol/l)	322.2862	2.4187
10^4k	0.9486	2.0710
n	2.1790	0.2613
R^2	0.9988	

A graphical method was also used, plotting dC/dt against $(C-C_\infty)$ on logarithmic axes. A plot of log dC/dt vs log $|C-C_\infty|$ will enable calculation of n and k. The C_∞ values calculated from the Sigmaplot curve fits were used (table 26). The results are shown in figure 91 for the 0.025 M copper solution, figure 92 for 0.1 M copper solution and figure 93 for the 0.5 M copper solution. Fitted values of k and n are given in table 27.

dC/dt was determined by straight lines through to the data for the first and last pair of datapoints in each set. For the datapoints in between these, a parabola was fitted to every three consecutive datapoints and the differential of this parabola used to find dC/dt at the central datapoint.

Table 27. Results of graphical fitting kinetic equation 32 to weathering data.

Copper concentration [M]	Equation of line	n	k
0.025	y=1.112x – 1.235	1.11	5.82E-2
0.1	y=3.409x – 5.936	3.41	1.159E-6
0.5	y=2.261x – 4.094	2.26	8.059E-5

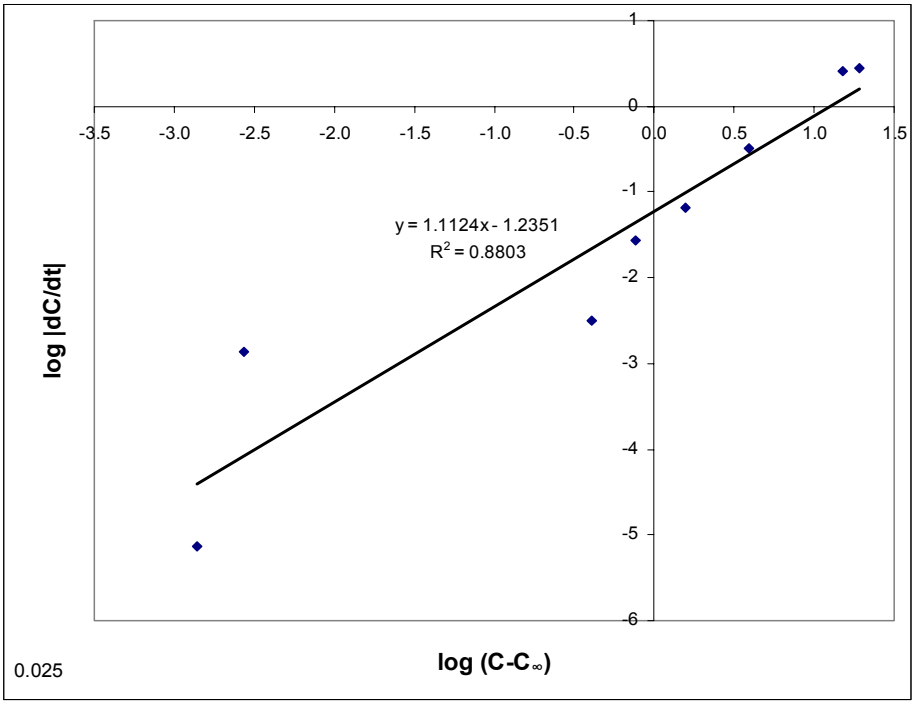

Figure 91. A plot of log dC/dt vs. log ($C-C_\infty$) for the 0.025 M copper weathering test. Time in hours, ($C-C_\infty$) in mmol/l and dC/dt in mmol/(lxh).

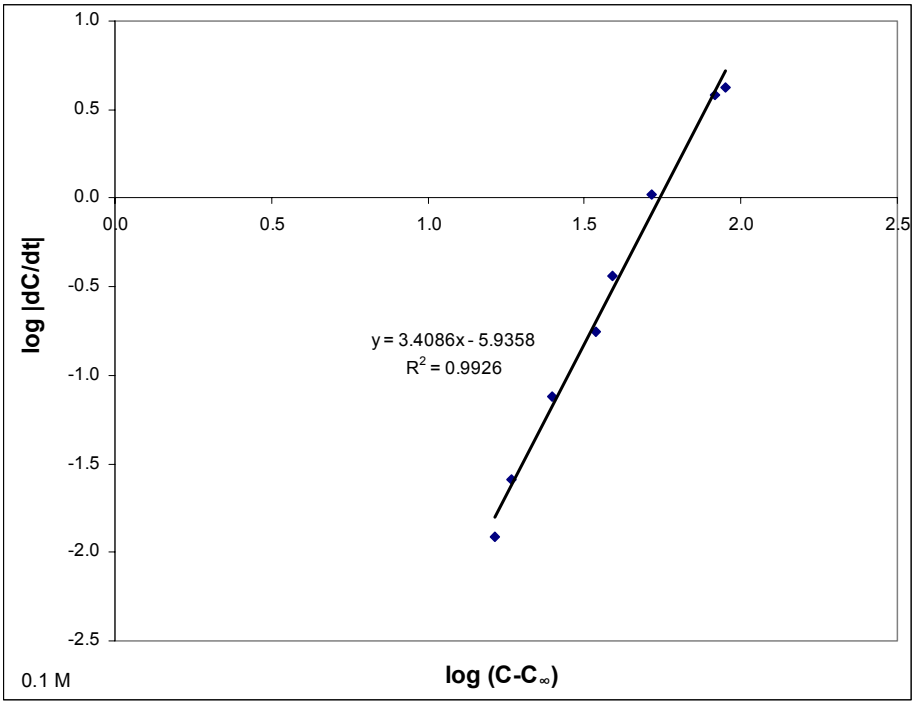

Figure 92. A plot of log dC/dt vs. log ($C-C_\infty$) for the 0.1 M copper weathering test. Time in hours, ($C-C_\infty$) in mmol/l and dC/dt in mmol/(lxh).

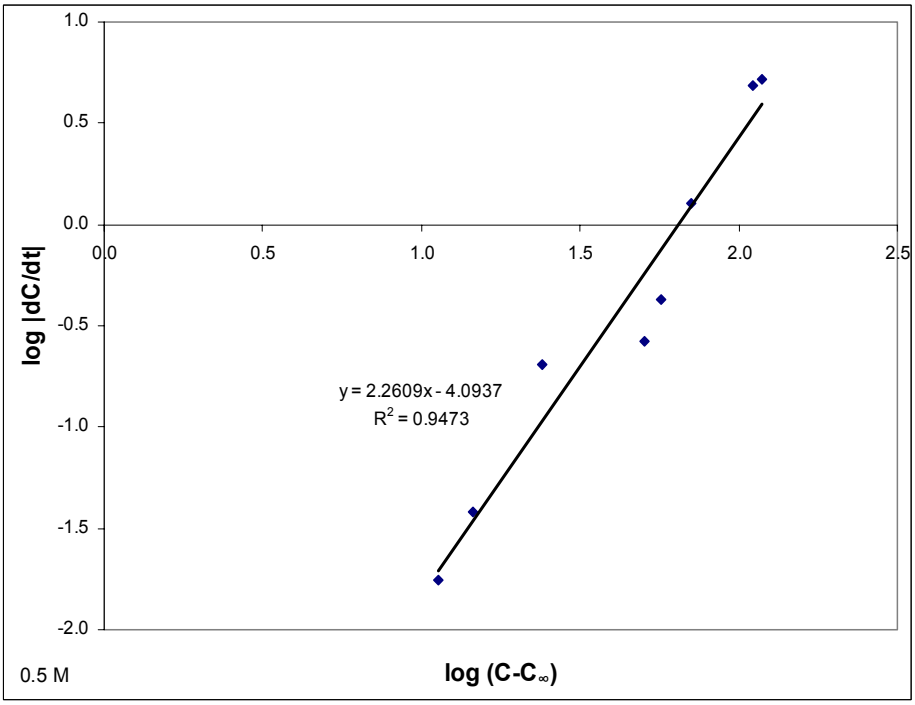

Figure 93. A plot of log dC/dt vs. log ($C-C_\infty$) for the 0.5 M copper weathering test. Time in hours, ($C-C_\infty$) in mmol/l and dC/dt in mmol/(lxh).

The two techniques used for interpretation of the data (graphical and by curve fitting) give very similar results for the apparent reaction order (within 5 %) and rate constants (taking into account the standard error as shown in table 26). The values for n and k are compared in table 28. The order of the reaction is close to 1 for the 0.025 M copper solution, which indicates a mass transfer control reaction. The apparent order is however considerably higher for the 0.1 and 0.5 M copper solutions indicating a different controlling mechanism of transfer due to the higher copper concentration. What reaction step determines the rate cannot be concluded. The dependence of apparent reaction order on initial concentration is unexpected, and cannot be explained at this stage.

Table 28. Results of fitting n^{th} – order kinetic equation to copper weathering data.

	Cu concentration [M]	Curve fitting	Graphical method
n	0.025	1.112	1.134
	0.100	3.409	3.531
	0.500	2.261	2.179
k	0.025	0.058	0.032
	0.100	1.159E-06	6.664E-05
	0.500	8.059E-05	9.486E-05

Kinetic and thermodynamic studies of copper exchange on Na montmorillonite were performed by El-Batouti *et al* (2003). The study utilised an Orion Cu-ion specific electrode. This was repeated in water, methanol and ethanol media and utilised only the < 1 μm fraction of the clay. They found an apparent order of 2.7 for water at temperatures 20 – 40 °C. The exchange took place within 270 s in the study by El-Batouti *et al* (2003), which is very fast compared to the current study. The main reason is the difference in particle size. El-Batouti *et al* (2003) used only < 1 μm material where this study utilised fine rocks (-16 + 13 mm). The much higher concentration used in this present study could also influence the kinetics of the exchange reaction. The lower adsorption rate for copper and the lower reaction order (close to 1 for the 0.025 M concentration) in this present work suggest a degree of mass transfer control in this study. The higher apparent reaction order for the 0.1 and 0.5 M copper concentrations agree well with the study of El-Batouti *et al* (2003). Mass transfer control could be tested in principle by using different sizes of kimberlite particles, but break-up of these particles during weathering changes the diffusion distance as copper take-up proceeds, so the effect of particle size will not follow simple shrinking core kinetic behaviour.

Mass balance for the cupric medium

The total charge of cations absorbed by the kimberlite (expressed as Cu^{2+} equivalents) should equal the total charge of other cations released. For the three copper concentrations, the moles of copper taken up by the kimberlite and the moles of other cations released are compared in table 29. The charge balance over the cation exchange reaction is fairly good, although the 0.1 M copper concentration does not agree very well. A small pH difference did occur which could account for the discrepancies.

Table 29. Mass balance of copper weathering tests.

Copper concentration	Moles of Cu taken up by ore	Moles of Na & K released	Moles of Mg & Ca released	Moles of Al released	Total equivalent moles of cations released*
0.025	**0.023601**	0.050046	0.000386	0.000000	**0.025409**
0.1	**0.081516**	0.111043	0.009406	0.000070	**0.065033**
0.5	**0.118025**	0.132279	0.042258	0.002817	**0.112623**

*Total equivalent moles of cations released = K /2 + Na/ 2 + Ca + Mg + 3/2 * Al

Potassium Medium

The kinetic study of the cation exchange reaction was repeated in a different solution with a different kimberlite. The Venetia kimberlite was used in this case, as the effect of potassium on the weathering behaviour of Venetia was already studied and the kinetic data could be used for optimising and understanding the application thereof on underground tunnels. The test utilised a potassium solution and 300 g of Venetia kimberlite (-16 + 13 mm) weathered in 0.1, 0.5 and 1 M potassium chloride solutions at room temperature (20 °C), using 1 litre of weathering medium. Solution samples were removed at 0, 4 hours, 8 hours, 24 hours, 48 hours, 72 hours and 216 hours (9 days) for ICP analysis to follow the uptake of potassium by the kimberlite. The ICP results are given in table 30 and include the concentration of sodium, calcium and magnesium.

The decrease in the concentration of potassium in the three solutions is shown in figure 94. The decrease in potassium concentration is initially rapid and then the reaction becomes slower at around 2-3 days and thereafter the concentration changes very little. This is faster than for copper, where exchange continued for up to 7 days.

The increase in sodium is shown in figure 95 and the increase in the sum of magnesium and calcium in figure 96. Similar to the copper kinetic evaluation it is essentially sodium that is replaced from the kimberlite for the 0.1 M potassium solution (up to ~ 48 mmol/l) while the

sum of calcium and magnesium is ~ 5 mmol/l. In the 0.5 M potassium solution the sodium replaced from the kimberlite goes up to 83 mmol/l and the sum of magnesium and calcium up to 30 mmol/l. For the 1 M solution the sodium goes up to 87 mmol/l and the sum of calcium and magnesium up to 39 mmol/l. The sum of calcium and magnesium replaced from kimberlite increases considerably with potassium concentration. (The detail of the cation exchange of the copper and potassium mediums cannot be compared directly as different kimberlites were used during these tests.)

Table 30. ICP analysis results of potassium weathering solution as a function of time.

0.1 M Potassium				
Time	K	Na	Ca	Mg
[hours]	mmol/l	mmol/l	mmol/l	mmol/l
0	99.75	0.96	0.05	0.03
4	69.06	24.36	2.12	0.53
8	63.94	29.58	2.74	0.74
24	53.71	37.84	3.24	1.03
48	48.60	43.50	3.24	1.11
72	43.48	47.85	3.49	1.15
216	40.92	47.85	3.49	1.19
0.5 M Potassium				
Time	K	Na	Ca	Mg
[hours]	mmol/l	mmol/l	mmol/l	mmol/l
0	485.95	3.35	0.04	0.09
4	434.80	38.28	9.73	1.73
8	409.22	52.20	13.47	2.55
24	383.65	65.25	17.71	3.37
48	358.07	73.95	21.21	4.11
72	352.96	78.30	22.95	4.94
216	350.40	82.65	24.20	5.35
1 M Potassium				
Time	K	Na	Ca	Mg
[hours]	mmol/l	mmol/l	mmol/l	mmol/l
0	946.33	6.52	0.05	0.13
4	895.18	38.28	10.73	1.65
8	856.81	60.90	18.71	2.88
24	818.45	73.95	23.45	3.66
48	818.45	82.65	28.69	4.53
72	805.66	87.00	32.44	5.35
216	792.87	87.00	32.44	6.17

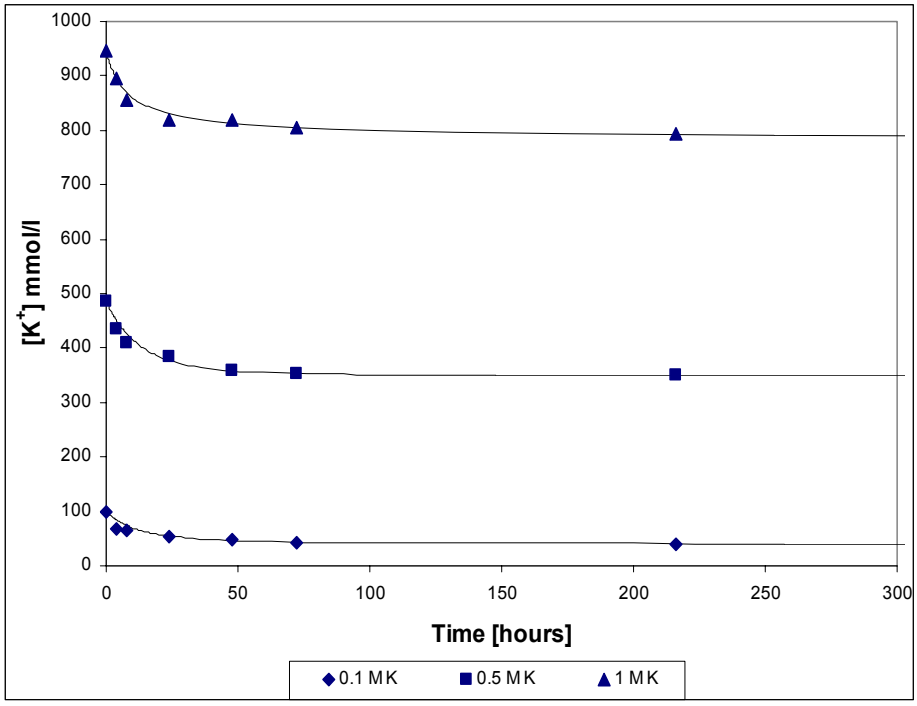

Figure 94. ICP analysis results displaying the steady decrease of the concentration of potassium in the weathering solution as functions of time. The lines are fitted curves for simple n th - order kinetics (parameters in table 30).

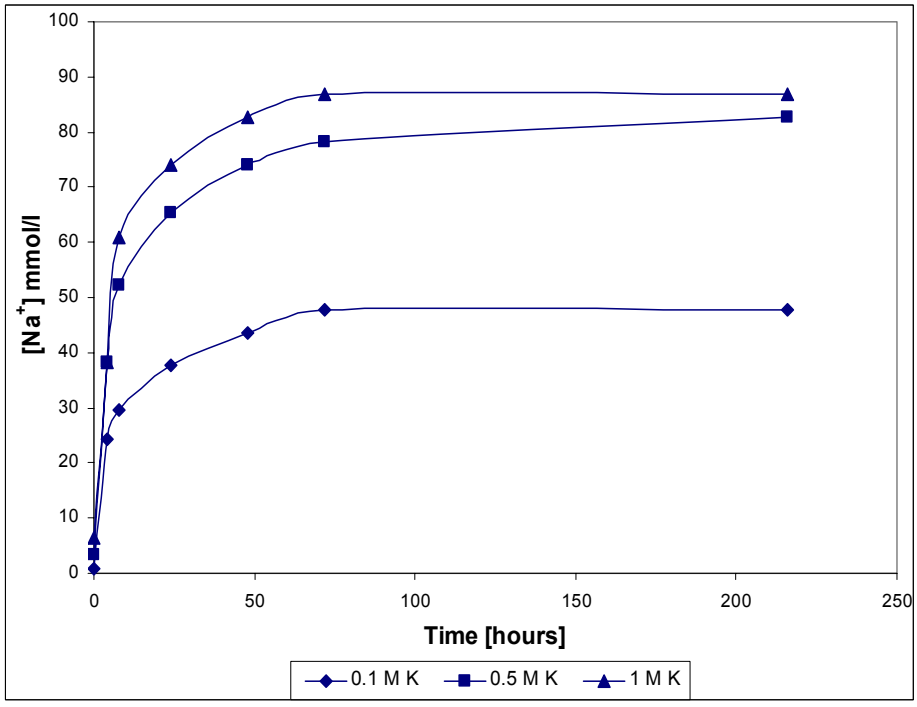

Figure 95. ICP analysis results displaying the increase in the concentration of sodium in the potassium weathering solution as functions of time.

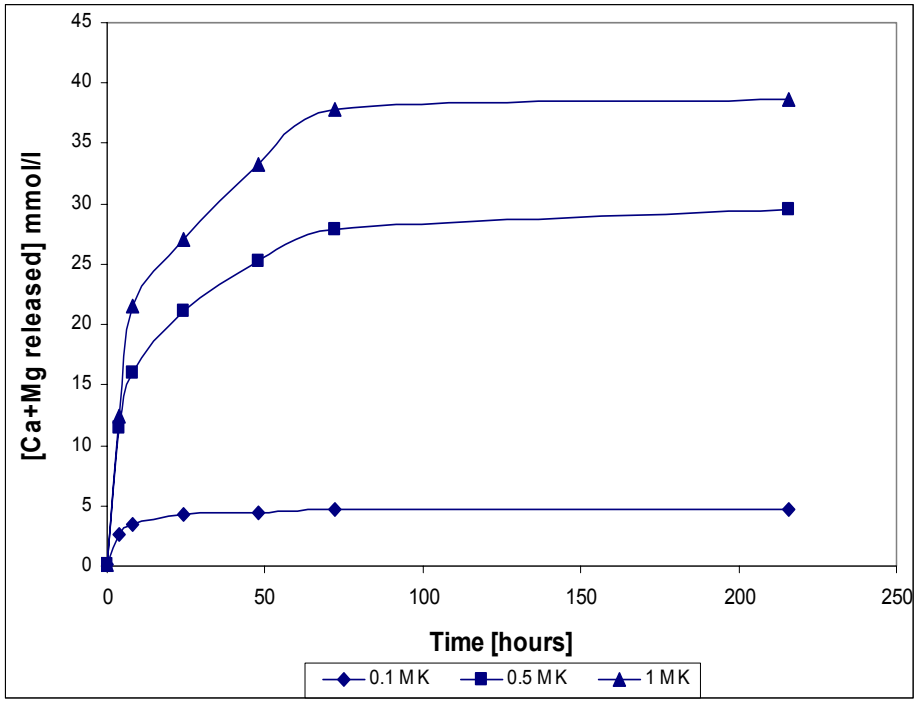

Figure 96. ICP analysis results displaying the increase in the concentration of the sum of calcium and magnesium in the potassium weathering solution as functions of time.

Table 31. Results of fitting kinetic equation 33 to weathering data.

Variable	Coefficient	Std Error
0.1 M		
C_o (mmol/l)	99.749	-
C_{∞}(mmol/l)	40.488	0.489
k	0.013	0.024
n	1.448	0.278
R^2	0.994	-
0.5 M		
C_o (mmol/l)	485.955	-
C_{∞}(mmol/l)	350.348	0.026
k	0.034	0.018
n	1.169	0.081
R^2	0.999	-
1 M		
C_o (mmol/l)	946.333	-
C_{∞}(mmol/l)	785.456	11.002
k	4.967E-04	4.644E-03
n	2.062	1.056
R^2	0.990	-

The potassium kinetic data was also fitted graphically and by Sigmaplot curve fitting. Results are given in tables 31 and 31. The apparent reaction order is ~ 1.5 for the 0.1 M solution, ~ 1 for the 0.5 M solution and ~ 2 for the 1 M potassium solution. The results of both these fitting methods are shown in table 33 for comparison.

Table 32. Results of graphical fitting of kinetic equation 32 to potassium weathering data.

Potassium concentration	Equation of line	n	k
0.1	y=1.644x – 1.963	1.6	0.011
0.5	y=1.310x - 1.585	1.3	2.6E-02
1	y=2.194x – 3.425	2.2	3.8E-04

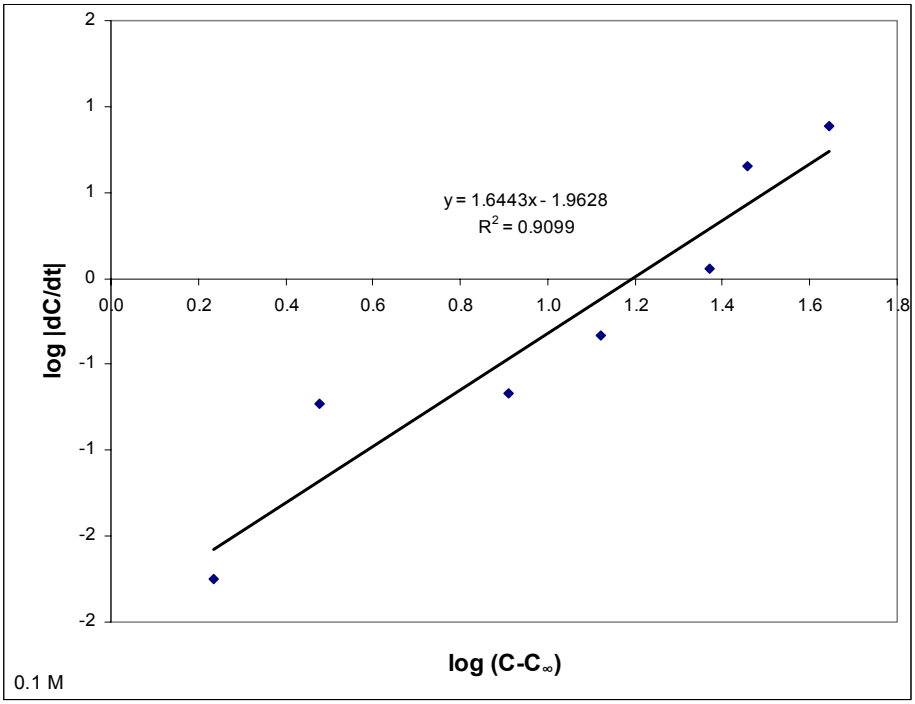

Figure 97. A plot of log dC/dt vs. log ($C-C_\infty$) for the 0.1 M potassium weathering test. Time in hours, ($C-C_\infty$) in mmol/l and dC/dt in mmol/(lxh).

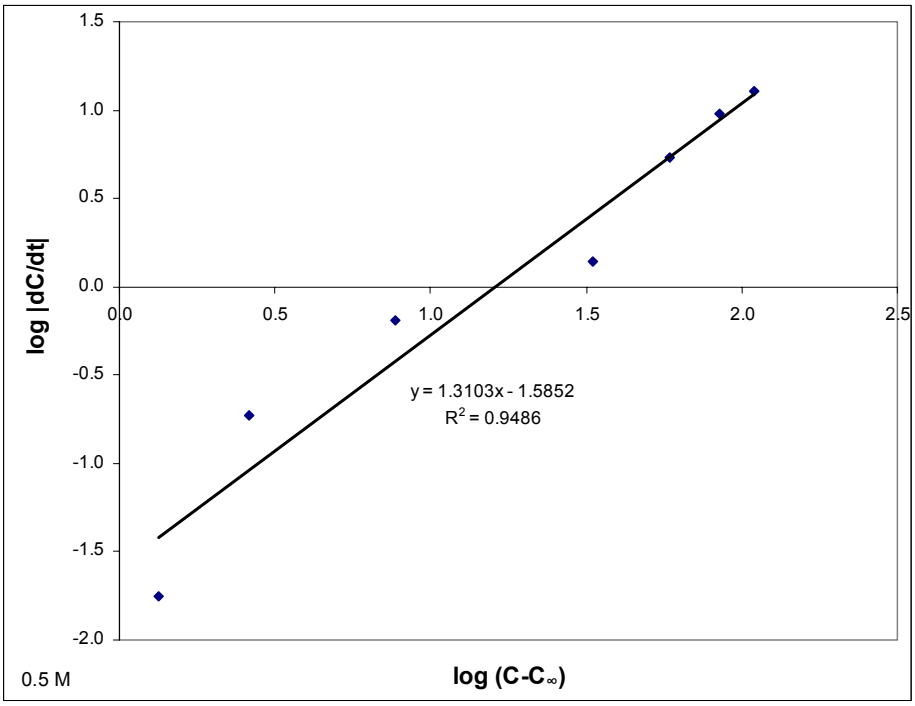

Figure 98. A plot of log dC/dt vs. log ($C-C_\infty$) for the 0.5 M potassium weathering test. Time in hours, ($C-C_\infty$) in mmol/l and dC/dt in mmol/(lxh).

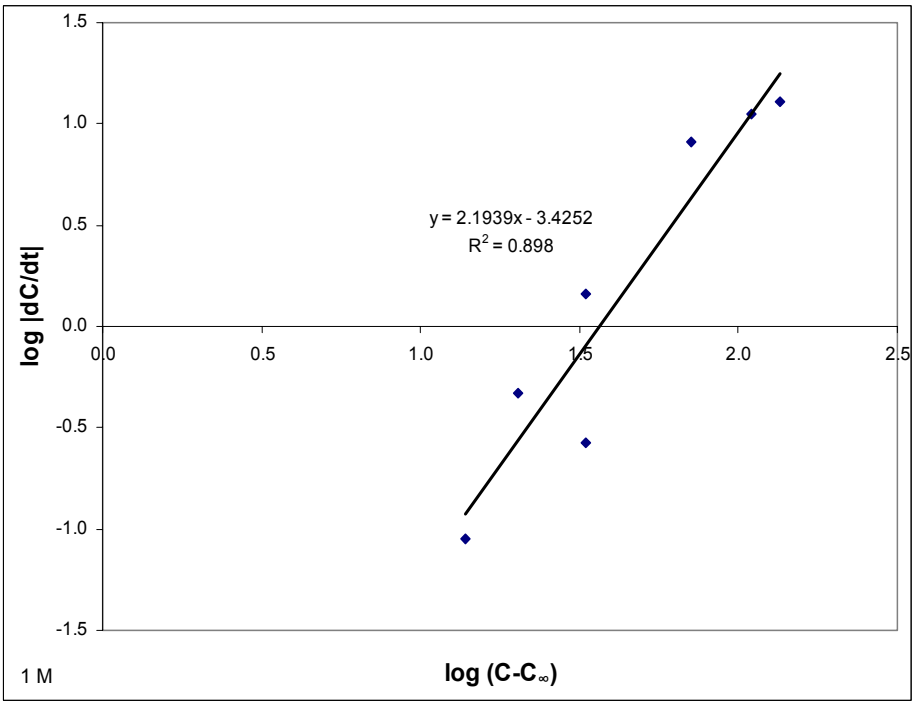

Figure 99. A plot of log dC/dt vs. log ($C-C_\infty$) for the 1 M potassium weathering test. Time in hours, ($C-C_\infty$) in mmol/l and dC/dt in mmol/(lxh).

Table 33. Results of fitting n^{th} – order kinetic equation to potassium weathering data.

	Cu concentration [M]	Curve fitting	Graphical method
n	0.1	1.644	1.448
	0.5	1.310	1.169
	1.0	2.194	2.062
k	0.1	0.011	0.013
	0.5	0.026	0.034
	1.0	3.757E-04	4.967E-04

To enable comparison of the potassium and copper data, a plot of $t_{0.5}$ vs. C_0-C_∞ is given in figure 100. The value of $t_{0.5}$ represents the time to reduce the difference between the copper concentration in solution and its equilibrium concentration, to half the original difference.

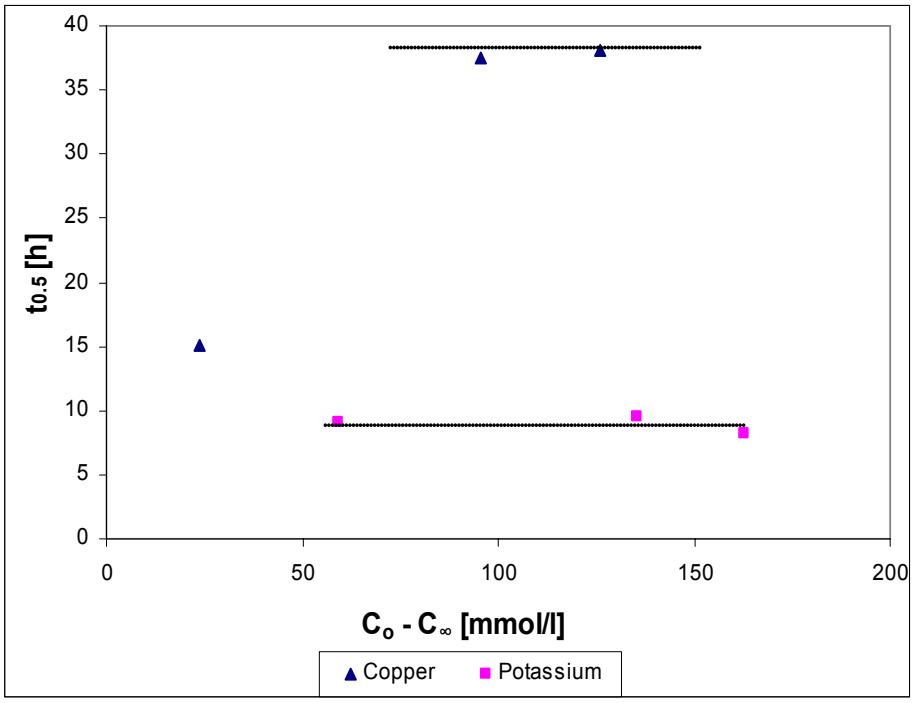

Figure 100. A plot of $t_{0.5}$ (time to reduce the difference between the exchanging cation concentration and the equilibrium concentration to half of the original difference) vs. log C_o-C_∞ for the copper and potassium data.

Figure 100 confirms the more rapid exchange of potassium, which is in line with its higher mobility: the room temperature diffusion coefficient for K^+ equals 1.957×10^{-5} cm^2 s^{-1} compared to 0.714×10^{-5} cm^2 s^{-1} for Cu^{2+} (Lide and Frederikse, 1994). For the case where k and n are not dependent on the initial concentration, it is expected that $t_{0.5}$ would be proportional to $(C_0 - C_\infty)^{n-1}$. For n > 1 (as in this case) it is hence expected that $t_{0.5}$ would decrease as C_0 increases, which is not the case in figure 100. This suggests that the exchange mechanism and reaction kinetics are not clearly understood at this stage.

Langmuir adsorption isotherms

The equilibrium data for copper and potassium can be plotted as adsorption isotherms as shown by Dahiya *et al* (2005), Herbert and Moog (1999) and Rytwo *et al* (1996). This is a plot of Qe (the quantity of cation uptake by the solid, units mol/l) vs. Ce (the final cation concentration in solution, units mol/l). Qe was not measured in this case but calculated from the cation concentration removed from the solution. The Langmuir equation is shown as equation 34 where Qe = X/M; X the amount of solute absorbed, M the weight of the solid, a and b are constants. A plot similar to Dahiya *et al* (2005) of Ce/Qe vs. Ce is shown in figure 100 for the three concentrations of copper and potassium. Note that Ce/Qe is dimensionless.

Langmuir equation: $$\frac{Ce}{Qe} = \frac{Ce}{a} + \frac{1}{b} \qquad (34)$$

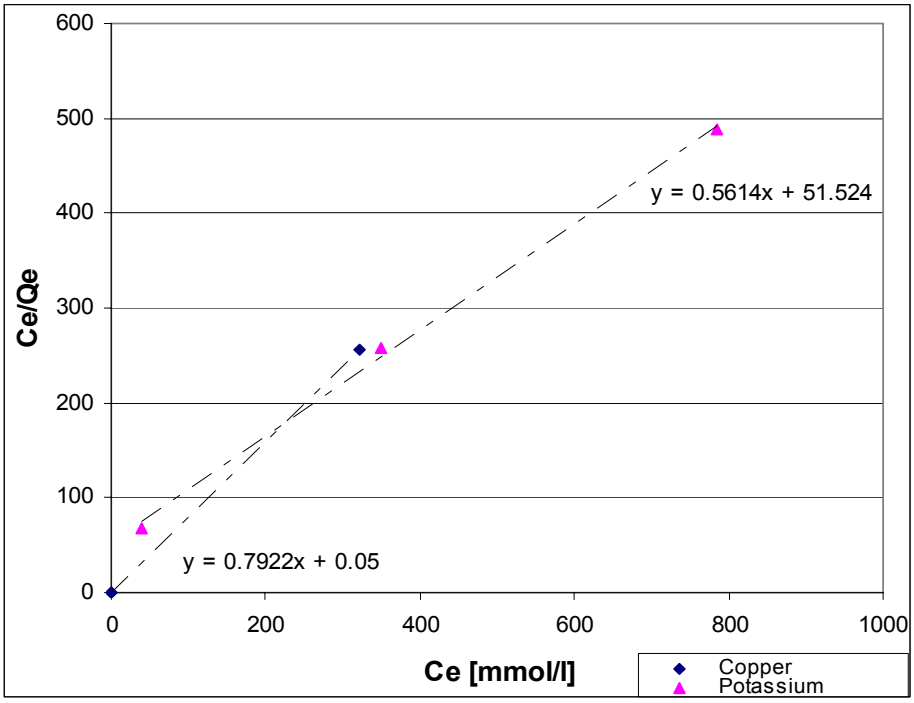

Figure 101. Langmuir adsorption isotherm for kimberlite treated with copper at 0.025, 0.1 and 0.5 M and treated with potassium at 0.1, 0.5 and 1 M.

Linear relationships are obtained in figure 101 according to the Langmuir equation although more data points would be useful. This is similar to zinc adsorption work by Dahiya *et al* (2005) on one specific soil they tested. Another soil tested in their work fitted the Freundlich adsorption equation. The concentration used in the present work is much higher and utilised copper rather than zinc. According to Dahiya *et al* (2005) the amount of zinc absorbed was determined by the type of soil (different clay minerals present), the initial concentration and temperature. The Langmuir equation represents the capacity of a soil to absorb a specific cation. In this case (figure 101) the capacity of absorption for copper is higher than for potassium (at higher concentrations), although this is difficult to compare directly as different kimberlites were used for the test work. Figure 101 also shows that the absorption is directly correlated with the cation concentration in solution (concentration of cations available for up-take). This correlates with the kinetic data which showed that as the cation concentration in solution increased, the amount of cations absorbed by the kimberlite increased.

6.5 Cation exchange behaviour

The cation exchange constant refers to the ease of replacing the interlayer cations with cations in the surrounding medium. The method used for calculation of the cation exchange constant (K_N) is discussed in section 3.2. The tabulated data by Bruggenwert and Kamphorst (1982) are compared with the ionic potential (as used in section 6.2.5.2) in figure 102. Note that the tendency to exchange monovalent Na^+ with other cations was compared by calculating the product $K_N(0.5c_B)^{(1/z_B-1/z_A)}$, where constant K_N is the equilibrium constant for the exchange of cation A (taken to be Na^+) with cation B. For this calculation, an arbitrary (but realistic) value of 0.1 M equivalent concentration of cation B was used. The Na-montmorillonite data was used for comparison, as experimental results (section 6.4) indicated that primarily Na^+ is replaced from the kimberlite, especially at low cation concentrations. No data is available for the iron species in Bruggenwert and Kamphorst (1982). Figure 102 shows that there is no correlation between the ionic potential and cation exchange constants.

The cation exchange constants were determined experimentally utilising finely milled Venetia Red kimberlite and 0.05 M K^+, Li^+, NH_4^+, Ca^{2+}, Mg^{2+}, Ni^{2+}, Fe^{2+}, Cu^{2+}, Fe^{3+} and Al^{3+} solutions. The cation exchange constants determined experimentally compared with the ionic potential are shown in figure 103. The experimental data were expressed simply as the ratio of the equilibrium concentration in the liquid of the exchanging cation B (raised to the power $1/z_B$) to that of the exhanged cation, Na^+ (with both concentrations expressed in mol/dm^3). There is a positive correlation between the experimental cation exchange behaviour and the ionic potential as shown in figure 103, with the exception of Fe^{2+} and Cu^{2+}.

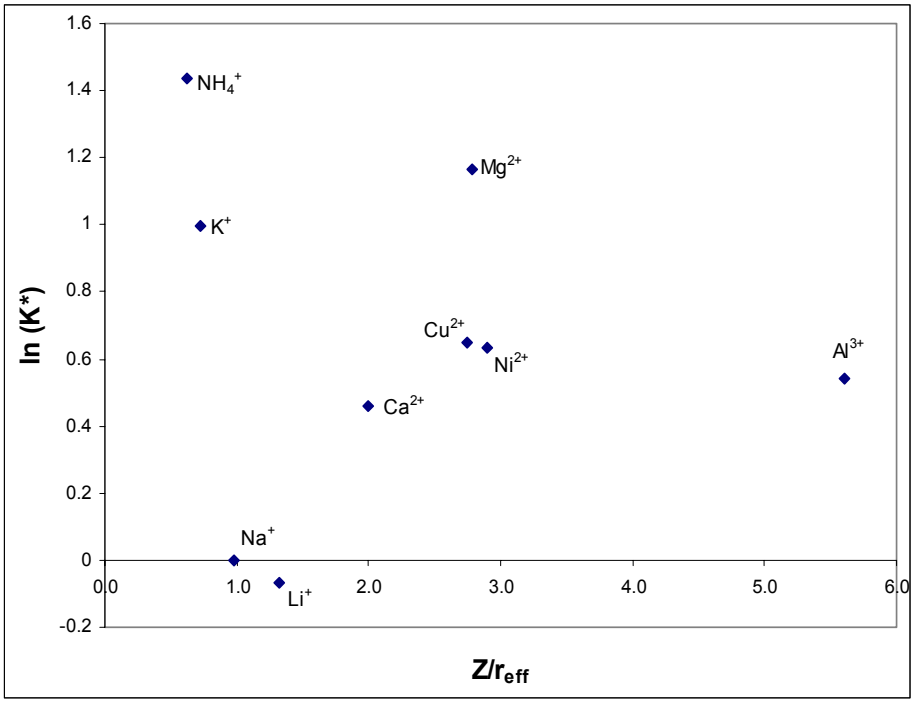

Figure 102. Cation exchange constants as published by Bruggenwert and Kamphorst (1982) as a function of ionic potential.

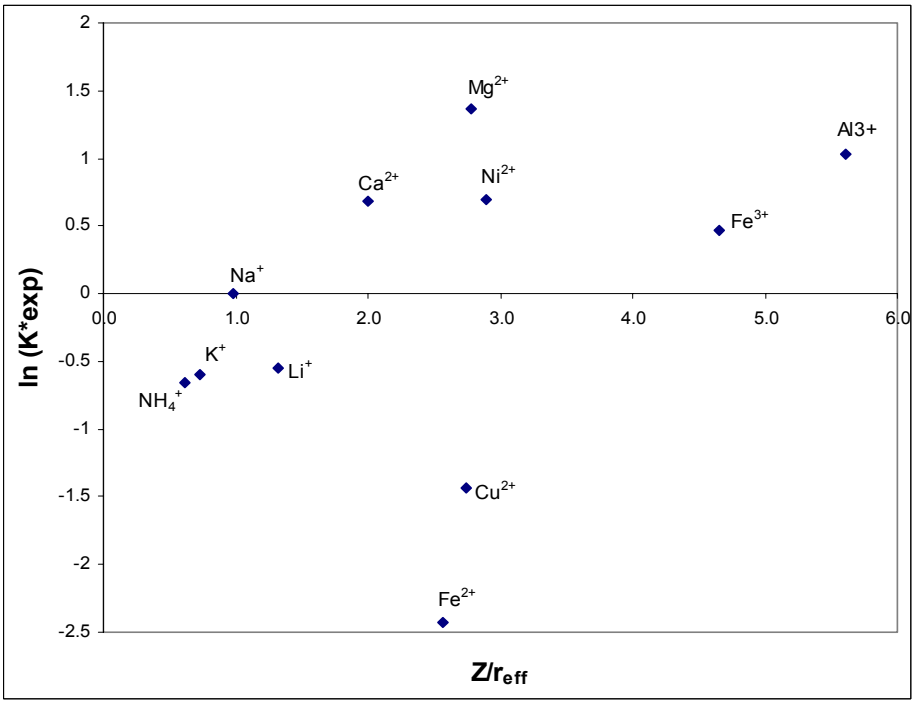

Figure 103. Experimentally determined cation exchange constants as a function of ionic potential.

6.6 Correlation between cation weathering and interlayer spacing (from XRD)

The relationship between changes in interlayer spacing of the clay mineral (measured by XRD) and cation exchange was studied. Dutoitspan kimberlite (250 – 300 g of the – 16 + 13.2 mm size fraction) was weathered in a 0.5 M copper solution for 4 hours, 8 hours, 1 day, 7 days and 30 days utilising 1.5 litres of weathering medium. XRD analysis was performed on the air dried kimberlite after weathering to determine the interlayer spacing (d value of the smectite peak). The results are shown in figure 104. The interlayer spacing is at 12.5 Å (7.1 ° 2 theta) after 4 and 8 hours exposure to the copper solution. At two days, two peaks are visible at 12.5 and 14.5 Å (6.1 ° 2 theta) indicating the presence of smectite with an interlayer spacings of both 12.5 and 14.5 Å, i.e. the smectite is in the process of swelling. After 7 days the 12.5 Å peak is totally collapsed and only the 14.5 Å peak is visible. All the smectite has therefore swollen to this value and it is shown that after 30 days the interlayer spacing is still at 14.5 Å. Only 2 spacing values are observed with no intermediate values. This could indicate stepwise swelling as suggested by Madsen and Müller-Vonmoos (1989). A spacing of 14.5 Å is associated with a double water layer.

The Venetia Red kimberlite interlayer spacing was determined on the untreated sample and then exposed to a 1.5 M potassium chloride solution for 4 hours before repeating the XRD scan (-16 + 13.2 mm). The untreated interlayer spacing is at 14 Å or 6.3 ° 2 theta (figure 105) and is collapsed to 12.5 Å (7.1 ° 2 theta) with the potassium chloride solution.

The d spacing was investigated as a function of the cation type by exposing Dutoitspan kimberlite to different 0.5 M cation solutions (sulphate and chloride anion) for six days. The final d spacings are shown in table 34. The weathering order for some of the cations are: $Cu^{2+} > Li^{1+} > Ca^{2} > Mg^{2+}$. The table shows that there is no correlation between the interlayer spacing and the severity of weathering. The differences between the interlayer spacing for Ca^{2+}, Mg^{2+} and Cu^{2+} exchange are very small whilst the weathering results are very different. For K^{+} the interlayer spacing relates to the collapsed form as expected. Ferrage *et al* (2005) showed that, for ambient conditions (room temperature and around 35 % relative humidity) montmorillonite with Mg^{2+} and Ca^{2+} in the interlayer had primarily 2 water layers in the interlayer. Na^{+} and Li^{+} on the other hand will display primarily 1 water layer spacings and K^{+} predominantly 0 water layers. The results for Ca^{2+}, Mg^{2+}, Li^{+} and K^{+} therefore agrees well with the work by Ferrage *et al* (2005). Cu^{2+} agrees with the Mg^{2+} and Ca^{2+} exchanged forms; a two water layer system under room temperature and humidity conditions.

Ferrage *et al* (2005) formulated equations for the interlayer thickness as a function of the ionic potential and relative humidy, which allows the quantification of the increase of layer thickness with increase in the relative humidity for single and double water layer systems. These formulations are given as equations 35 and 36 with ν the cation charge, r the effective radius and RH the relative humidity as a fraction. For room conditions these equations could predict the experimentally determined cation interlayer spacings within a 7 % interval as shown in table 34 (assuming 2 water layer systems for Cu^{2+} and Al^{3+} at room conditions).

Layer thickness (1W) = 12.556 + 0.3525 x (ν/r-0.241) x (ν x RH – 0.979) (35)

Layer thickness (2W) = 15.592 + 0.6472 x (ν/r-0.839) x (ν x RH – 1.412) (36)

From these results it is concluded that the interlayer spacing (swelling) can not in itself explain the weathering behaviour of kimberlite. The other factors for example cation charge, hydrated radius, type of clay mineral and layer charge all contribute towards the weathering mechanism.

Table 34. Interlayer spacing for Dutoitspan kimberlite weathered in solutions containing different cations.

Cation Type	Measured d spacing	Ferrage *et al* (2005) predicted spacing
	Å	Å
Ca^{2+}	15.1	15.06
Mg^{2+}	14.6	14.70
Cu^{2+}	14.9	14.72
Al^{3+}	14.6	14.47
K^{+}	10.1	10.00
NH_4^{+}	12.5	12.47
Na^{+}	13.3	12.40
Li^{+}	12.9	12.30

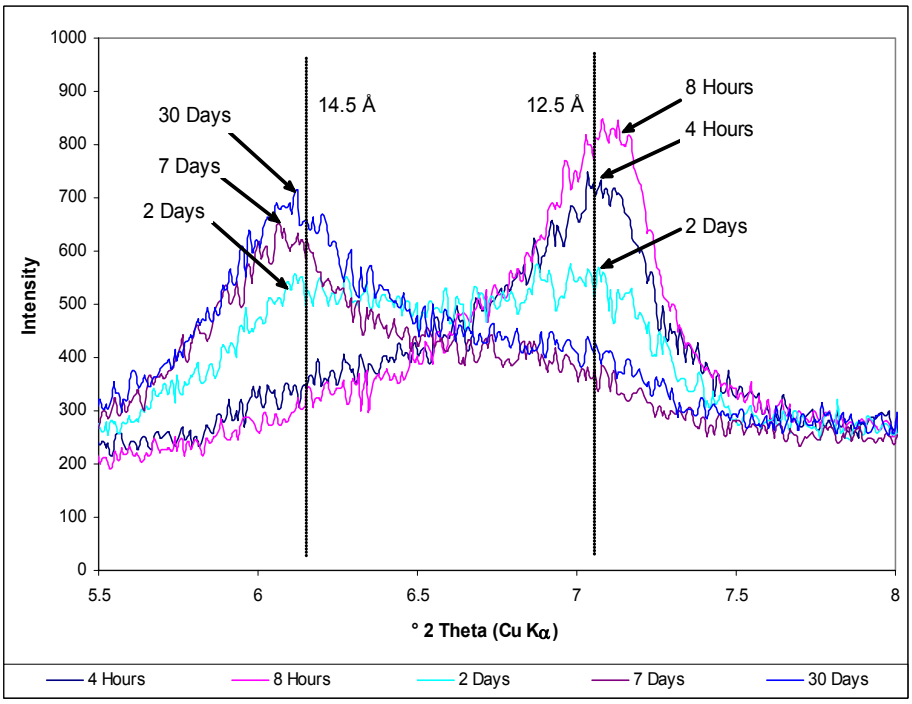

Figure 104. XRD scans (5.5 – 8 ˚ 2θ) of Dutoitspan kimberlite after exposure to copper solutions for 4 hours, 8 hours, 2 days, 7 days and 30 days.

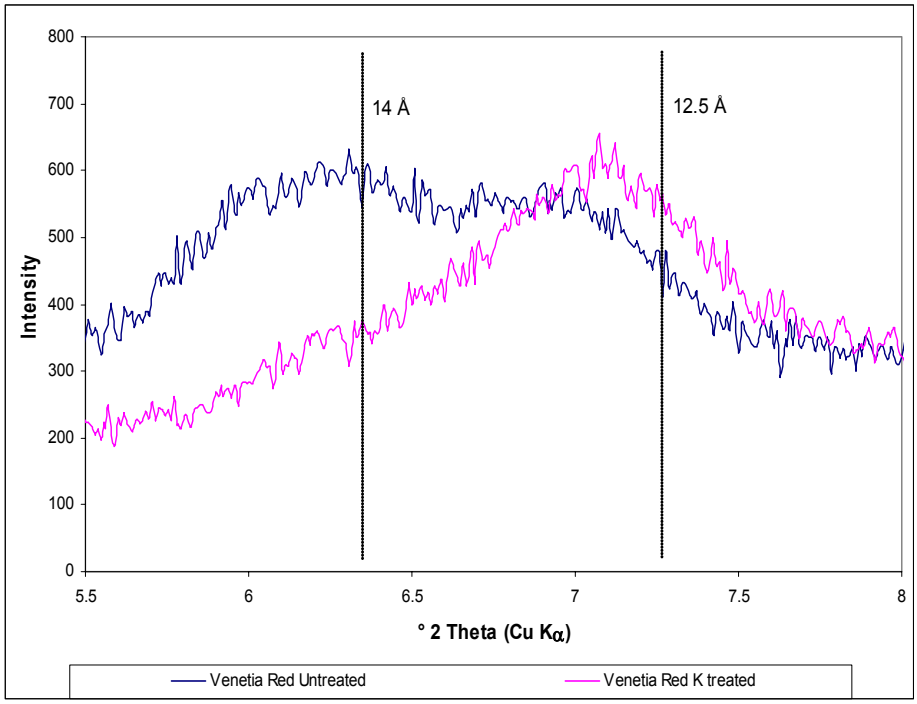

Figure 105. XRD scans (5.5 – 8 ˚ 2θ) of Venetia Red kimberlite after exposure to a 1.5 M potassium chloride solution for 4 hours.

The absence of an effect of cation type on the extent of smectite swelling is in apparent contradiction with the central role of swelling clay in kimberlite weathering which is proposed in this work. To state the apparent contradiction simply: swelling causes kimberlite weathering; kimberlite weathering is strongly affected by the identity of cations in the solution; yet cation identity has little effect on swelling.

This apparent contradiction can be resolved by invoking other elements of the failure process. Griffith-style fracture of brittle materials depends on defect length, applied stress and surface tension. Of these, the defect length is expected to depend on the kimberlite structure, and this does not change if the weathering solution is changed. The stress is applied by swelling; this can be seen to be little affected by cation identity. By elimination, this leaves an effect of cation identity on the surface energy of the crack; such an effect could arise from cation adsorption on the crack surface. The study of Cu^{2+} sorption on montmorillonite by Stadler et and Schindler (1993) suggested that for $3 < pH < 5$ the Cu^{2+} sorbs in the interlayer of montmorillonite through ion exchange, but for $pH > 5$ forms surface complexes with surface hydroxyl groups, which could influence the crack surface energy. This effect was not explored further in this study (careful study of fracture behaviour is severely impeded by the rapid disintegration of the kimberlite). However, it would be a worthwhile direction for future work, especially where solutions with more than one cation are used (perhaps the solution could be designed to contain one cation which exchanges with sodium to cause swelling and another cation/s which changes the crack surface energy).

The type of cation expressed as the ionic potential (cation valence and effective radius) show correlation with the observed weathering behaviour. The type of clay and layer charge will also influence the degree of weathering and the effect of cations. The adsorption mechanism has been shown to differ for different cations (section 6.2.5.2) which also influences the effect of cations on the clay structure and properties. In summary it was shown that Cu^{2+}, Fe^{2+} and Li^{+} can absorb in different positions than only the interlayer rendering the adsorption very effective. Fe^{3+} and Al^{3+} on the other hand have the tendency to form hydroxy species in the interlayer and therefore exhibit a very different mechanism of adsorption. The relationship between ionic potential and observed weathering behaviour holds well for all cations except the trivalent species. It is suggested that the different adsorption mechanism accounts for the weak correlation observed in this case.

6.7 Agglomeration test results

The results of this test are given in table 35. Visual observations of the agglomeration effect were also recorded and shown in figure 106. The results broadly agreed with the weathering results. The Wesselton and Cullinan ores, that showed no and very little weathering, had very little ore agglomerated on the metal piece while Geluk Wes had 2.5 % and Koffiefontein 13.6 %. Figure 107 shows the correlation between this test and weathering results of the Venetia ores.

Table 35. Results of the agglomeration test.

Ore type	Mass retained on metal pieces	% Material retained on metal pieces
Dutoitspan	26.03	13.01
Geluk Wes	5.02	2.51
Koffiefontein	27.32	13.66
Cullinan	1.85	0.92
Wesselton	0.28	0.14
Venetia K1 HYP NE	0.17	0.09
Venetia K1 HYP S	0.81	0.41
Venetia K1 TKB E	2.25	1.13
Venetia K2 NE	6.82	3.41
Venetia K2 S	4.64	2.32
Venetia K2 W	4.76	2.38
Venetia K8	0.11	0.05
Venetia Red	8.59	4.29

Koffiefontein	Dutoitspan

Geluk Wes	Cullinan TKB

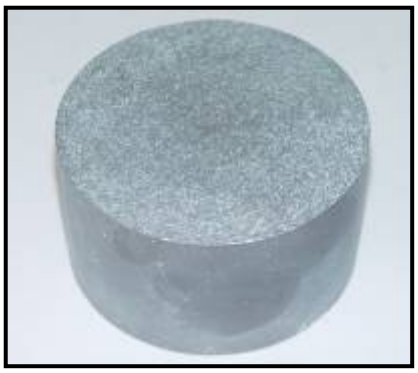

Wesselton	Venetia K1 HYP NE

Figure 106. Visual results of the agglomeration test showing the degree of agglomerated ore on the metal piece.

Venetia K1 HYP S	Venetia K1 TKB E

Venetia K2 NE	Venetia K2 S

Venetia K2W	Venetia K8

Figure 106. Visual results of the agglomeration test showing the degree of agglomerated ore on the metal piece.

Venetia Red

Figure 106. Visual results of the agglomeration test showing the degree of agglomerated ore on the metal piece.

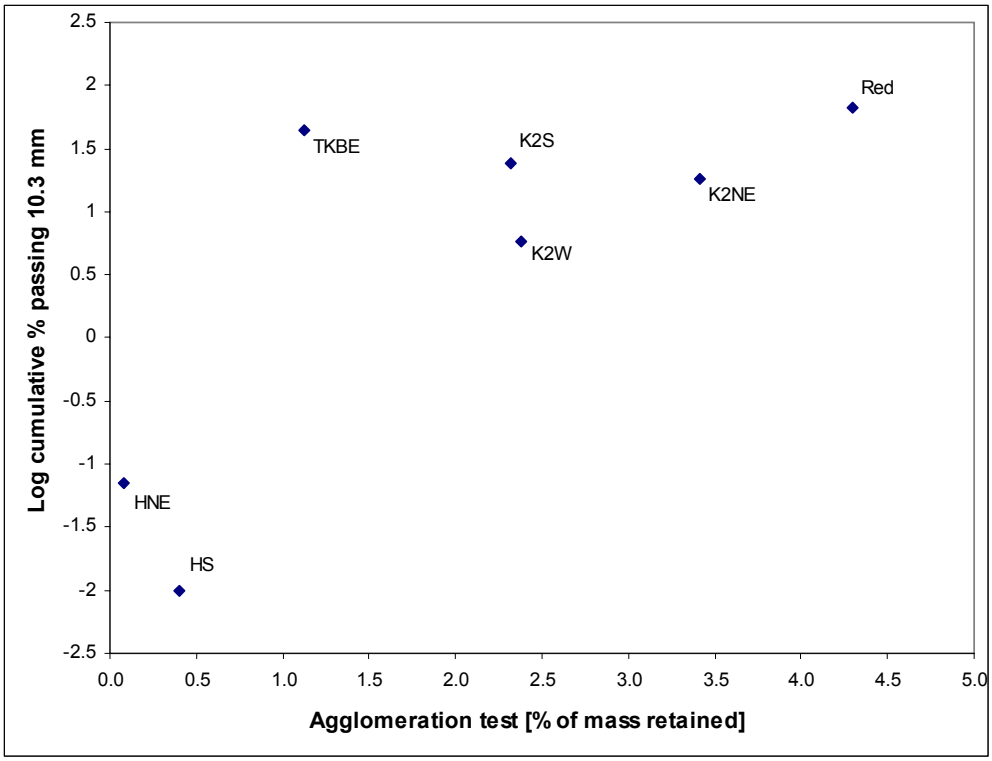

Figure 107. Comparing weathering results with the agglomeration test of Venetia ores. Weathering is shown as log cumulative % passing at 10.3 mm from figure 82 (6 days' weathering in 0.05 M copper sulphate).

Figure 107 shows the relationship between observed weathering behaviour and the agglomeration test for Venetia ores. The poor correlation is evident. This can be due to differences in inherent water content or differences in the histories of these samples, as the

samples were not dried prior to testing. It was therefore suggested that a standard test be developed based on this idea, which should include drying all samples so that it will allow for comparison. This was done as part of a final year undergraduate project (Morkel and Bronkhorst, 2005). The results showed that initial drying at 100 °C for 4 hours and then wetting in distilled water for 2 hours gave good results (figure 108). A R^2 of 0.91 was obtained. This is a simple test for prediction of an ore's likely behaviour during weathering.

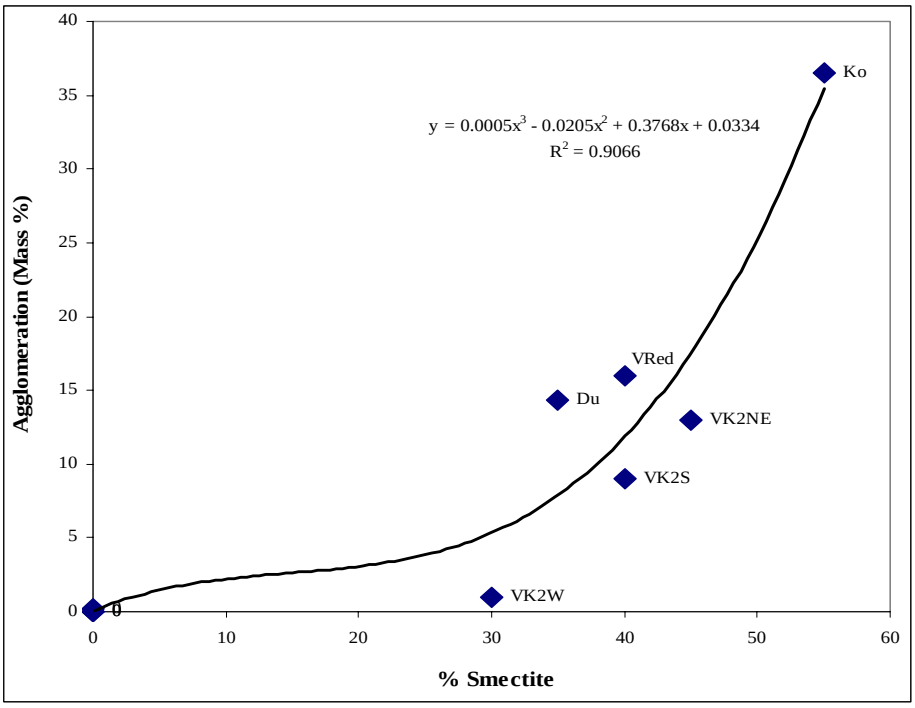

Figure 108. Agglomeration test results for kimberlites dried at 100 °C and then wetted in distilled water for 2 hours.

7 INDUSTRIAL APPLICATION

7.1 % Smectite vs. CEC for some De Beers Mines

Plots of the analysed % smectite and CEC for kimberlites from some De Beers mines are shown in figures 109 - 113. This data was obtained from the Ore Dressing Study group at De Beers Technical Services. De Beers has previously determined their % smectite at Agricultural Research Council (ARC) and therefore the XRD analysis was done on the -2 μm fraction only. This data therefore can not be compared to data in this thesis. We expect a linear increase in CEC as % Smectite increases.

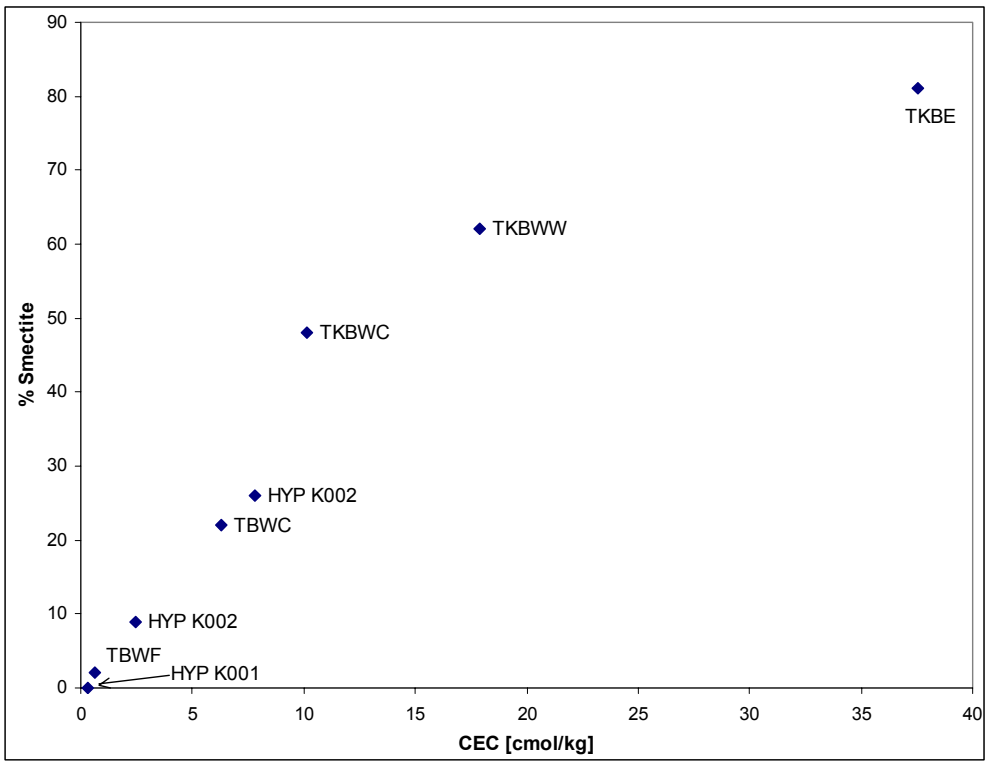

Figure 109. Smectite vs. CEC for Venetia ores / kimberlites from the De Beers geological database. Symbols of kimberlites shown in table 36.

Figure 109 shows the CEC and % smectite for Venetia kimberlites. Very good correlation between these parameters is observed. It is shown that Venetia has kimberlites over the whole spectrum from unweatherable (hypabyssal kimberlite) to highly weatherable (TKB East and West). No kimberlites in this group have a cation exchange capacity larger than 40 cmol/kg.

Table 36. Venetia ores / kimberlites from the De Beers Geological database.

Ore / Kimberlite type	Label
Hypabyssal K001	HYP K001
Tuffisitic Breccia West Fine	TBWF
Hypabyssal K002	HYP K002
Tuffisitic Breccia West Coarse	TBWC
Tuffisitic Kimberlite Breccia West Competent	TKBWC
Tuffisitic Kimberlite Breccia West Weathered	TKBWW
Tuffisitic Kimberlite Breccia East	TKBE

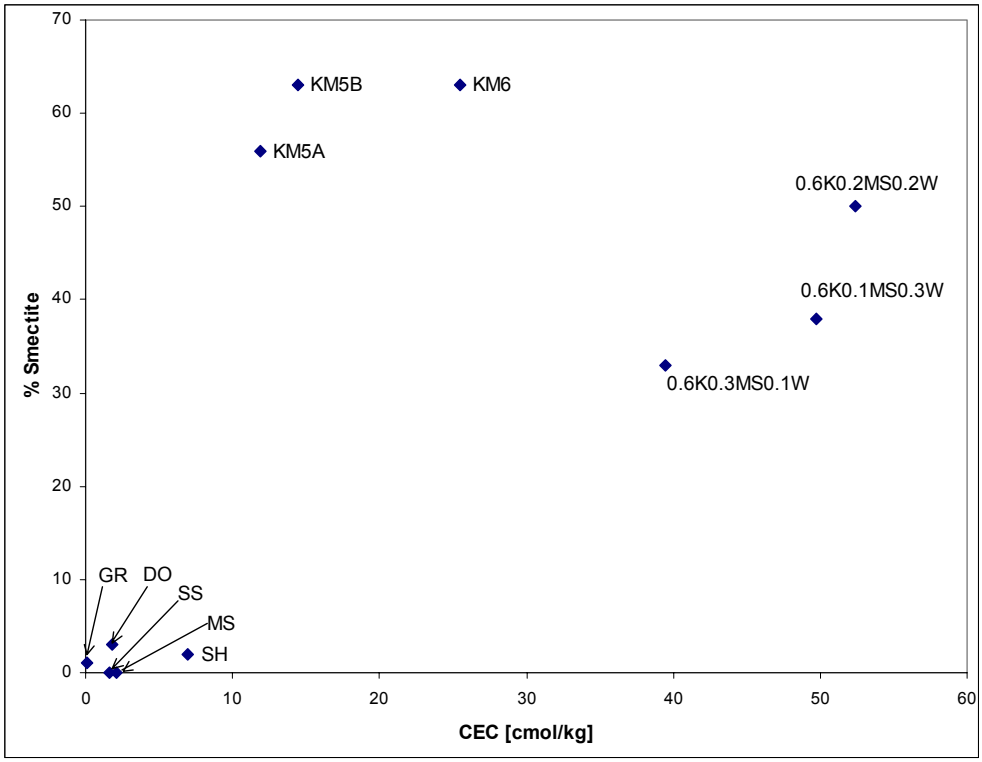

Figure 110. Smectite vs. CEC for Koffiefontein ores / kimberlites from the De Beers geological database. Symbols of ores / kimberlites shown in table 37.

Figure 110 shows the CEC and % Smectite for Koffiefontein ore / kimberlite. Although the correlation between the two parameters is not very good, a prediction of the behaviour of these kimberlites during weathering can be made based on the cation exchange capacity. There are a few ores / kimberlites that should show no weathering (granite, dolomite, mudstone, sandstone and shale) and then progressively the kimberlites will become more prone to weathering as the CEC increases with the kimberlite; mudstone and whittworth mixed ore being the most vulnerable. Note that the highest CEC value here is ~ 55 cmol/kg compared to the highest value for Venetia kimberlite which is below 40 cmol/kg.

Table 37. Koffiefontein ores / kimberlites from the De Beers Geological database.

Ore / Kimberlite type	Label
Granite	GR
Dolomite	DO
Sandstone	SS
Mudstone	MS
Shale	SH
Kimberlite KM5A	KM5A
Kimberlite KM5B	KM5B
Kimberlite KM6	KM6
60 % Kimberlite, 30 % Mudstone, 10 % Whittworth	0.6K0.3MS0.1W
60 % Kimberlite, 10 % Mudstone, 30 % Whittworth	0.6K0.1MS0.3W
60 % Kimberlite, 20 % Mudstone, 20 % Whittworth	0.6K0.2MS0.2W

Figure 111 shows the % smectite, CEC results for Cullinan kimberlites and slimes. The correlation between these two parameters is good. All four kimberlites present in the database have CEC values below 10 cmol/kg indicating these ores to be non weatherable. The CEC of C-Cut slimes is reported as 27 cmol/kg.

Table 38. Cullinan ores / kimberlites from the De Beers Geological database.

Ore / Kimberlite type	Label
Piebald Kimberlite	PBK
Tuffisitic Kimberlite Breccia	TKB
Black Kimberlite	Black
Brown Kimberlite	Brown
C-Cut Slimes	CSlimes

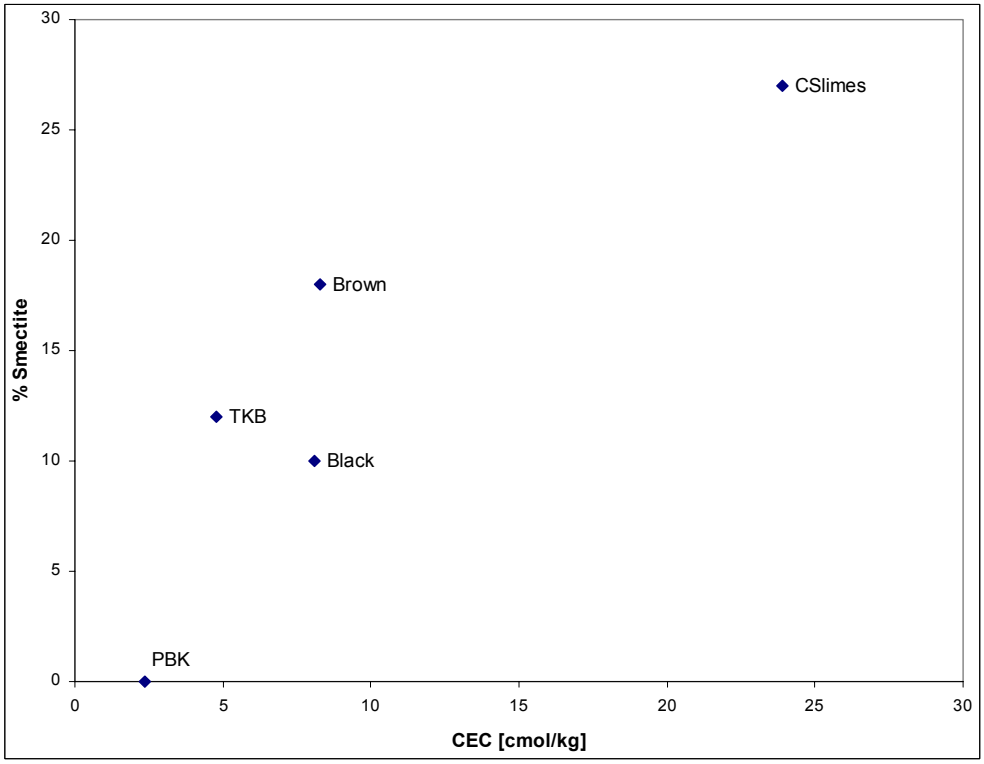

Figure 111. Smectite vs. CEC for Cullinan ores / kimberlites from the De Beers geological database. Symbols of ores / kimberlites given in table 38.

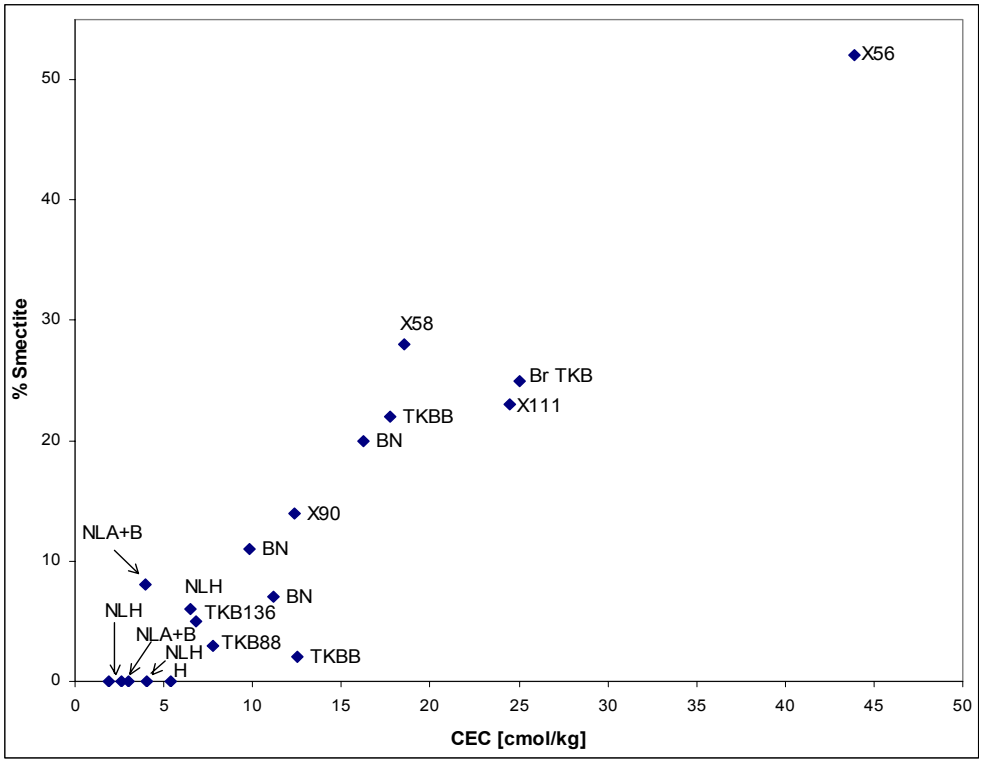

Figure 112. Smectite vs. CEC for Oaks ores / kimberlites from the De Beers geological database. Symbols used for the ores/ kimberlites are given in table 39.

Table 39. Oaks Kimberlite types from the De Beers Geological database.

Ore / Kimberlite type	Label
North Lobe Hypabyssal	NLH
North Lobe Amphibole and Biotite	NLA + B
Hypabyssal Kimberlite	H
TKBB136	TKB136
TKB88	TKB88
TKBB	TKBB
Breccia Neck (TKB)	BN
Xenolith (58 – 82 m)	X58
Xenolith (56 – 70 m)	X56
Xenolith (90 – 107 m)	X90
Xenolith (111 – 124 m)	X111
Br TKB (193 – 217 m)	Br TKB

The % smectite vs. CEC for the Oaks De Beers mine is shown in figure 112. The correlation between the parameters is also good with almost all the ores / kimberlites having CEC values below 30 cmol/kg. These ores therefore will mostly not be prone to weathering although some of the kimberlites (with CEC values close to 30 cmol/kg) might show some signs of degradation. There is however one data point at 43 cmol/kg which should be a kimberlite exhibiting degradation by weathering.

The data for these mines are combined in figure 113.

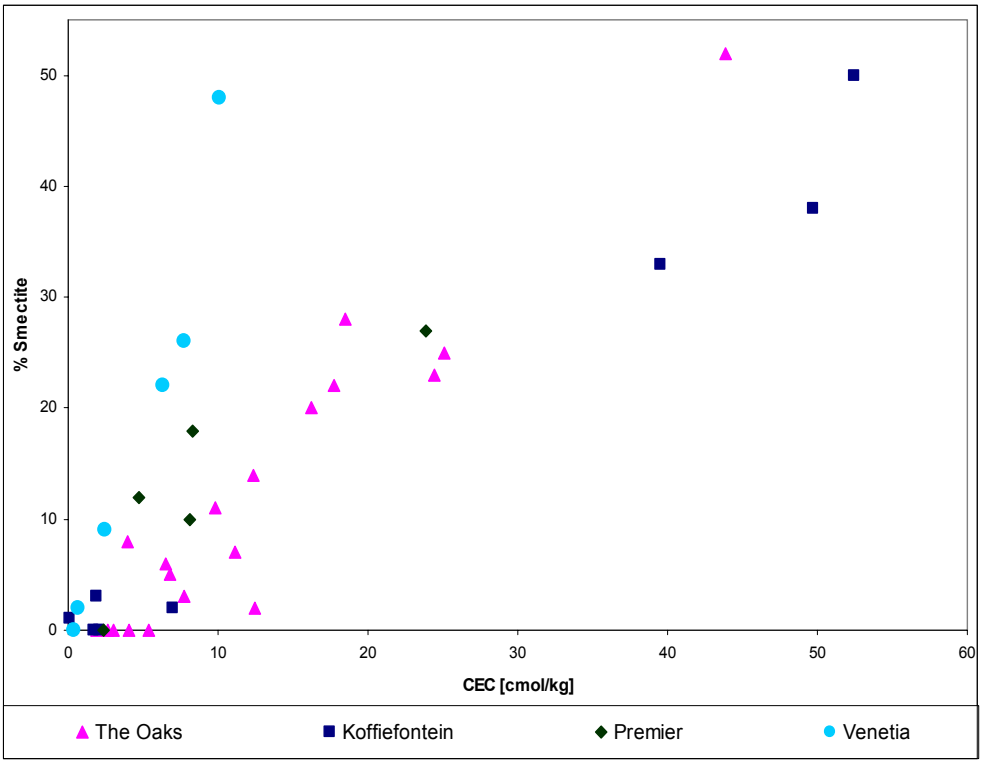

Figure 113. Smectite vs. CEC for the Oaks, Koffiefontein, Cullinan and Venetia mines from the De Beers geological database.

7.2 Potassium as stabiliser of kimberlite

7.2.1 Background

Understanding kimberlite weathering is also important in terms of underground mining techniques as De Beers currently experiences many problems with creating stable underground tunnels. Currently the kimberlite is sprayed with a sealant (commonly with an epoxy or polyurethane basis) and then sprayed with shotcrete (a concrete produced for underground mining). The function of the sealant is to seal off the kimberlite from the surroundings and the shotcrete is then applied to provide mechanical strength. The sealants however typically contain ~ 20 % of calcium sulphate and ~ 30 % water and therefore have been found to actually cause weathering of the kimberlite and then peel off. Typically adhesion tests are used to evaluate the adhesion property of sealants, and also allows for evaluation of whether the kimberlite has been affected by the sealant. This project looked at chemically altering the kimberlite to a more stable state, and also investigated altering the

sealant properties to minimise the effect on kimberlite. Some of the test results obtained during this study are shown in the next section.

7.2.2 Slake durability test results

The slake durability test discussed in section 2.3.1.4 was used to evaluate the weathering behaviour of the kimberlite. For these tests some Cullinan and Venetia kimberlites were obtained. Figure 114 shows the results for these kimberlites in distilled water (data are given in Appendix D).

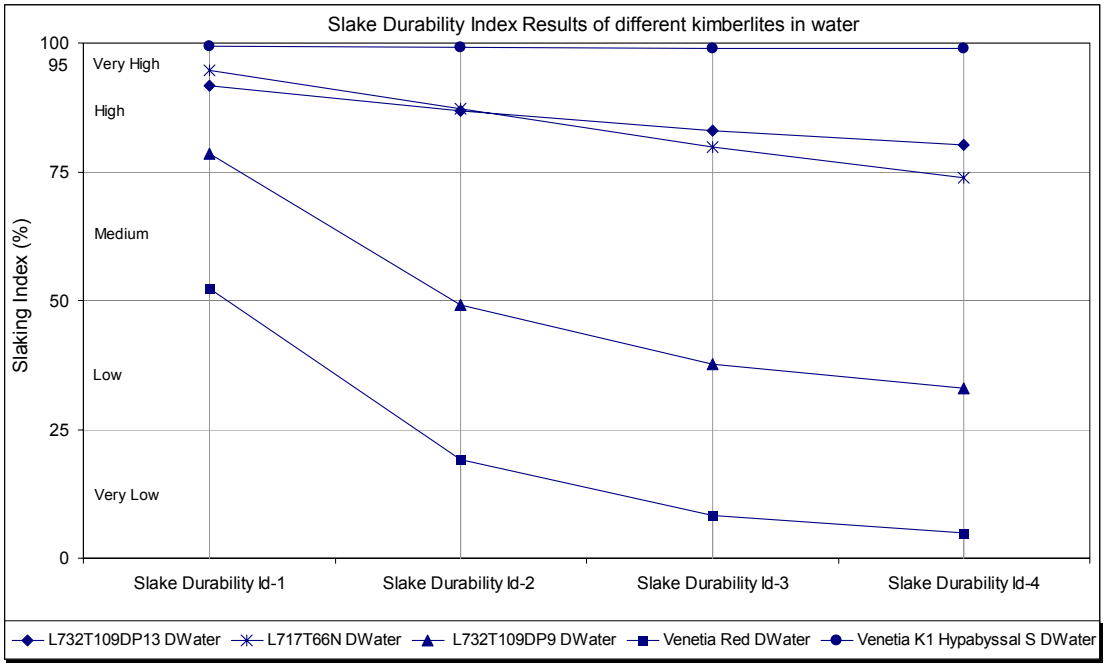

Figure 114. Slake durability test results for three different Cullinan kimberlites (L732T109DP9, L717T66N, L732T109DP13) and Venetia Red and Venetia Hypabyssal kimberlites in distilled water.

The slake results for Cullinan and Venetia kimberlites in distilled water are shown in figure 114. Venetia Hypabyssal shows high slaking durability with almost all the mass retained after four cycles. Cullinan L732T109DP13 and L717T66N show strong slaking durability, whilst Cullinan L732T109DP9 kimberlite displays medium to low slaking durability. Venetia Red kimberlite has been shown to be very weatherable, which agrees with the very low slaking durability observed. The effect of utilising a potassium weathering medium was evaluated and results are shown in figure 115. Potassium has been shown a clay stabiliser (collapses swelling clays) and therefore is expected to provide more integrity to clay rich kimberlite. For these tests Venetia Red and Cullinan L732T109DP9 was chosen as these kimberlites showed the most slaking.

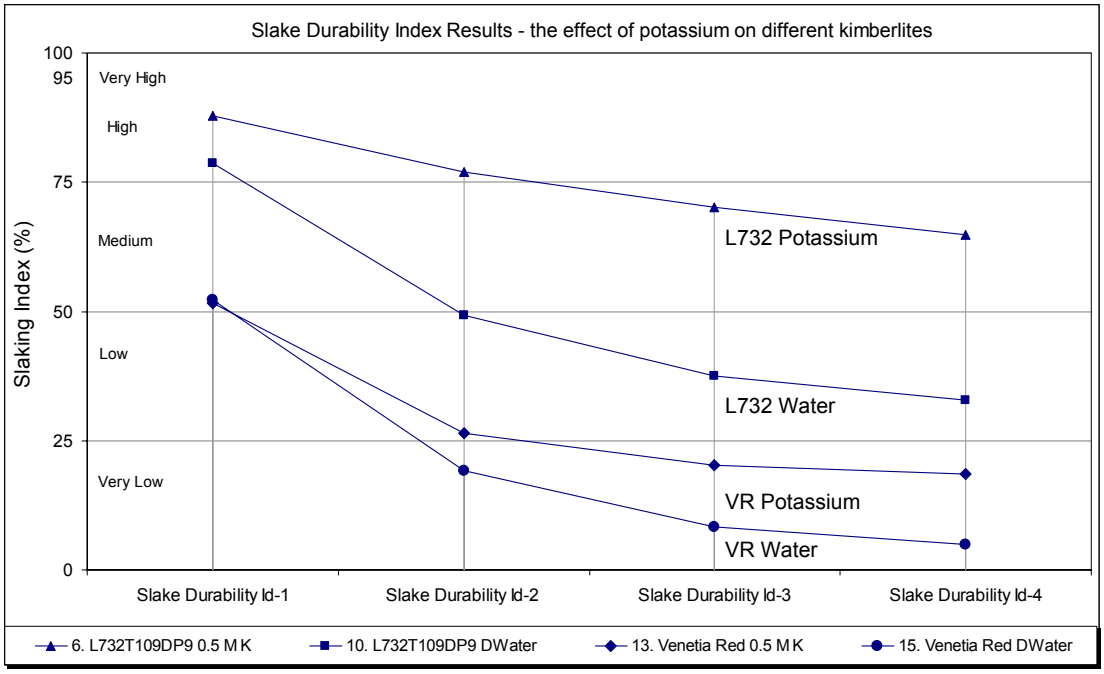

Figure 115. Slake durability test results for Venetia Red and Cullinan L732T109DP9 in a distilled water and a potassium chloride solution.

The addition of potassium to the weathering solution was investigated (0.5 M solution) and results shown in figure 116. Venetia Red was improved from a final slake durability index of 5 to 20 %. Similarly Cullinan kimberlite (L732) was improved from ~ 30 to 65 %. The weathering improvement obtainable depends on the abundance of smectite; Cullinan with less swelling clay can be improved more (35 %) that Venetia Red at 15 %.